FLUORINATED NANOFIBERS
FOR POTENTIAL BIOMEDICAL APPLICATIONS

by

BURCU SANER

Submitted to the Graduate School of Engineering and Natural Sciences
in partial fulfillment of the requirements for the degree of
Master of Science

Sabancı University
Spring 2007

FLUORINATED NANOFIBERS
FOR POTENTIAL BIOMEDICAL APPLICATIONS

APPROVED BY

Assoc. Prof. Yusuf Menceloğlu .....
(Thesis Supervisor)

Prof. Dr. Yuda Yürüm .....

Asst. Prof. Alpay Taralp .....

Assoc. Prof. Hikmet Budak .....

Asst. Prof. Melih Papila .....

DATE OF APPROVAL: 14/08/07

© Burcu Saner 2007

All Rights Reserved

To my grandfather and grandmother

Asım & Fadile SANER

ACKNOWLEDGMENTS

I would like to express my gratitude to all those who gave me the possibility to complete the thesis. Firstly, I would like to give my special thanks to my advisor Yusuf Menceloğlu for his patient guidance, encouragement and excellent advises throughout the research. Also, I would like to express my deepest sense of appreciation to our beloved Gürsel Sönmez who lives in my heart and I will never forget him.

Very special thanks go out to Levent Toppare without whose motivation and encouragement, I would not have considered to continue academic career. Also, my sincere thanks go to Yuda Yürüm, Alpay Taralp and Hikmet Budak for their encouragement and their valuable comments and suggestions.

I'm thankful to Burçin Yıldız for her essential assistance and guidance during my 2-years at Sabanci University.

Many thanks go in particular to my colleagues "Burak Birkan, and Nalan Öncü" for their friendly help in my research. I also wish to thank my friends to "Cenk Gümeci, Aslı Nalbant, Özlem Kocabaş, Funda İnceoğlu, Ayşe Özlem Sezerman, Ayça Erden, and Canan Barıştıran" for their friendship and support at Sabancı University.

I would like to express my warmest thanks to my dear friends "Pınar Demirel, Pınar Özge Çetinyürek, Mehtap Önler, Serhat Varış, Başak Yiğitsoy, Günseli Sezigen, Ayşe Nur Pinar, and Özlem Velioğlu" for their friendship and moral support during my undergraduate and graduate years.

I consider myself as a very lucky person to know Gönül Ungan and Ercüment&Güzin Yürüten who always help and support me in any conditions of my life.

Finally, I owe my loving thanks to my sister Tuğçe and my parents for their moral support and patience during my study at Sabanci University.

FLUORINATED NANOFIBERS
FOR POTENTIAL BIOMEDICAL APPLICATIONS

Burcu Saner

Materials Science and Engineering, M. Sc. Thesis, 2007

Thesis Advisor: Assoc. Prof. Yusuf Z. Menceloğlu

Keywords: Supercritical Carbon Dioxide, Biodegradation, Polymers, Fibers

ABSTRACT

The application of supercritical carbon dioxide has been attracting more attention in the synthesis of biodegradable polymers. Highly pure products without residues can be recovered after the polymerization in supercritical carbon dioxide. In the present work, three types of block poly(L-lactide-co-ε-caprolactone), with a central fluorinated segment and polylactide/polycaprolactone side chains were synthesized by sequential ring-opening polymerization in supercritical carbon dioxide. Perfluoro polyethers can be used as blood substitutes to deliver oxygen to tissues so that these materials are promising for biomedical applications. In the first part of the work, fluorinated reactive stabilizers (prepolymers) with inner fluorinated segment and polylactide or polycaprolactone side chains were synthesized in bulk from three different fluorinated alcohols. The prepolymers were then utilized for the synthesis of copolymers in supercritical carbon dioxide, where polylactide segments were successively incorporated to the ends of the prepolymer, forming a block structure with polyester side chains. Solubility tests of the prepolymer and the pentablock copolymer in supercritical carbon dioxide showed effective solubilization at the reaction temperature and pressure. In the second part of the work, with the process of electrospinning, nanofiber webs were prepared from these biodegradable materials. Material characterization was carried out by nuclear magnetic resonance spectroscopy (NMR), differential scanning calorimetry (DSC), gel permeation chromatography (GPC), optical microscopy and scanning electron microscopy (SEM).

BİYOMEDİKAL UYGULAMALARDA KULLANILABİLECEK FLORLU NANOFİBERLER

Burcu Saner

Malzeme Bilimi ve Mühendisliği, Yüksek Lisans Tezi, 2007

Tez Danışmanı: Doç. Dr. Yusuf Z. Menceloğlu

Anahtar Kelimeler: Superkritik karbon dioksit, biyoayrışma, polimerler, lifler

ÖZET

Biyo-çözünebilen polimerlerin sentezinde süperkritik karbon dioksit kullanımı giderek önem kazanmaktadır. Süperkritik karbon dioksit kullanılarak gerçekleştirilen polimerizasyonların sonucunda yüksek saflıkta ürünler elde edilmektedir. Bu çalışmada, halka açılma polimerizasyon yöntemi ile superkritik karbon dioksit ortamında, ortasında florlu grup ve uçlarında polilaktit ya da polikaprolakton içeren üç çesit blok poli(L-laktit-ko-ε-kaprolakaton) sentezlenmiştir. Bu malzemeler, oksijen taşıma özelliklerinden dolayı biyomedikal uygulamalarda büyük ilgi görmektedir. Çalışmanın ilk bölümünde, üç çeşit florolink kullanılarak ortasında florlu grup ve uçlarında polilaktit ya da polikaprolakton bulunan florlu stabilizatörler sentezlenmiştir. Daha sonra, bu stabilizatörleri kullanarak süperkritik karbon dioksit ortamında blok kopolimer sentezleri yapılmıştır. Stabilizatörler ve kopolimerler, süperkritik karbon dioksit ortamında yüksek çözünürlükler göstermiştir. Çalışmanın ikinci bölümünde, elektrodokuma yöntemiyle blok kopolimerler nanofiber yapılar haline getirilmiştir. Malzemelerin karakterizasyonunda, nükleer manyetik rezonans spektroskopi (NMR), Diferansiyel Taramalı Kalorimetri (DSC), Jel Geçirgenlik Kromatografisi (GPC), optik mikroskop ve taramalı elektron mikroskopu (SEM) kullanılmıştır.

TABLE OF CONTENTS

LIST OF FIGURES

LIST OF TABLES

LIST OF ABBREVIATIONS

SCF	:	Supercritical Fluid
$scCO_2$	:	Supercritical Carbon Dioxide
ROP	:	Ring Opening Polymerization
PMFC	:	Polymer Membrane Fuel Cell
FDA	:	US Food and Drug Administration
NMR	:	Nuclear Magnetic Resonance
DSC	:	Differential Scanning Calorimetry
GPC	:	Gel Permeation Chromatography
SEM	:	Scanning Electron Microscopy
PLLA	:	Polylactide
PCL	:	Polycaprolactone
FLK-D	:	Fluorolink D
FLK-E	:	Fluorolink E
FLK-T	:	Fluorolink T
T_c	:	Critical Temperature
P_c	:	Critical Pressure

CHAPTER 1

INTRODUCTION

1.1. Supercritical Fluids

Baron Charles Cagniard de la Tour discovered the critical point of a substance in his famous cannon barrel experiments in 1822. Over the course of the last several years, essential studies have been conducted in a wide variety of areas using supercritical fluids. The continued constructive development of the science employing these fluids is dependent upon a unique bridging of scientists from many disciplines involved in supercritical fluid work.

1.1.1. What is a Supercritical Fluid?

A one-component fluid is loosely defined to be supercritical when its temperature and pressure exceed its critical temperature and pressure, respectively, while it is not far from its critical state. The critical point represents the highest temperature and pressure at which the substance can exist as a vapor and liquid in equilibrium.

The most outstanding quality of supercritical fluid (SCF) is that equilibrium and transport properties can be adjusted with minor changes in pressure, temperature or both.

In Figure 1.1 illustrates a pressure-temperature phase diagram for SCF. The critical point is observed as the end of the transition line between liquid and gas.

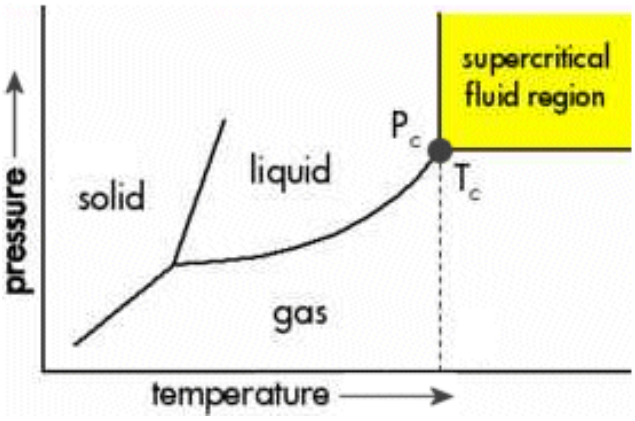

Figure 1.1. Pressure-Temperature Phase diagram.

Tunable densities of SCF (comparable to organic solvents) are sufficient to provide good solvent capability, but low enough for high diffusivity. In Table 1.1, some typical thermophysical properties of gases, liquids and fluids are compared.

Phase	Density (kg/m^3)	Viscosity ($mPa\ s$)	Diffusion coefficient (m^2/s) x10^4	Surface Tension ($dynes/cm$)
Gas	1	0.1	0.1	45-60
Supercritical Fluid	~500	0.03-0.1	0.0001	0
Liquid	1000	1	0.00001	n/a

Table 1.1. Physical properties of gas, liquid, and supercritical fluid of typical organic fluid [1]

The critical temperature (T_c) and pressure (P_c) are characteristic points for the fluid. In table 1.2, the critical parameter values of some fluids are listed [2].

Fluid	P_c/Mpa	T_c/K	Molecular Weight (g/mol)	Density (g/cm^3)
Methane	4.592	190.56	16.02	0.162
Ethane	4.872	305.33	30.07	0.203
Carbon Dioxide	7.377	304.13	44.01	0.469
Water	22.064	647.096	18.02	0.348

Table 1.2. Critical parameter values for some frequently used SCFs.

To sum up, a fluid is said to be supercritical when its temperature and pressure are both above those of its critical point. The properties of SCFs theoretically offer alternative routes for polymer formation, purification and modification. With SCFs, a smooth transition in solvent quality between liquid-like and gas-like properties is possible by external control over pressure and temperature. Moreover, the viscosity of the supercritical fluid is far less than that of the liquid solvent, which is an essential advantage in supercritical processing. The density (solubility), polarity, and other properties of SCFs can be controlled over a wide range.

1.1.2. Supercritical Carbon Dioxide ($ScCO_2$)

Carbon dioxide (CO_2) is the most used supercritical material due to its inherent advantages over other supercritical fluids. These include: accessible critical state (T_c (Critical Temperature) = 304.25 K; P_c (Critical Pressure) = 73.8 bar), properties adjustable with small changes in pressure or temperature, good solvent strength, compatibility with solutes, lack of toxicity and it is commercially available, inexpensive, nonflammable, odorless, and readily recoverable [3]. The surface tension of $scCO_2$ is zero and this allows complete wetting of complex substrates.

$ScCO_2$ is an excellent non-polar solvent for many organic compounds. By adjusting the pressure of the fluid, the solvent properties can be adjusted to be more ‘gas-like’ or more ‘liquid-like’, which allows ‘tuning’ of the solvent properties. Most of

the monomers exhibit high solubility in $scCO_2$ because $scCO_2$ has capability to dissolve the small molecules [4]. DeSimone *et al.* have shown that $scCO_2$ is a versatile solvent for both homogeneous [5] and heterogeneous [6] polymerizations. SCFs are highly compressible, and the density (and therefore solvent properties such as viscosity and dielectric constant) can be tuned by varying the pressure or temperature of the system. The solubility of $scCO_2$ can be improved by adding cosolvents to the system [7].

Since CO_2 is non-polar (unlike water) and has weak Van Der Waals forces (unlike lipophilic phases), nonpolar and polar non-volatile molecules are often insoluble. Therefore, many lipophilic or hydrophilic substances may be dispersed in a CO_2 continuous phase. Various kinds of surfactants (like block copolymers) have been designed recently for stabilizing polymer latexes [8], microemulsions [9], emulsions [10] and inorganic suspensions [11] in CO_2.

In Table 1.3, the properties of $scCO_2$ are categorized into four main fields: environment, health and safety, chemistry and process and benefits of $scCO_2$ are listed for each field [3].

Environmental Benefits	**Health and Safety Benefits**	**Chemical Benefits**	**Process Benefits**
Does no contribute to smog	Noncarcinogenic	High miscibility with gases	No solvent residues
Does not damage ozone layer	Nontoxic	Altered cage strength	Facile separation of products
No acute ecotoxicity	Nonflammable	Variable dielectric constant	High diffusion rates
No liquid waste		High compressibility	Low viscosity
		Local density augmentation	Adjustable solvent power
		High diffusion rate	Adjustable density
			Inexpensive

Table 1.3. Benefits of $scCO_2$ as an industrial solvent

1.1.3. Applications of Supercritical Fluids

Over the course of the last several years, supercritical fluids have been an essential issue for both industrial and academic laboratories. Especially chemical industry prefer to use supercritical fluids as processing aids, cleaning agents and dispersants instead of volatile organic compounds (VOCs). SCFs have been used as solvents for extracting specific compounds [12] such as coffee and tea decaffeination [13], chromatographic techniques [14], polymer synthesis, purification and processing [15]. Most of polymer syntheses occur at high temperatures so that SCF has attracted great attention in these fields. $ScCO_2$ is used for the synthesis of porous polymers since CO_2 provides 'solvent-free' preparation of the materials with pore sizes in the range from microcellular foams down to macroporous resins, and mesoporous/microporous aerogels [16].

SCF is used in polymer processing applications which are polymer fractionation and extraction. In supercritical fluid extraction, SCF is used for extracting specific compounds from a solid or liquid matrix. $ScCO_2$ is the best choice in the extraction of fragrance compounds due to its nontoxicity and easy accessibility to the critical points. $ScCO_2$ extraction of essential oils is one of the most widely used methods among the other analytical techniques [17]. Supercritical fluid chromatography uses compressed gases in the critical temperature range as mobile phases into the capillary columns in order to separate the substances with low migration rates and/or low thermal stabilities. Schneider *et al.* [18] focused on this chromatographic methods using $scCO_2$ as a mobile phase.

SCF is an excellent alternative to conventional organic solvents in the production of controlled drug delivery systems. The main role of these systems is to keep constant the concentration of active compounds in tissues or blood for a long time. In drug delivery systems, the residual solvent left can give hazardous effects in patients so that all residual solvents should be removed. At this point, researchers have concentrated on SCFs in order to prepare solvent-free drug products. Supercritical CO_2 is used as an extracting agent in the manufacture of pharmaceuticals to receive high-purity products. The removal of dichloromethane from a therapeutic system containing polyvinylpirrolidone and megestrol acetate is an illustration of pharmaceutical product

purification [19]. Here, $scCO_2$ is used for extracting dichloromethane and the amount of residual solvents in matrix is relatively minimized. Furthermore, some studies were performed to produce fine powders of polymer materials that can be used with drugs for the production of the controlled release systems. Recently, synthetic polymers such as polyesters, polyurethanes and polyanhydrides have been examined for use in these systems [20].

1.1.4. Polymerizations in $ScCO_2$

Polymerization is the process of forming large molecules from small units (monomers). The properties of polymers depend on the type of monomer and reaction. The polymers can be distinguished with their unique features such as the molecular weight, molecular weight distribution, chain end groups, repeat unit orientation and chain regularity, monomer sequence distributions, crystallinity, branching, or crosslinking.

$ScCO_2$ possesses many properties that have allowed it to emerge as the most extensively studied supercritical fluid for polymerization reactions [21]. The possibility of easily tuning the solvent properties of $scCO_2$, by simply varying pressure or temperature, makes this solvent highly appealing for synthetic applications [22]. Reactions are carried out in an environmentally more acceptable manner because the polymer end-product, the unreacted monomer and solvent, CO_2, can be conveniently separated. $ScCO_2$ in polymerizations has also plasticization effect which results in the lowering of the polymer's glass transition temperature (T_g) [23]. Polymers become highly plasticized by CO_2. There are important effects of plasticization: the removal of residual monomer from the polymer, incorporation of additives and formation of foams.

Solubility plays a significant role in the polymerization reactions in $scCO_2$. CO_2 is a good solvent for most nonpolar and some polar molecules of low molar mass [4] but it is a poor solvent for most high molar mass polymers under mild conditions(<100 °C, <350 bar).

$ScCO_2$ has attracted great interest as an alternative solvent in the area of polymer synthesis as a result of these properties mentioned above. Polymerizations in $scCO_2$ are divided into two major categories: chain addition and step growth polymerizations.

1.1.4.1. Chain Addition Polymerizations

The chain addition polymerizations need monomers with double bonds. A variety of copolymers or terpolymers are synthesized by the chain addition polymerizations of two or three different monomers including double bonds. The types of chain addition polymerizations are free radical, cationic, anionic and transition metal catalyzed reactions.

1.1.4.1.1. Free Radical Polymerizations

Free radical polymerizations can be divided into two groups: homogeneous and heterogeneous polymerizations. Heterogeneous polymerizations can be classified as precipitation, dispersion, emulsion, and suspension reactions.

1.1.4.1.1.1. Homogenous Solution Polymerizations

In homogeneous polymerizations, all components including monomer, initiator, and polymer are soluble during the reaction. Homogenous solution polymerizations are proper for amorphous or low-melting fluoropolymer synthesis and low conversion operations. Using $scCO_2$ as the solvent, DeSimone *et al.* [5] [24] used free radical initiators to affect the synthesis of high molar mass amorphous fluoropolymers. Due to the high solubility of the polymers in the CO_2 continuous phase, the polymerization can be kept homogeneous throughout the reactions.

Homogeneous free radical polymerizations of traditional monomers such as styrene start with the establishment of phase boundaries for monomer, polymer and fluid [25]. Beuermann *et al.* [26] reported that to maintain homogeneous conditions in mixtures of polystyrene+styrene+CO_2, pressure should be higher than about 750 bar at 80^oC if the molecular weight of the polymers is about 10,000 gr/mol.

1.1.4.1.1.2. Heterogeneous Precipitation Polymerizations

In heterogeneous precipitation polymerization, the monomer and the initiator are initially immiscible in fluid but at the end of the reaction, the polymer that forms phase separates. Phase separation stems from the solubility of polymer in the fluid and unreacted monomer. Many early studies in CO_2 were concentrated on the free radical polymerizations of vinyl monomers [27]. Most of vinyl monomers are highly soluble in CO_2 [4] but their polymers exhibit considerably low solubilities in CO_2. Recently, researchers are focused on the precipitation polymerizations of semicrystalline fluoropolymes in CO_2 such as copolymerization of tetrafluoroethylene monomer [28] with perfluoro(propylvinyl ether).

1.1.4.1.1.3. Heterogeneous Dispersion and Emulsion Polymerizations

In the last few decades, researchers have focused on dispersion and emulsion polymerizations in order to design and synthesize spherical polymer particles. In dispersion polymerization, the monomer and the initiator are soluble in the continuous phase, the polymer phase separates. The end product is obtained as spherical particles. In emulsion polymerization, the initiator is preferentially dissolved in the continuous phase and the solubility of monomer in the continuous phase is low.

Surfactant has an essential role for successful dispersion and emulsion polymerization. Its role is to adsorb or chemically attach to the surface of the growing

polymeric particle and prevent the particles from aggregating by electrostatic, electrosteric, or steric stabilization.

A major application of dispersion polymerization in SCFs is in coating systems for many fields, such as textiles, biomedical material, and paper coatings [29]. Dispersion polymerizations in CO_2 can be performed at high polymerization rates to obtain high molecular weight and to recover spherical particles as 1-3 micron. The majority of the work in dispersion polymerizations in supercritical CO_2 has focused on methyl methacrylate (MMA). In 1994, DeSimone reported the dispersion polymerization of MMA in $scCO_2$ [30].

1.1.4.1.1.4. Polymer Blend Synthesis

The plasticization effect of $scCO_2$ favors the synthesis of polymer blends. The main idea is used CO_2 in polymerizations for to swell a CO_2-insoluble polymer substrate and to infuse a CO_2-soluble monomer and initiator into substrate. This provides to generate the polymer blends by the polymerization of monomer.

1.1.4.1.2. Ring Opening Polymerizations

Ring opening polymerization (ROP) is easy method to generate linear aliphatic polyesters such as polycaprolactone, poly(L-lactide), and polyglycolide which are biodegradable polymers used for biomedical applications [31].

High boiling compounds are necessary for performing a thermal ROP in a solvent but it is diffult to remove the solvent from the reaction media. However, this problem can be overcome using $scCO_2$.

1.1.4.2. Ionic Polymerizations

Ionic polymerizations are carried out in two ways: anionic and cationic. In cationic way, polymerization proceeds by adding monomers to a terminal cation while in anionic way, monomers add to a negatively charged terminal cation.

In cationic polymerizations, the high reactivity of carbocations leads to fast polymerization and this results in unwanted side reactions. Due to these side products, the cationic polymerizations are generally conducted at low temperatures (-10 to -100^{o}C). Using CO_2 as a solvent in these polymerizations may be a disadvantage because CO_2's critical temperature (31.1^{o}C).

Recently, living cationic polymerization methods have been developed to obtain well defined-polymers [32]. These methods provide to perform the reactions in a control manner. This means that the molecular weight, molecular weight distribution, and reactivity can be controlled. Also, some experiments on cationic dispersion polymerizations in scCO_2 using polymeric surfactants have been reported [33].

1.1.4.3. Step Growth Polymerizations

Step growth polymerizations in supercritical fluid media have been gaining important attention. These polymerizations are advantageous due to obtain high molecular weight polymers and easier processing. Melt-phase condensation, sol-gel, and oxidative coupling polymerizations are given as examples for step growth type polymerizations. In melt-phase condensation reactions, highly viscous high molecular weight polymers are generated by using organic solvents and this can be disadvantage but if CO_2 is used as a solvent, the plasticizing effect of CO_2 at the melt phase increases the free volume of melt and lowers the viscosity. Poly(ethylene terephthalate) (PET) are commonly synthesized following melt-phase polycondensation method. PET is an important plastic that sees widespread use in fiber, film, and food packaging applications for materials. Sol-gel polymerizations are essential for producing amorphous and porous silica. In these reactions, shrinkage and cracking during drying of

sol-gels should be avoided because this forms the limitations in the commercial applications. For this reason, drying should be performed above the critical temperature and critical pressure of the solvents [34]. In oxidative polymerizations, polypyrrole is synthesized in the controlled manner in $scCO_2$ [35].

1.1.5. Drawbacks of $ScCO_2$

Instead of many advantages of $scCO_2$, it has some disadvantages, too. The high cost of liquid pressure equipments is one of the main drawbacks of $scCO_2$. $ScCO_2$ has a low dielectric constant. Polar molecules such as water, amides, ureas, urethanes and azo dyes show poor solubility in carbon dioxide. However, because CO_2 has a strong quadrupole moment, it solubilizes some polar molecules such as methanol. Therefore, CO_2 is a rather poor solvent and it is adequate only for substances with low or medium molar mass and polarity [36].

1.2. Surfactant Systems

Surfactants are amphiphilic-emulsifying agents including hydrophobic groups (“tail” parts) and hydrophilic groups (“heads” parts). Surfactants lower the surface tension of water by absorbing at liquid-gas interphase. Aggregation occurs due to the interactions of tails with water and the chain molecules consequently form clusters with tails. These aggregates are known as micelles. Same principle is applied for CO_2 and various surfactants are designed.

Surfactants have various industrial applications in detergency, dispersion stabilization, foaming, emulsification, cosmetic formulations, along with more specialized applications in pharmaceuticals (e.g., drug solubilization and control drug

release), bio-processing (i.e., protection microorganism from mechanical damage) and separations (i.e., solubilization of organic in aqueous solutions).

1.2.1. Solubility in Supercritical Fluids (SCFs)

Solubility (γ) is the ratio of vapor pressure (p_v) to total pressure (p_t). In SCFs, the increase in solubility is due to the increase in density of the fluid. Increase in solubility is defined by the enhancement factor (E) that is the ratio of the actual solubility to the one predicted by the ideal gas law.

$$(E)=\gamma.p_t/p_v \qquad (1.1)$$

Solubilities in SCFs are of great importance in a wide variety of applications [37]. These applications are production of controlled drug delivery systems, powder processing, pollution prevention and remediation, methods for spraying paints and coatings, precipitation/crystallization processes, bioseparations, and food processing. The significant variation of solubility is observed with the change of pressure and temperature during supercritical fluid processes when the solvent is a SCF.

The ability to correlate and predict the solubility of solids in supercritical fluids is important in the design and evaluation of supercritical extraction processes [38]. The solubility of the solid in a certain solvent or solution depends on three main factors: the nature of the solute and solvent, temperature and pressure. The solubility of components in SCFs can be enhanced by the addition of a substance referred to as an entrainer, or cosolvent. The addition of a cosolvent provides a further dimension to the range of solvent properties in a given system by influencing the chemical nature of the fluid. The solvent power of the supercritical phase is a function of fluid density. The density of a SCF can be determined by changing its temperature and pressure. With an increase in the density of the SCF, a solute starts to dissolve in the fluid, and with a decrease in the density, the solute can be easily recovered and the solvent can be recycled [39]. The solid solubility in supercritical fluid can be calculated by equation of state (EOS)

method, activity coefficient models, semi-empirical equations or chemical equilibrium approach. EOS method is usually preferred to calculate the solid solubility in SCFs [40].

The level of polymer solubility in $scCO_2$ depends on polarity and backbone flexibility [41]. Most of the compounds like polymers and polar species are not CO_2-soluble [42]. However, fluoropolymers and polysiloxanes are the few materials that are readily soluble in CO_2 even at high molecular weight [43,44].

1.2.2. Fluorinated Surfactants

Fluorine is the most electronegative and reactive of all elements. It has a high ionization potential and very low polarizability [45]. C-F bond is the most stable single bond and the bond strength increases by increasing fluorine substitution. Therefore, perfluorocarbons are thermally and chemically very stable. They also have higher fluidity, lower dielectric constants, higher compressibility and higher gas-dissolving capacities. Fluorocarbons are not only extremely hydrophobic, they are lipophobic as well.

The development of fluoropolymers began with the invention of polytetrafluoroethylene (PTFE) in 1938 by Dr. Roy Plunkett of DuPont Company. Then, a soluble perfluoropolymer (Teflon_ AF) was invented in 1992 and fluoroplastics polymerized in $scCO_2$ were introduced in 2002. Using CO_2 for the synthesis of fluorinated polymers has advantages because of its availability, recyclable and biocompatible properties. Beckman *et al.* [46] synthesized the first effective fluoro-surfactants for CO_2 based on the fact that fluorocarbons and CO_2 are compatible. After this work, DeSimone *et al.* [5] reported the first homogeneous solution polymerization of 1,1-dihydroperfluorooctyl acrylate in $scCO_2$ by employing free radical methods.

A variety of fluorinated surfactants are synthesized for different usage areas. Triblock semifluorinated n-alkanes $F(CF_2)_n(CH_2)_m(CF_2)_nF$ were synthesized and they have interesting and useful physical and chemical properties [47]. Their melting points are lower than those of the perfluoro-n-alkanes of the same molecular weight but their

quite high molecular weight provide low vapor pressure. Also, surface properties can be controlled by varying the chain length of blocks.

1.2.3. Applications of Fluorinated Materials

Fluorinated materials and surfactants have unique properties that make them highly suitable for many industrial processes and consumer applications [48]. Their applications are changed based on their chemical structures. Some fluorocarbons have been used for biomedical applications. These type materials include high purity, aptitude to forming stable emulsions, absence of clinically significant side-effects, and large scale, cost-effective industrial feasibility. These properties are important in vivo oxygen delivery. When the hemoglobin level decreases in blood, delivering oxygen to tissues becomes vital. With perfluorochemicals (PFCs), oxygen can be dissolved and delivered to tissues [49]. The PFCs are injected into bloodstream as emulsions and these emulsions are called as blood substitutes due to the properties of respiratory gas-carrier [50]. The PFCs are unreactive in body and excreted primarily as a vapor through the lungs. By changing the concentration of PFC, the amount of oxygen can be controlled. In addition, fluorinated surfactants have a tendency to self-aggregate into stable and well-organized supramolecular assemblies and these materials can be used for the design of multi-phase colloidal systems including microemulsions, gels, dispersions and aerosols. Most of the colloidal systems have a great potential as drug delivery systems [51]. Fluorinated polymers are also utilized in firefighting applications, cosmetics, greases and lubricants, paints, polishes, and adhesives [52].

1.3. Biodegradable Polymers

Bidegradable polymers have significant potentials in biomedical and pharmaceutical applications such as surgical sutures [53] and matrices for drug delivery [54]. Before the application of biomaterials, the compatibility within the human body should be tested. There are several factors that affect the degradability rate which are chemical composition and configurational structure, processing steps, molecular weight (Mw), polydispersity (Mn/Mw), environmental conditions, stress and strain, crystallinity, porosity, chain orientation, the ratios of chemically reactive compounds within the matrix, and additives [55, 56]. Polymers are tested in a natural or simulated environment. The moisture level, nutrient supply, pH and temperature level of environments leads to a change of degradability [57]. An amount of polymer mass compared to its volume and the chemical composition strongly influences the degradation characteristics. Furthermore, the mechanical properties of biodegradable polymers can be changed according to the chemical structures of the building blocks.

Biodegradable polymers are divided into two major groups: natural and synthetic biodegradable polymers. The natural based materials are polysaccharides such as starch, alginate, chitin/chitosan or proteins such as collagen, fibrin gels, silk. The natural biodegradable polymers are preferable materials because of a high affinity to the environment, and the compatibility within a living body, a high affinity to the environment but they are typically expensive. Synthetic biodegradable polymers have many advantages compared to the natural ones. Crystallinity, degradability, solubility, hydrophobicity, glass transition and melting temperatures can be controlled by changing the synthesis routes. Among the synthetic biodegradable polymers, aliphatic polyesters are mostly developed. Poly(ε-caprolactone) (PCL), polylactide (PCL) and their copolymers have been widely used in medicine. Copolymers of PCL and PLLA are of major importance for drug delivery systems, especially as semi-crystalline materials, the properties of which can be adjusted according to the relative copolymer composition

[58, 59]. In the following parts, characteristic properties of PCL and PLLA will be explained briefly.

1.3.1. Poly(ε-caprolactone) (PCL)

Polycaprolactone is a biodegradable thermoplastic polymer derived from the chemical synthesis of crude oil. PCL is also hydrophobic and semicrystalline material (50% crystalline). Although not produced from renewable raw materials, it is fully biodegradable. However, the degradability of PCL is slow since its crystallinity makes it difficult to be hydrolyzed [60]. The degradability rate of PCL can be controlled by the copolymerization with other lactones such as glycolide and lactide [61, 62]. It has a low melting-point (58-60 °C) and low viscosity, and it is easy to process. PCL can be synthesized by anionic ring opening polymerization of ε-caprolactone using metal hydroxide initiators [63].

PCL has a long degradation time, which is generally a drawback in biomedical applications and this is only proper for drug delivery systems because of its high permeability towards drugs [64].

PCL is used mainly in thermoplastic polyurethanes, resins for surface coatings, adhesives and synthetic leather and fabrics. It also serves to make stiffeners for shoes and orthopedic splints, and fully biodegradable compostable bags, sutures, and fibers.

1.3.2. Polylactide (PLA)

Lactic acid (2-hydroxypropanoic acid) can exist as either L(+) or D(-) lactide due to the chiral nature. Polylactide (PLA) is a biodegradable, thermoplastic, aliphatic polyester derived from renewable resources. Homopolymers of L-lactide and D-lactide are semicrystalline materials (poly(L-lactide): 30-40% crystalline, poly(D-lactide): 60-70% crystalline, for high molar mass). Poly(L-lactide) is one of the most useful in the biomedical field for porous scaffolds and load bearing applications, and also in

orthopedic fixations and sutures due to its high elongation strength and low ultimate elongation [65]. Also, PLA can be processed like most thermoplastics into fibers, films, thermoformed or injection molded and used for compost bags, plant pots, diapers and packaging.

1.4. Polymeric Nanofibers

Nanotechnology and nanoscience are widely developed fields covering a broad range of topics. In these research areas, polymeric nanofibers have attracted much attention due to the ease of fabrication, controllable size/shape, and properties. They are used for diversified applications, including filtration, barrier fabrics, wipes, personal care, biomedical, and pharmaceutical applications [66]. There are many preparation techniques for the fabrication of nanofibers. Among these techniques, electrospinning is the practically unique technique which produces polymeric nanofibers with low cost and high amounts.

1.4.1. Electrospinning

Electrospinning is a unique approach of forming polymer fibers with diameters in the micro- to nanometer range by using electric fields. The electrospinning technology dates back the early 1930s. In 1934, electrospinning was patented by Formhals [67] and Reeneker *et al.* [68] conducted the detailed research. The production of electrospun polymer fibers has widely great interest due to its potential to form fibers with a high surface area and a small pore size.

The elements required for electrospinning include a polymer solution, a high voltage supply and a collector [69]. A voltage is applied to the polymer solution, which causes a jet of the solution to be drawn toward a grounded collector. As the jet moves the collector, it is elongated by electrostatic interactions between charges on nearby segment

of the same jet. The fine jets dry to form polymeric fibers, which can be collected on a web. The electrospinning process is categorized in Table 1.4. [70]. Most of soluble polymers can be electrospun into nanofibers. It is important to choose the suitable solvent such as water and organic solvents. The solvent evaporation and solubility will have an effect on the fiber morphologies.

1. The polymer solution	2. Launching the jet	3. Elongation of the straight segment of the jet	4. The onset of bending, with continuing elongation	5. Solidification of the nanofiber	6. Collection of the nanofiber

Table 1.4. The major steps for the electrospinning process

During the electrospinning, the molecular weight of the polymers has an essential role in controlling the fiber formation and fiber diameter. Low molecular weight leads to bead formation but as molecular weight increases, bead formation is reduced and fiber formation is observed mostly [71].

1.4.1.1. Advantages of Electrospinning

Electrospinning has many advantages:

i. low cost
ii. high production rate
iii. highly controllable
iv. the formation of scaffolds with high porosity and surface area
v. the filtration efficiency
vi. the fabrication of submicron fibers from a variety of organic polymers
vii. the ability to cover complex three-dimensional surfaces with a uniform surface layer

Among these advantages mention above, the filtration efficiency is significant. This can be observed from porous membrane-like fabrics and the high surface area organic fibers [72].

1.4.1.2. Disadvantages of Electrospinning

Instead of the advantages, electrospinning process has some disadvantages:

i. toxicity due to usage of highly volatile organic solvents
ii. web strength
iii. jet instability

Most of the polymers are dissolved in organic solvents and this may result in hazardous explosions in the presence of high voltages during the process. Therefore, manufacturing costs increase for removing the solvents from the media. Also, the polymer type affects the fiber strength and toughness in the final electrospun web.

The electrical and fluid flow conditions alter dramatically in a few milliseconds required to form a jet and to adjust the shape of the region from which the jet emerges. The creation of the jet leads to start the phenomenon that happens within the few milliseconds after the electrical potentials is applied [73]. In addition, the jet undergoes a fluid instability which leads to a whip-like motion of the jet; thereby the formation of individual fibers is reduced.

1.4.2. Potential Applications of Electrospun Nanofibers

Electrospun nanofibers have been searched for use in various application areas. The major areas are health care, biotechnology and environmental engineering, defense and security, and energy storage and generation.

Electrospun fibers can be used in tissue/organ repair and regeneration, as vectors to deliver drugs and therapeutics, as biocompatible and biodegradable medical implant

devices, in medical diagnostics and instrumentation, as protective fabrics against environmental and infectious agents in hospitals and general surroundings, and in cosmetic and dental applications [74]. Especially nonwoven fabrics are used as scaffolds for tissue engineering applications [75]. Scaffold architecture can be designed to provide the mechanical properties to support cell growth, proliferation, differentiation and motility.

In biotechnology and environmental engineering applications, electrospun nanofibers become a promising material for membrane preparation if high porosity, interconnectivity, microscale interstitial space and a large surface-to-volume ratio are provided. The nanofiber membranes attach with ligand molecules, biomacromolecules, or cells in the purification of protein, the treatment of waste water, and chemical analysis [74, 76].

For military, firefighters and medical personnel, nanofiber membranes are fabricated as protective garments (i. e. facemasks) to protect chemical and biological risks [77].

In the energy generation applications, electrospun nanofiber membranes are well suited for polymer batteries [78], photovoltaic cells [79], and polymer membrane fuels cells (PMEFCs).

1.4.3. Polymer Scaffolds

Tissue engineering is an interdisciplinary field of engineering and life sciences. This promising scientific field provides a significant opportunity for many patients who are seeking organ transplant to replace their diseased organs. The tissue engineered organ is transplanted into the patient without the slightest risk of tissue rejection of foreign cells by the body [80]. In this approach, a new set of tools and techniques are emerging to restore, maintain and improve tissue functions. Polymer matrices play a central role to mimic the mechanical and biological properties of living cells and extracellular matrix in tissue engineering. These matrices can be used to achieve cell

delivery with high loading and efficiency to specific sites [81]. Levenberg *et al.* [82] also proved that scaffolds seeded with stem cells let local cell function adaptation by differentiation of stem cells. The scaffold depending on its design may act as a physical barrier to immune system components of host or act as a matrix to conduct tissue regeneration [83].

There are a few basic requirements that have been widely accepted for designing polymer scaffolds; a scaffold has to have high porosity, proper pore size, and a high specific surface area. Biodegradability is generally required, and must have the required mechanical integrity to maintain the pre-designed tissue structure. The scaffold should positively interact with cells, including enhanced cell adhesion, growth, migration, and differentiated function. The more proper method for the adequate space for the growth of the cells and, material and energy exchanges is to keep the pore size and pore surface area much bigger [84]. The high porosity of tissue scaffolds enables enough space for the cell accommodation and an easy passage for the nutrient intake and metabolic waste exchange [85]. The modulus of elasticity and strain at failure are the essential mechanical properties for the usage of electrospun nanofibers as tissue scaffolds [86].

Natural scaffolds like collagen, alginate and fibrin can be used to obtain the biological information they contain, or modified by enzymes [87]. Degradation of natural scaffolds occurs by enzymes in the matrix. However, these materials have some disadvantages like poor mechanical strength, immunogenicity and potential disease transmission [88]. Synthetic polymers have been synthesized in order to overcome these problems. Polylactide, poly(glycolic acid), and polycaprolactone are the most widely used materials as structural elements in the scaffolds. Both of these homopolymers and their block copolymers can be used in tissue engineering due to produce nontoxic degradation products. Moreover, these materials are designed to modify the surface in order to provide optimal cell-polymer interactions [89].

The method of electrospinning provides a new way to produce an ideal tissue engineering scaffold. With this method, various shapes of scaffolds can be constructed as controlling the fiber orientation, composition and dimensions. Also, the mechanical properties and the degradation rates of electrospun scaffoldings can be controlled with the characteristics of fibers. The scaffolds formed by the fibers under 200 nm show

substantial structural strength for ease of handling during scaffold sterilization, cell seeding, and transferring to subsequent culture environment [90]. Yashimoto *et al.* [91] electrospun PCL at 10 weight percent in chloroform for a bone tissue engineering application.

CHAPTER 2

2. EXPERIMENTAL

This work was divided into three main parts: the synthesis of fluorinated surfactants, the synthesis of fluorinated block copolymers and the synthesis of biodegradable nanofiber webs via electrospinning.

2.1. Materials

Dry CO_2 (99,5%) and Ar (99.99%) were received from Karbogaz. ε-Caprolactone monomer (ϵ-CL, MW = 114.14 g/mol, purity > 99%, Aldrich), L-lactide monomer (LLA, MW = 114.13 g/mol, purity > 98%, Purac) and the ring opening catalyst tin(II) ethyl hexanoate ($Sn(Oct)_2$, MW = 405.11 g/mol, purity > 97%, Sigma) were used as received. Fluorolinks were supplied by Solvay Chemicals. Methanol (CH_3OH, MW = 32.04 g/mol, purity > 99.9%), Tetrahydrofuran (THF, MW = 72.11 g/mol, purity > 99%, Aldrich), Dichloromethane (CH_2Cl_2, MW = 84.93 g/mol, purity > 99%), Chloroform ($CHCl_3$, MW = 119.38 g/mol, purity > 99.9%), and N,N-dimethyl formamide (DMF, MW = 73.09 g/mol, purity > 99.5%) were purchased from Merck. Dimethyl sulfoxide (DMSO, MW = 78.13 g/mol, purity > 99%) and Acetone (CH_3COCH_3, MW = 58.09 g/mol, purity > 99.8%) were purchased from LabKim. They were used as received.

The structures of ϵ-CL, LLA and fluorolinks are shown in Figure 2.1.

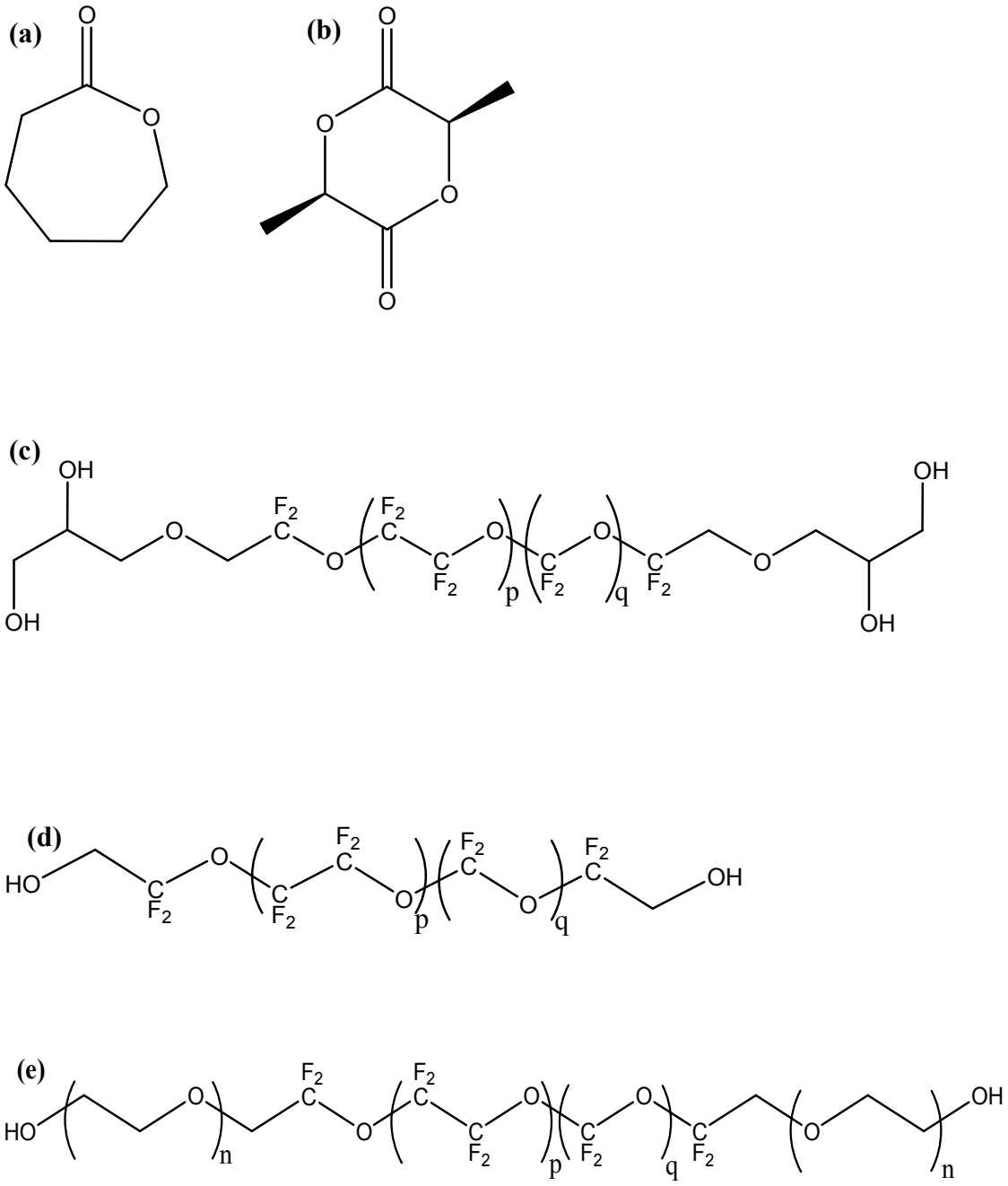

Figure 2.1. Structures of **(a)** ε-caprolactone **(b)** L-lactide **(c)** Fluorolink-T (FLK-T, MW = 2200 g/mol) **(d)** Fluorolink-D (FLK-D, MW = 2000 g/mol, p/q = 0.9) and **(e)** Fluorolink-E (FLK-E, MW = 2000 g/mol, n~1.5, 0.8≤p/q≤1.25)

2.2. Characterization

2.2.1. Nuclear Magnetic Resonance

Structural characterization of the materials was carried out with ^{1}H, ^{13}C and ^{19}F-NMR spectroscopy utilizing Unity Inova 500 spectrophotometer (Varian) and deuterated chloroform ($CDCl_3$) as a solvent.

2.2.2. Gel-Permeation Chromatography

Gel-permeation chromatography (GPC) analyses were performed with a Waters 410 differential refractometer, connected to a Waters 515 HPLC pump equipped with three Waters Ultrastyragel columns (HR series 4, 3, 2 narrow bore). Tetrahydrofuran running at a flow rate of 0.3 ml/min was utilized as an eluent. The molecular weights and the distribution of the polymers were calculated on the basis of a calibration curve recorded with monodisperse polystyrene standards.

2.2.3. Differantial Scanning Calorimetry

Thermal analysis of the materials was carried out by Differential Scanning Calorimetry (DSC, 204 Phoenix, Netzsch) at N_2/LN_2 atmosphere. Polymer samples of 10 mg were heated, quenched, and again heated, respectively in the range of -150°C to 400°C. Initial heating was carried out from 25 to 200°C at a heating rate of 10°C/min, and then rapid cooling to -150°C at 50°C/min, followed by a heating from -150 to 400°C again at a heating rate of 10°C/min was performed. Isothermal steps were included between the heating-cooling sequences, in order to ensure stabilization. The glass transition temperature (T_g) (from second heating) and the melting temperature (T_m) were

determined. The first heating was performed to eliminate the thermal history of the samples [92].

2.2.4. Scanning Electron Microscopy

Investigation of prepolymers', polymers' and fiber morphologies and fiber diameters was carried out with Scanning Electron Microscope (SEM) analyses (Supra 35VP Field Emission SEM, Leo). The samples were coated with gold and carbon under Ar atmosphere with an EMITECH K950X.

2.2.5. Optical Microscopy

Nikon Eclipse ME600 Optical Microscopy was used to measure the fiber diamers and investigate the fiber morphologies as well.

2.3. Reaction Set-up's

2.3.1. $ScCO_2$ Set-up

The schematic representation of $scCO_2$ set-up and the photos belonging to our set-up can be seen in Figure 2.2 and Figure 2.3. Block copolymer were synthesized in a 100-mL high pressure stainless-steel vessel (Thar) with a mechanical stirrer (Thar). The reactor is designed with two quartz windows to observe the reaction. P-50 High Pressure Pump Contrivance (Thar) was utilized to pump CO_2 through the columns. Heating was achieved by a heating band (Omega, FGS0041-006 model) and the temperature was controlled by a thermocouple adapted to the vessel (Omega, TJ-36 ICIN- 18U- 12 Model).

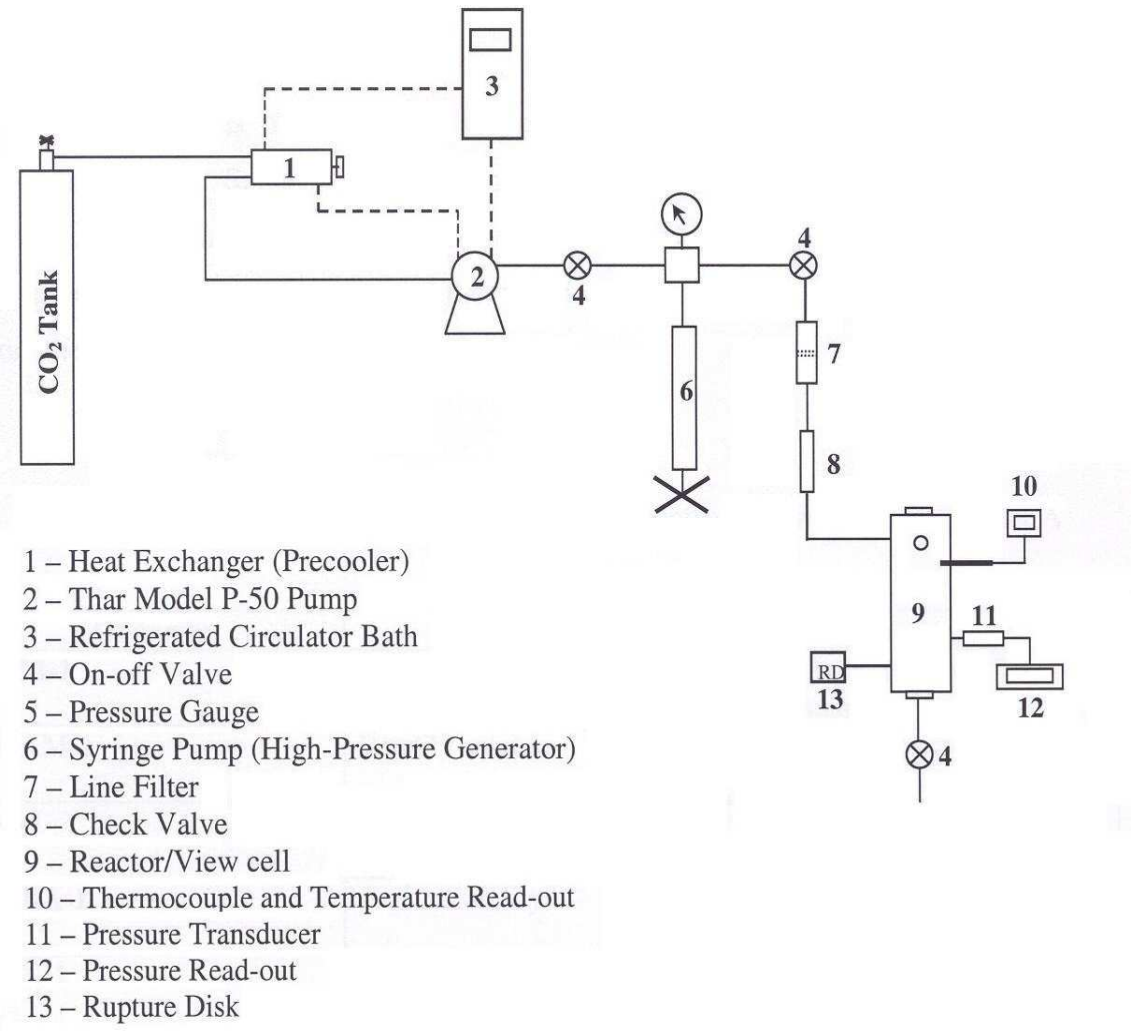

Figure 2.2. Schematic representation of $scCO_2$ set-up

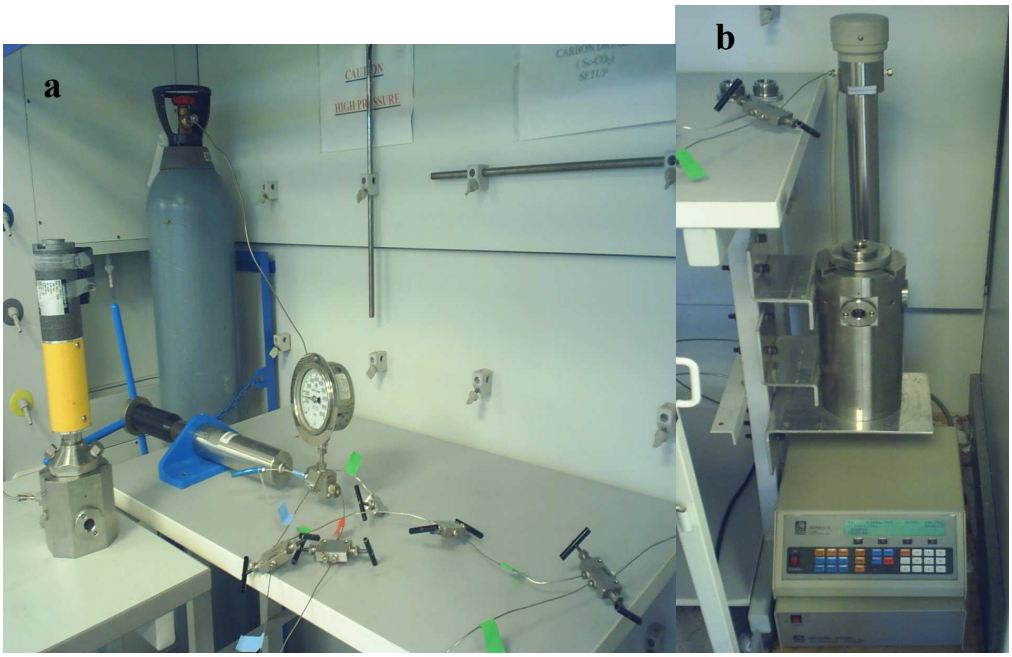

Figure 2.3. Photos of **(a)** $scCO_2$ set-up and **(b)** High Pressure Pump

2.3.2. Electrospinning Set-up

Electrospinning system (Figure 2.4) that was used in this study was a home made system consist of: (i) a high voltage power which can generate voltages of up to 30 kV (ii) a glass capillary in which a copper probe inserted (iii) a collector which is a grounded aluminum sheet.

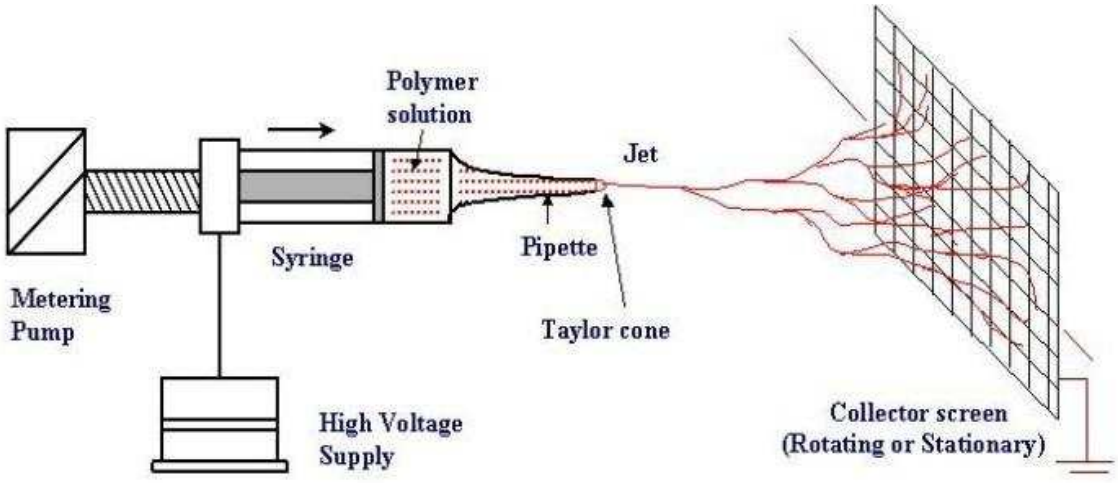

Figure 2.4. Schematic description of the electrospinning system.

2.4. Material Synthesis

2.4.1. Synthesis of reactive fluorinated stabilizers via Ring Opening Polymerization

Prepolymers were synthesized using different fluorolinks in bulk and the results were compared. Initially, branched type block copolymers were synthesized via using Fluorolink-T (FLK-T). Then, linear block copolymers were synthesized via using Fluorolink-D (FLK-D) and Fluorolink-E (FLK-E). Each fluorolink was used as an initiator and $Sn(Oct)_2$ was used as a catalyst. All reactions were carried out without using organic solvents.

For the synthesis of branched block copolymers, FLK-T (7.5 g) was reacted with ϵ-CL (16.6-mL, 1:40 FLK-T:ϵ-CL molar ratio) using $Sn(Oct)_2$ (0.8 ml) catalyst in a three-necked round bottom flask, equipped with a thermometer, condenser, and a magnetic stirring bar. Figure 2.5 displays the reaction mechanism of the prepolymer synthesis (PCL-FLKT-PCL). The flask containing the reactants was initially purged with Ar and then was immersed in an oil bath at 120^{o}C. The mixture was refluxed for 18 h. After reaction completion and cooling to room temperature, the mixture was gradually diluted with CH_2Cl_2. Continuous stirring was applied with a magnetic stirring bar during the precipitation, and then the mixture was poured into an excess of cold methanol. The prepolymer product was filtered off and collected through filtration, and then was dried at room temperature *in vacuo* for 3 d. The same procedure applied for the synthesis of prepolymers starting with FLK-D and FLK-E.

Two types of monomer were used for the synthesis of fluorinated prepolymers: ϵ-caprolactone and L-lactide. Table 2.1 gives the information about the characteristic properties of fluorolinks and also Table 2.2 shows the reaction conditions for each prepolymer synthesis.

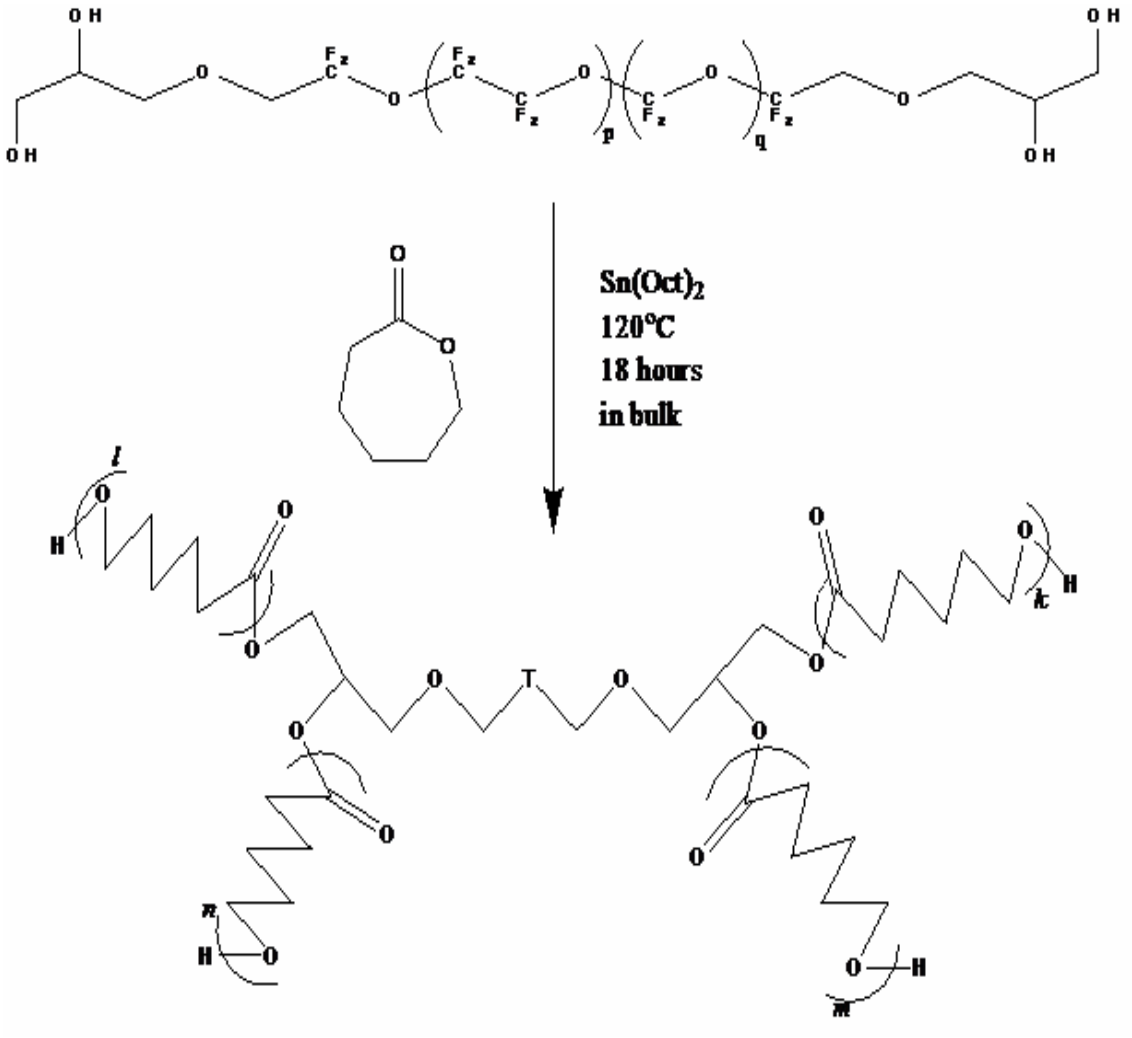

Figure 2.5. Reaction scheme for the synthesis of prepolymer PCL-FLKT-PCL

Fluorolinks	Properties	Molecular weight (g/mol)	Specific Gravity (g/ml)	Glass Transition (^{o}C)	Fluorine Content (%)
Fluorolink-T	Alcohol	2200	1.75	-85	58
Fluorolink-D	Alcohol	2000	1.81	-110	62
Fluorolink-E	Alcohol	2000	1.73	-110	58

Table 2.1. The characteristic properties of fluorolinks

Monomer	Fluorolink	Fluorolink /Monomer[a]	$SnOct_2$ (ml)	Temperature (^oC)	Reaction Time (hr)
ε-CL	FLK-T	1:40	0.800	120	8
ε-CL	FLK-D	1:20	0.400	120	8
ε-CL	FLK-E	1:20	0.400	120	8
ε-CL	1,4-Butanediol	1:20	0.177	120	8
LLA	FLK-T	1:40	0.056	130	8
LLA	FLK-D	1:20	0.056	130	8
LLA	FLK-E	1:20	0.056	130	8
LLA	1,4-Butanediol	1:20	0.056	130	8

[a] Fluorolink to monomer ratios were determined by calculating their mole numbers.

Table 2.2. The reaction conditions for each prepolymer synthesis

2.4.1.1. Solubility Tests

Before starting the reactions in $scCO_2$ media, behavior of the prepolymers in $scCO_2$ was examined through solubility tests. Prepolymer samples of 1.00 g were placed into a 100 ml fixed volume view cell equipped with two sapphire windows at a loading rate of 0.01 g/ml. Then the vessel was pressurized and the pressures and temperatures were adjusted, while a stirring rate of 100 rpm was applied. Samples from the vessel at different temperatures and pressures were collected by spraying onto glass substrates and reserved for morphology characterization. In this way, quenching was applied in order to lock a structure that is closest to the one in the vessel before emptying.

2.4.2. Synthesis of Fluorinated Block PLLA/PCL Copolymers

Polymerizations held in $scCO_2$ were performed by adjusting the pressure in a 100-mL high-pressure stainless-steel vessel with a mechanical stirrer. Three types of prepolymers were synthesized to produce block copolymers in $scCO_2$ media. Most of the experiments were conducted by using the branched type prepolymer. The reaction scheme for the branched copolymer synthesis is illustrated in Figure 2.6. The prepolymer (PCL-FLKT-PCL) used as an macroinitiator was reacted with LLA monomer using $SnOct_2$ catalyst (1:8, $SnOct_2$:LLA) at 75^{o}C for 1 d (24 h). High catalyst ratio was preferred due to the highest conversion in $scCO_2$ media and pressure was tried to keep constant for each reaction. The stirring rate was adjusted during reactions. After the reaction was completed, the heater was turned off and the autoclave was allowed to cool to room temperature while stirring. The product was then collected from the reaction vessel and yield and conversion were determined by gravimetric and ^{1}H NMR measurements. The determined yields are not exact, because not all the products could be recovered from the reactor. For the purification process, the polymer samples were dissolved in CH_2Cl_2 and precipitated into an excess of cold methanol. The polymer product was filtered off, and dried at room temperature *in vacuo* for 3 d. A set of reactions were carried out by changing monomer concentration to control the chain length of PLLA and PCL (Table 2.3). Catalyst to monomer ratios are calculated by weight percentage as 1:8 except experiment 6 in which the ratio is 1:80.

Run	Prepolymer	L-Lactide/ Prepolymer[a]	Pressure (psi)	Temp. (^{o}C)	Stirring Rate (rpm)	Yield (%)
1	PCL-FLKD-PCL	1:3	2500	80	30	ND
2	PCL-FLKD-PCL	1:3	5000	80	30	ND
3	PCL-FLKE-PCL	1:3	2500	80	30	69
4	PCL-FLKT-PCL	1.45:1	4500	75	30	65
5	PCL-FLKT-PCL	1.45:1	4000	75	60	64
6	PCL-FLKT-PCL	1.45:1	4300	75	30	71
7	PCL-FLKT-PCL	3:1	4300	75	60	50
8	PCL-FLKT-PCL	0.35:1	4500	75	60	72
9	PCL-FLKT-PCL	1.45:1	4500	75	60	60

ND: Not Detected

[a] L-lactide to prepolymer ratios were determined with their molar ratios.

Table 2.3. Reaction conditions for the synthesis of fluorinated block copolymers in $scCO_2$

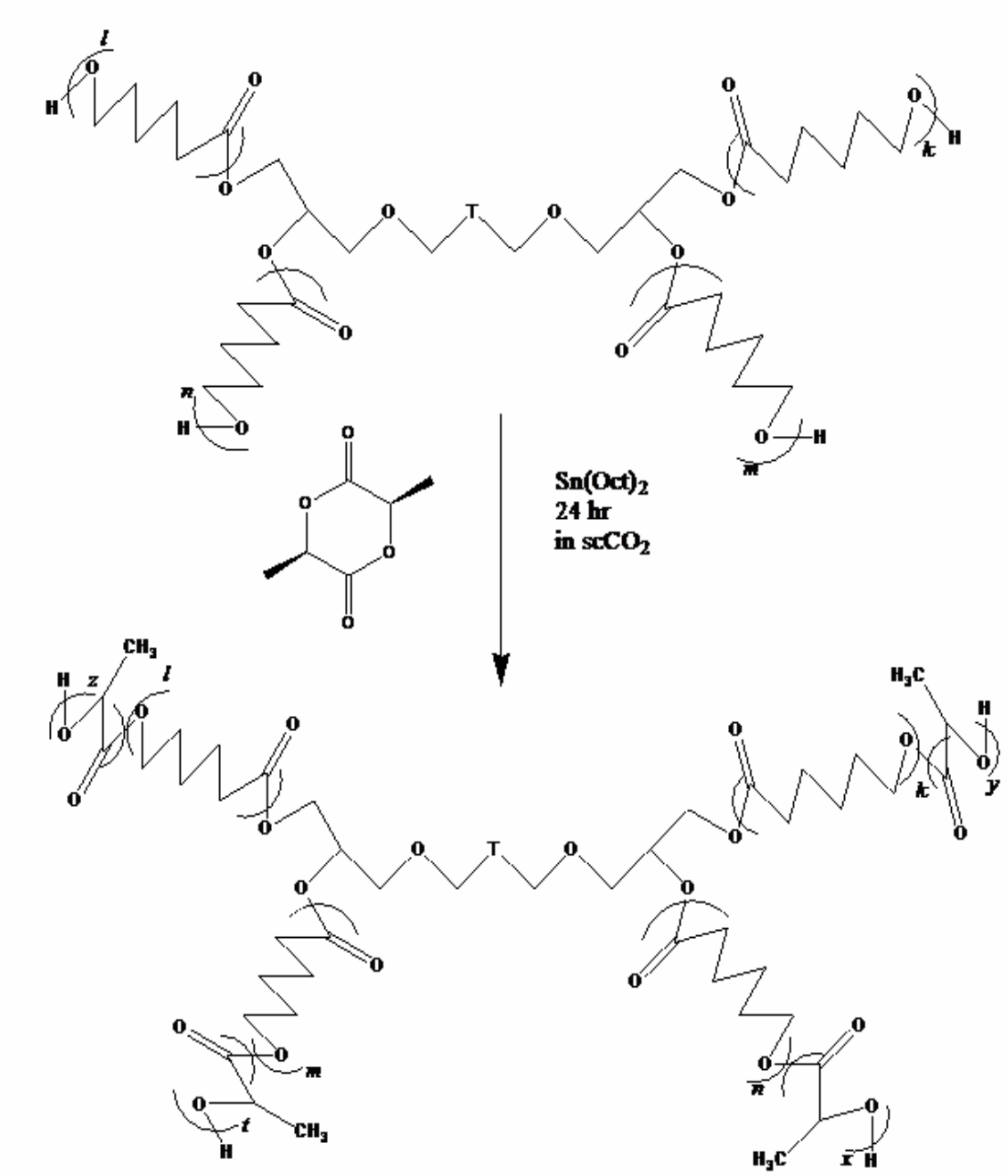

Figure 2.6. Reaction scheme for the synthesis of branched pentablock copolymer

Pentablock copolymers were also synthesized using each fluorinated stabilizer as an macroinitiator in bulk. Experiments with different ratios of monomer and prepolymer were studied to obtain high molecular weight polymers. For the synthesis of linear block copolymer, fluorinated prepolymer (PCL-FLKD-PCL, 1 gr) was reacted with ε-CL (5 gr) by using $SnOct_2$ (1:100, catalyst:monomer) without using solvent at 140°C for 18 hr. Also, this experiment was repeated without catalyst to observe the effect of catalyst on molecular weight. Several experiments listed in Table 2.4 were performed to obtain high molecular weight.

Run	Prepolymer	Monomer	Prepolymer/ Monomer[a]	Catalyst/ Monomer[b]
1	PCL-FLKD-PCL	LLA	1:1	No catalyst
2	PCL-FLKD-PCL	LLA	1:1	1:8
3	PCL-FLKE-PCL	LLA	1:2	1:1000
4	PCL-FLKT-PCL	LLA	1:2	1:1000
5	PLLA-FLKD-PLLA	ε-CL	1:5	1:100
6	PCL-FLKD-PCL	LLA	1:3	1:100

Each reaction was performed at 140°C and reaction time is 18 hr.

[a] The ratio of prepolymer and monomer was calculated by weight percentage.

[b] Catalyst to monomer ratios were determined with their molar ratios.

Table 2.4. The reaction conditions for the synthesis of fluorinated block copolymers in bulk

2.4.3. Preparation of Biodegradable Nanofiber Webs via electrospinning

The fluorinated pentablock copolymers in mixtures of methanol (CH_3OH) and N,N-dimethyl formamide (DMF) were processed into nanofibers by electrospinning. The polymer concentration in solvent (20-50 gr /100 ml), DMF volume percentage in the solvent mixture (0-100%), the applied voltage (10-25 kV) and the capillary tip-collector distance (5-20 cm) were changed in the process of electrospinning.

The polymer solutions were prepared with the polymer:solvent ratio of 1:2, 1:2.5 and 1:3 (w/w) using solvents as 100% DMF or 50% CH_3OH + 50% DMF composition. During the electrospinning process, the prepared polymer solution was placed in the glass capillary. The copper probe of the voltage generator was inserted into the capillary. The grounded aluminum sheet was positioned opposite to the tip of the capillary. The electrical field was applied and electricity was conducted through the solution. The output voltage between the copper probe and the grounded aluminum sheet was adjusted in the range between 10-25 kV and the distance between the capillary tip and the grounded aluminum sheet was measured from 5 to 20 cm for each experiment. The solution was ejected from the capillary tip towards the grounded collector. During the ejection of the polymer solution towards the collector, the solvent evaporated and the polymer fibers were deposited on the collector in the form of non-woven fabric.

CHAPTER 3

3. RESULTS AND DISCUSSION

3.1. Synthesis of Reactive Fluorinated Stabilizers via Ring Opening Polymerization

A commonly accepted mechanism of ring opening entails the activation of the ester-carbonyl of the cyclic monomer with an inorganic or organic catalyst such as stannous octate, stannous chloride and diethyl or dibutyl zinc [93]. Especially, $Sn(Oct)_2$ is a suitable catalyst for biomedical applications, since it has very low toxicity compared to other initiators and is approved for in vivo use by the US Food and Drug Administration (FDA) [94]. A ring opening reaction can occur to produce linear polyesters with a hydroxyl end group in the presence of a hydroxyl-bearing compound in the vicinity of the activated carbonyl group. Block copolymers of PCL and PLLA were synthesized by sequential ROP.

In the present study, the prepolymers prepared in bulk were previously obtained by similar procedures carried out by Howdle *et al* [95] and by Pilati *et al* [96]. Pilati *et al* had shown that the fluorinated alcohols are able to efficiently initiate the polymerization of ε-CL, and the PCL blocks grow on the terminal groups. The utilized alcohols are FLK-D, FLK-E and FLK-T. The reactions with FLK-D and FLK-E proceed from two ends leading to the formation of linear polymers, whereas, the one with FLK-T proceeds from four ends, leading to the formation of a branched prepolymer structure with PCL or PLLA side chains. The stabilizers are white-powder. The analyses such as NMR,

GPC, DSC and SEM were carried out in order to characterize the products. After being sure that the analyses results supported the successful polymerization, the solubility of these stabilizers was examined in $scCO_2$.

3.1.1. Structure Characterization

Nuclear Magnetic Resonance spectroscopy is a powerful and complex analytical tool. Nuclear magnetic resonance spectroscopy, commonly referred to as NMR, has become the widely used technique for determining the structure of organic compounds [97]. In this work, the molecular structures and chemical compositions of prepolymers were determined by ^{1}H, ^{13}C, and ^{19}F-NMR. The NMR characterizations for all reactions were evident that the hydroxyl end groups of fluorolinks had reacted with lactones as ϵ-CL and LLA. NMR spectra of the polymers recorded in $CDCl_3$.

3.1.1.1. Linear Polymers

^{1}H NMR spectra are fully representative that the reactions occurred successfully. For the linear triblock copolymer including FLK-D, repeating units of PCL were calculated as 40 from the signal integral ratio of α-methylene protons of PCL and terminal methylene protons of FLK-D from ^{1}H-NMR (Figure 3.1.a). The same integration was done for prepolymer synthesized via FLK-E and repeating units of PCL were calculated as 20 from figure 3.2.a. The characteristic proton peaks for PCL-FLKD-PCL in ^{1}H-NMR (recorded in $CDCl_3$) are δ 1.4 ppm ($-CH_2-\underline{CH_2}-CH_2-$), δ 1.65 ppm ($-O-CH_2-\underline{CH_2}-CH_2$), δ 2.3 ppm ($-CH_2-CO-$), δ 4.05 ppm ($-O-CH_2$), and δ 4.45 ppm ($-O-CH_2-CF_2$) (Figure 3.1.a). The proton peaks belonging to polycaprolactone in the other two prepolymers observed in the expected ranges similar to the peaks of PCL-FLKD-PCL (Figure 3.2.a and Figure 3.3.a).

^{13}C-NMR spectra were also support the polymerization (Figure 3.1.b and 3.2.b). However, in ^{13}C-NMR, only the PCL portion of the stabilizer is visible because carbons in fluorolinks have much longer relaxation times [98]. Characteristic carbon peaks on

the PCL block are δ 25 ppm (-CH_2-$\underline{CH_2}$-CH_2-CO-), δ 26 ppm (O-CH_2-$\underline{CH_2}$-CH_2), δ 29 ppm (-CH_2-$\underline{CH_2}$-CH_2-), δ 34 ppm (-$\underline{CH_2}$-CO-), δ 64 ppm (-$\underline{CH_2}$-O-), and δ 174 ppm (-CO-).

^{19}F-NMR analyses were also utilized to confirm fluorinated segments. The peaks belonging to fluorolink were similar to the assignment of Karis *et al* [99]. The characteristic flor peaks for FLK-D in order are δ -80 ppm (-CH_2-CF_2-O-), δ -92 ppm (O-$\underline{CF_2}$-CF_2-O-), δ -94 ppm (O-CF_2-$\underline{CF_2}$-O-), δ -54 ppm (-O-CF_2-O-) and δ -82.5 ppm (O-CF_2-CH_2-) (see Figure 2.1.d for the structure of FLK-D). The flor peaks for FLK-E are δ -80.5 ppm (-CH_2-CF_2-O-), δ -92 ppm (O-$\underline{CF_2}$-CF_2-O-), δ -93.5 ppm (O-CF_2-$\underline{CF_2}$-O-), δ -56 ppm (-O-CF_2-O-) and δ -83 ppm (O-CF_2-CH_2-) (see Figure 2.1.e for the structure of FLK-E).

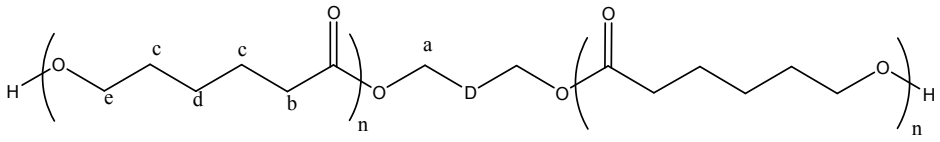

(a)

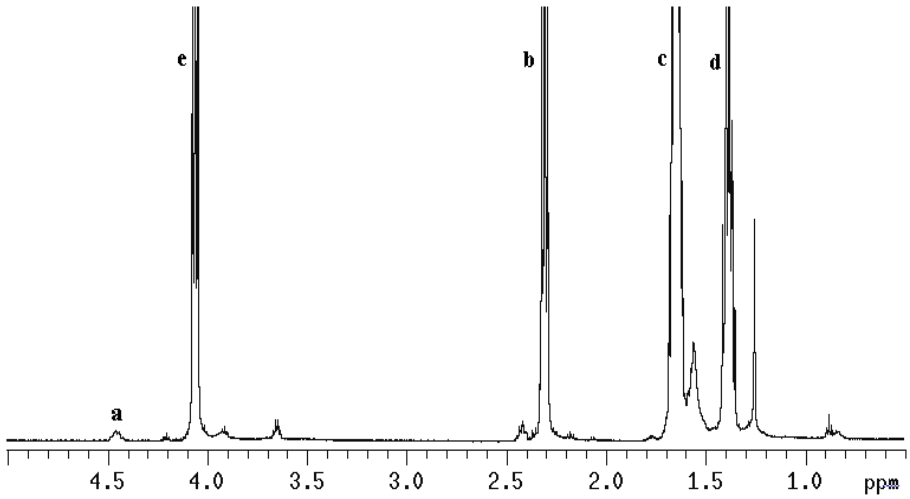

(b)

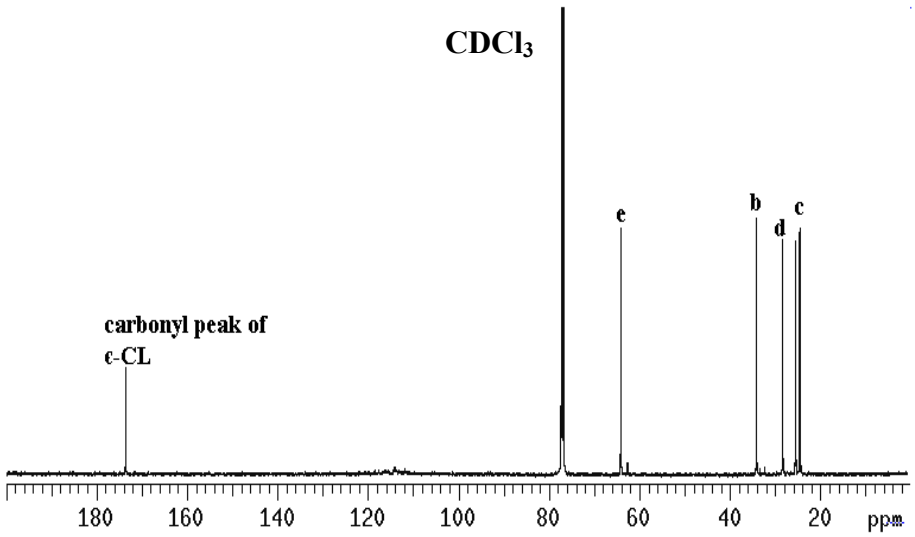

Figure 3.1. (a) ^{1}H-NMR and **(b)** ^{13}C-NMR of prepolymer PCL-FLKD-PCL recorded in $CDCl_3$.

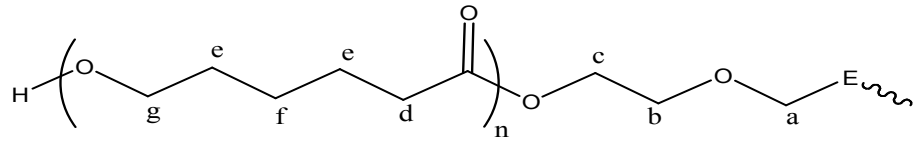

(a)

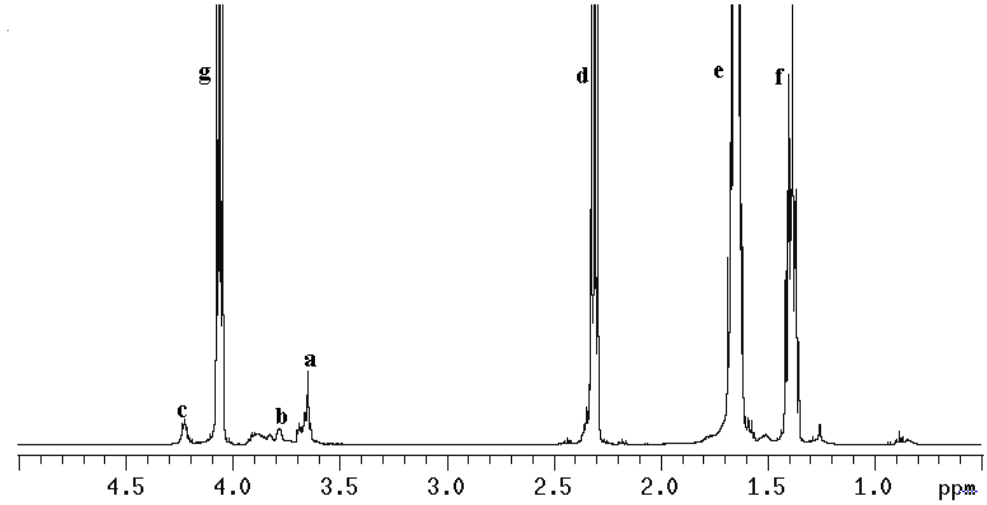

(b)

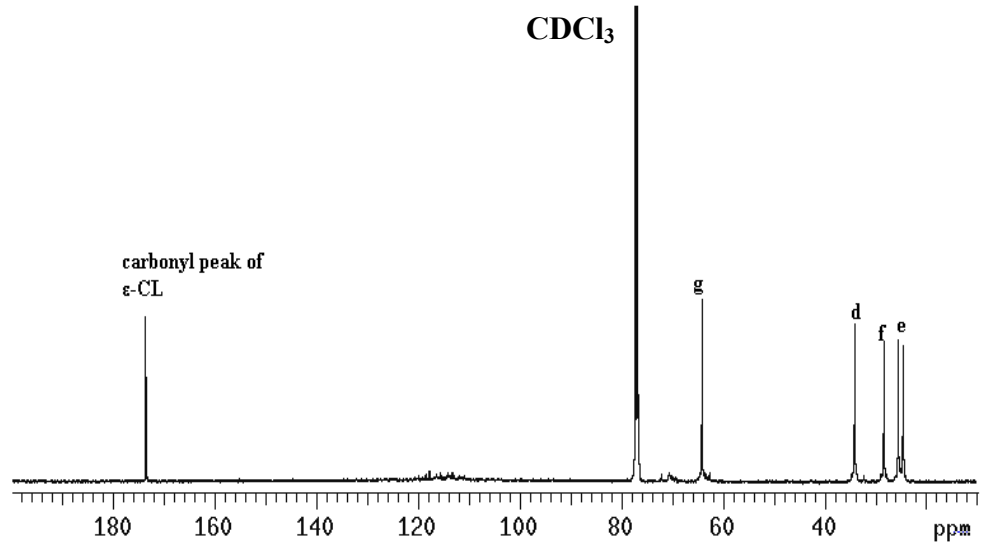

Figure 3.2. (a) ^{1}H-NMR and **(b)** ^{13}C-NMR of prepolymer PCL-FLKE-PCL recorded in $CDCl_3$.

3.1.1.2. Branched Polymers

The ^{1}H-NMR representative of prepolymer synthesized in bulk is illustrated in figure 3.3.a. The PCL repeating units were calculated as 180 from the signal integral ratio of the terminal methylene protons of FLK-T and α-methylene protons of PCL. The ^{13}C-NMR of the prepolymer is illustrated in figure 3.3.b, with the designed groups of carbons. In ^{13}C-NMR spectrum, only PCL portion of the stabilizer is visible due to the longer relaxation time of the carbons on the Fluorolink-T [98]. ^{19}F-NMR analysis was also utilized to confirm fluorinated segments. The peaks belonging to FLK-T were again similar to the assignment of Karis *et al* (δ -83 ppm (-CH_2-CF_2-O-), δ -92 ppm (O-$\underline{CF_2}$-CF_2-O-), δ -93.5 ppm (O-CF_2-$\underline{CF_2}$-O-), δ -56.5 ppm (-O-CF_2-O-) and δ -81 ppm (O-CF_2-CH_2-)) (see Figure 2.1.c for the structure of FLK-T) [99].

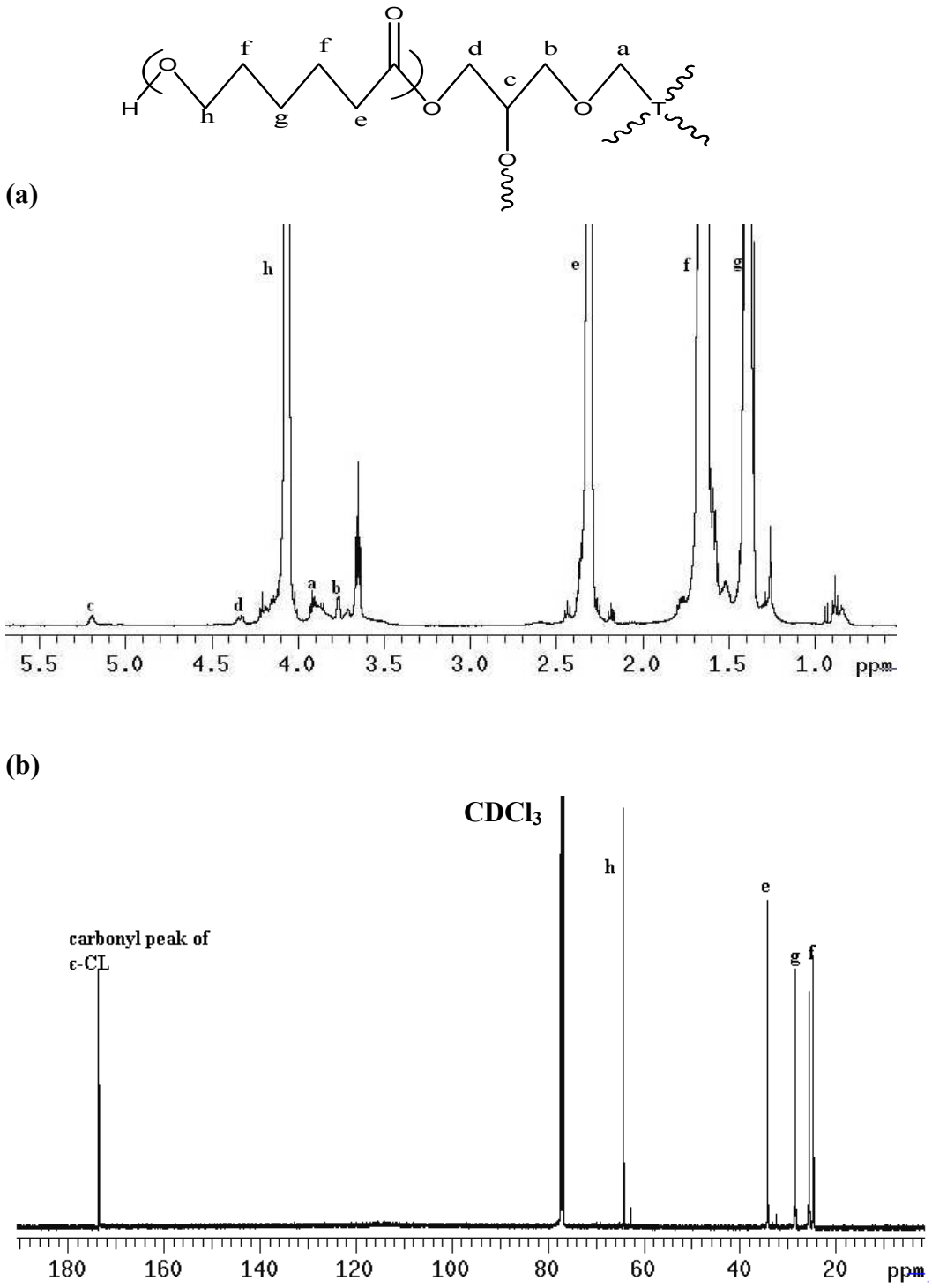

Figure 3.3. (a) ^{1}H-NMR and **(b)** ^{13}C-NMR of prepolymer PCL-FLKT-PCL recorded in $CDCl_3$. Only the PCL portion of the stabilizer is visible in ^{13}C-NMR spectrum.

3.1.2. GPC Results

The molecular weight (M_w), the number average molecular weight (M_n), and polydispersity index (PDI) were calculated from GPC. PDI was estimated against monodisperse polystyrene standards. The PDI values of the stabilizers are low (Table 3.1), that is, the propagation was controlled. In addition, M_n values were also calculated from NMR. To illustrate, M_n was found for PCL-FLKT-PCL prepolymer as 21,000 g/mol, where the GPC analysis gave M_n of 13,000 g/mol. Variations between M_n calculated from NMR and M_n measured by GPC are expected, since GPC results are calculated from the average of several data collected on number of measurements and include errors based on operator and on change in conditions during operation. On the other hand, NMR calculations are not informative of the distribution of various chains that have a M_n values showing deviations from the average. The PDI value of this polymer is 1.34 and M_w was found as 18,000 g/mol from the GPC analysis.

Prepolymer	Mn[a]	PDI[a]	Conv. of ε-CL(%)[b]	FLK:ε-CL[b]	*Tg* (°C)[c]	T*m*(°C)[c]
PCL-FLKD-PCL	13000	1.27	100	1:40	-62.7	56.9
PCL-FLKE-PCL	13900	1.22	100	1:20	-62.4	50.5
PCL-FLKT-PCL	15500	1.34	99	1:200	-68.4	54.9

[a] Mw, Mn and PDI values were measured by GPC.

[b] Conversion and the ratio between fluorolink (FLK) and polycaprolactone (PCL) were calculated from ^{1}H-NMR

[c] T_g and T_m were determined by DSC.

Table 3.1. GPC, NMR and DSC results of the prepolymers

3.1.3. Thermal Anaylses

The thermal analysis of the product supported triblock formation. From the second endotherm of the DSC analysis, the glass transition temperature (T_g) of each stabilizer was measured. T_g's for PCL-FLKD-PCL, PCL-FLKE-PCL, and PCL-FLKT-PCL are -62.7, -62.4 and -68.4^{o}C (Table 3.1). FLK-D, FLK-E and FLK-T display T_g's at -110, -110 and -85^{o}C. PCL display a typical T_g at -60^{o}C. The presence of fluorinated block has an effect of lowering the T_g [100, 101], however the low amount of the fluorinated segment compared to PCL segments (FLK-D:PCL = 1:40, FLK-E:PCL = 1:20, FLK-T: PCL = 1:180, from the ^{1}H-NMR analyses) results in a slight decrease of the T_g of the material.

3.1.4. Solubility Tests in $ScCO_2$

The solubilities of the reactive stabilizers in $scCO_2$ were investigated prior to copolymer synthesis in order to evaluate its stabilizing effectiveness in the given polymerization temperature and pressure. After the stabilizer was placed into the vessel at 1% loading by weight, the autoclave was pressurized at different temperatures. With the help of the windows of the reactor, the behaviors of these materials are observed. For more evidence of solubilities of the stabilizers, the photos were taken while miscible and immiscible (Figure 3.4a and 3.4b).

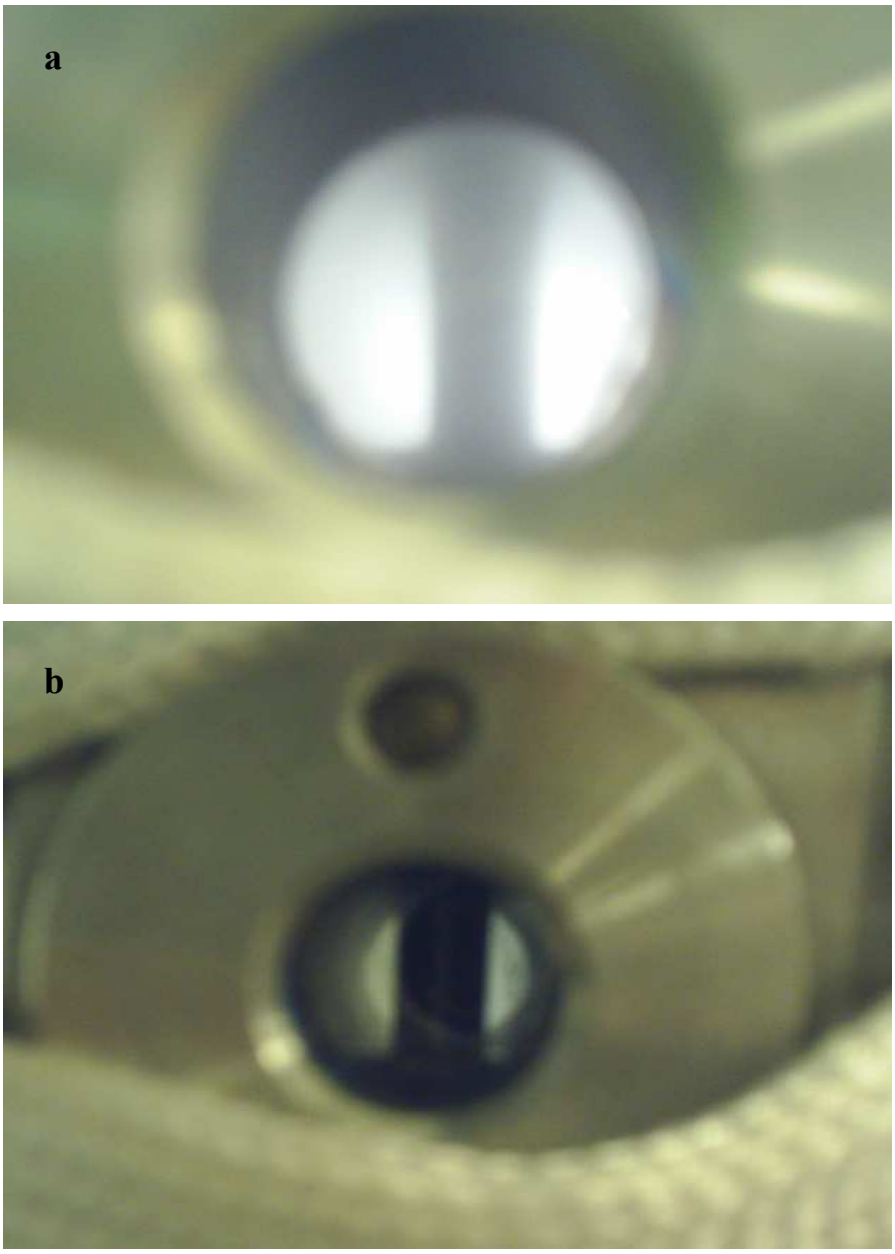

Figure 3.4. Prepolymer PCL-FLKD-PCL **(a)** immiscible at 1500 psi and room temperature **(b)** miscible at 2500 psi and 35^{o}C.

For the branched stabilizer (PCL-FLKT-PCL), the autoclave was pressurized up to 1200 psi at 17^{o}C (this temperature was detected by thermocouple before heating, and is lower from room temperature due to the $scCO_2$ entering the system). At this point, CO_2 started to diffuse into the reactor and the prepolymer dispersed with CO_2 by stirring. Gradual increase in pressure by heating the vessel was provided and at 1800 psi and 25^{o}C, the material started to form a cloudy mixture. This phase change stems from the segregation behavior of block copolymers. In the intermediate and strong segregation regimes, chain conformation takes place; therefore the interfacial energy changes affect the conformational entropy and the strength of the chains, leading to micelle formation in $scCO_2$ [102]. Over pressures of 4000 psi and 75^{o}C -the polymerization pressure and temperature- the material was effectively solubilized in $scCO_2$. All these observations were seen from the view windows of reactor.

Figure 3.5 displayed the morphology of PCL-FLKT-PCL stabilizer before loading to the CO_2 reactor, so that the differences can be distinguished easily by comparing the images after solubilization in CO_2. The solubility behavior of this stabilizer is represented in the SEM micrographs in figure 3.6.a, 3.6.b, and 3.6.c and in figure 3.7.a, 3.7.b, and 3.7.c. In figure 3.6a, the pressure and the temperature are 1200 psi at 17^{o}C, respectively and discrete particles can be seen clearly. This shows that CO_2 did not diffuse into of the polymer sample completely. When pressure and temperature are increased to 1800 psi and 25^{o}C, the material started to solubilize in $scCO_2$ (figure 3.6.b). The disappearing of the discrete particles and the sticky appearance accounts for the plasticization effect of $scCO_2$, which is typical especially to amorphous polymers. Similar observation was also stated by Howdle et al [95]. At higher temperature and pressure (4000 psi and 60^{o}C), the material was sparingly soluble and fibrous-like morphology is observed with an increased plasticization effect (figure 3.6.c).

Pressure effect on the solubility of the stabilizers was also investigated. In these experiments, temperature is held constant at 25^{o}C and pressure is gradually increased from 1200 psi to 3000 psi (figure 3.7.a), to 3500 psi (figure 3.7.b) and then to 4500 psi (figure 3.8.c) to observe the effect of temperature on the morphologies comparing the images at different temperatures. At 1200 psi, prepolymer displayed solution-cast like formation on the surface of glass substrate, which is evidence for complete dissolution at this pressure. There are no distinct differences in the morphologies observed, when

pressure is increased from 3000 psi to 3500 psi and both images have sticky structure. At 4500 psi, the polymer becomes more branched and discrete fibrils are observed. Therefore, the changes of the morphologies can be seen more clearly increasing temperature while pressurizing.

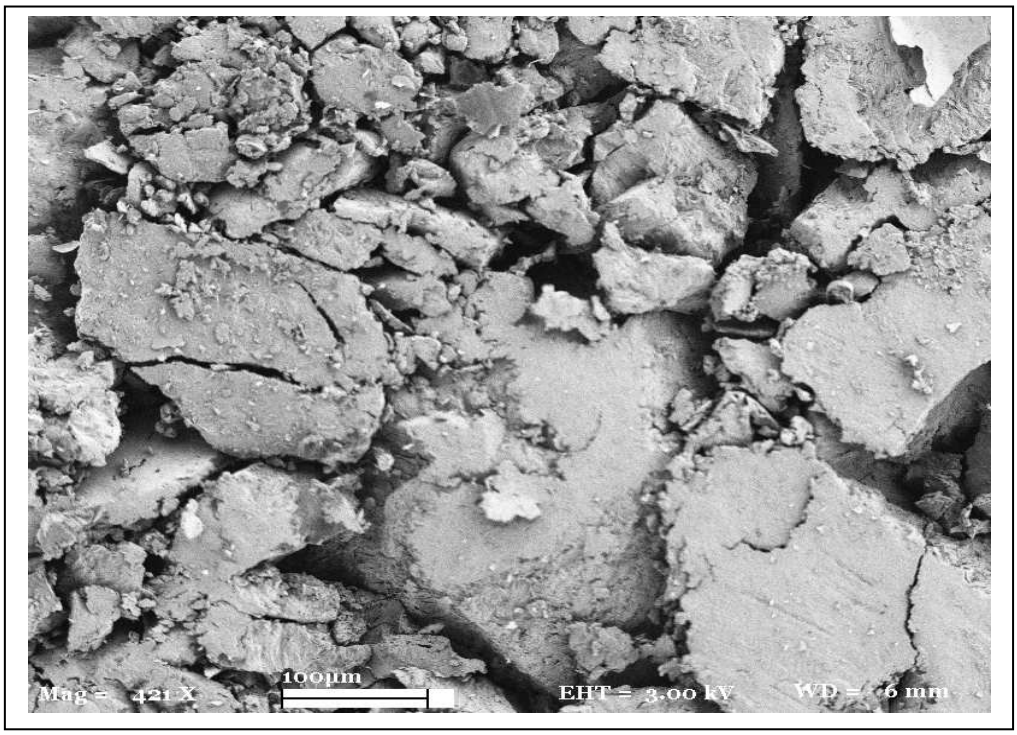

Figure 3.5. SEM image of prepolymer PCL-FLKT-PCL before loading into CO_2.

(a)

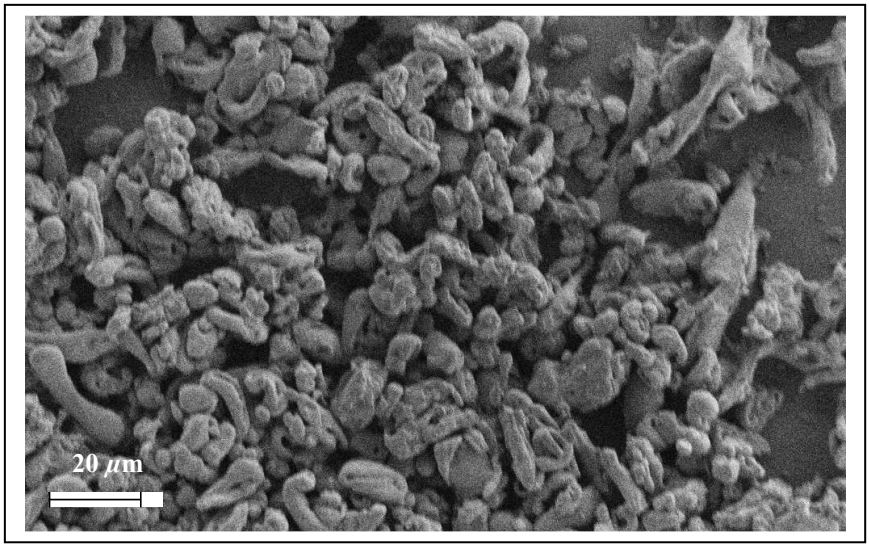

(b)

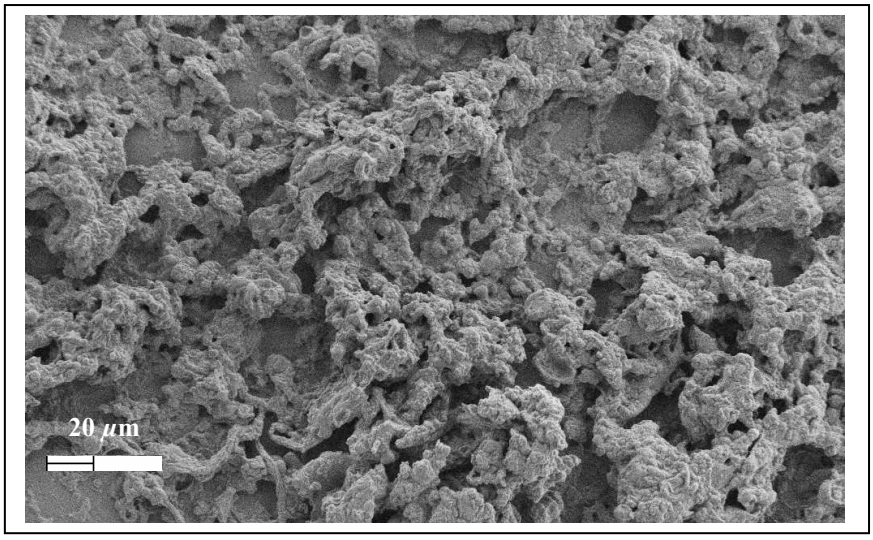

(c)

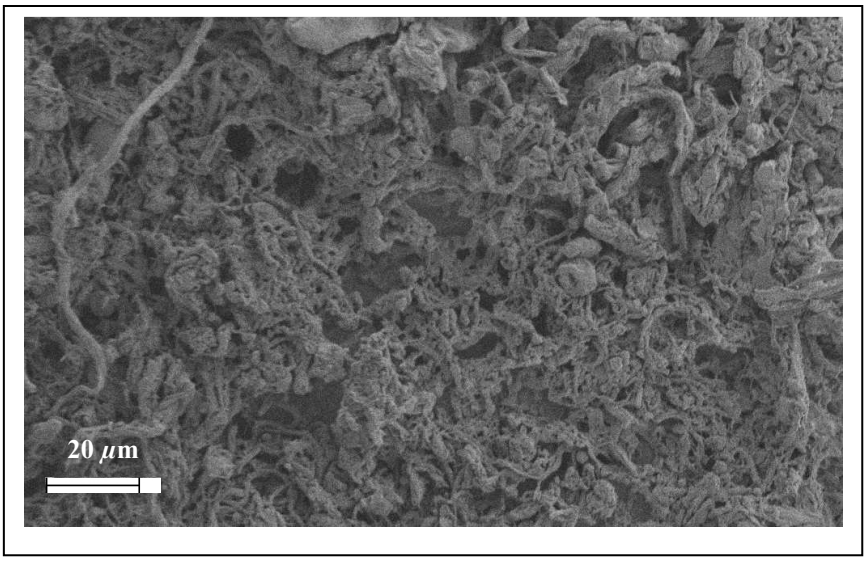

Figure 3.6. SEM micrographs of prepolymer PCL-FLKT-PCL at **(a)** 1200 psi and 17°C **(b)** 2000 psi and 25°C, and **(c)** 4000 psi and 60°C.

(a)

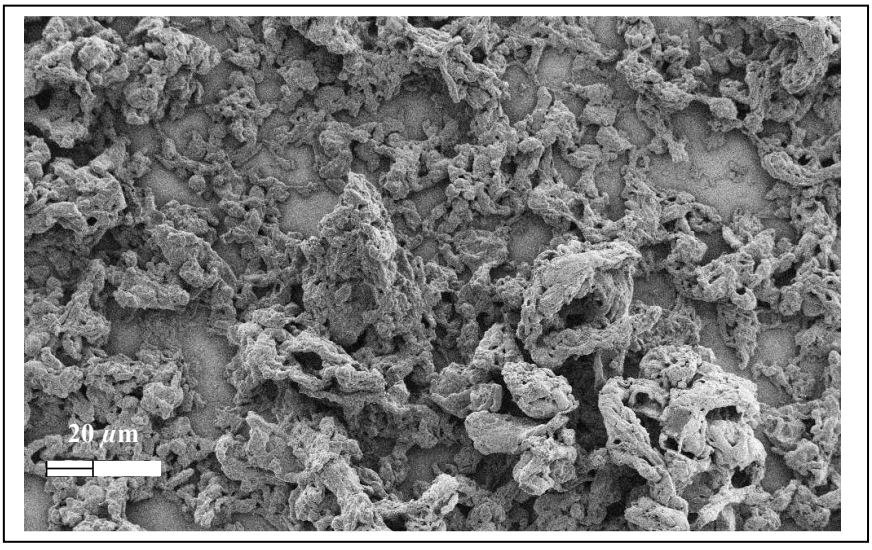

(b)

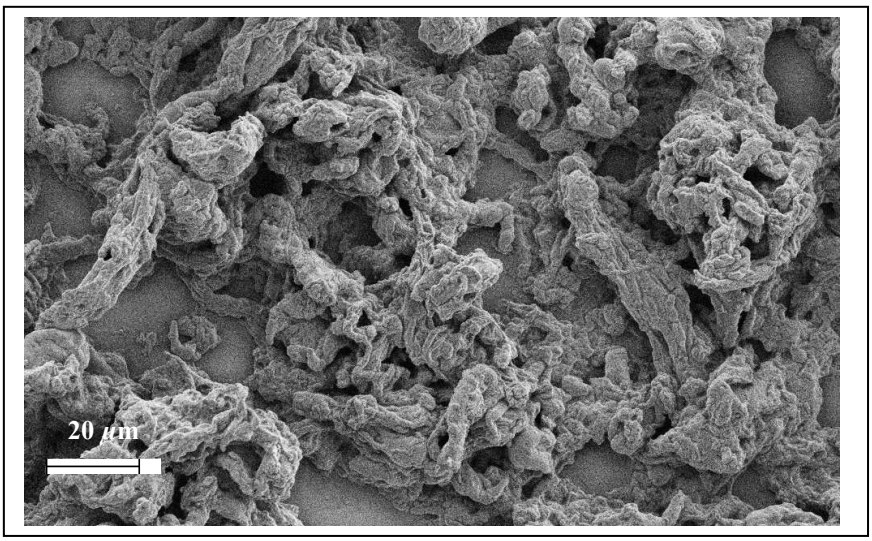

(c)

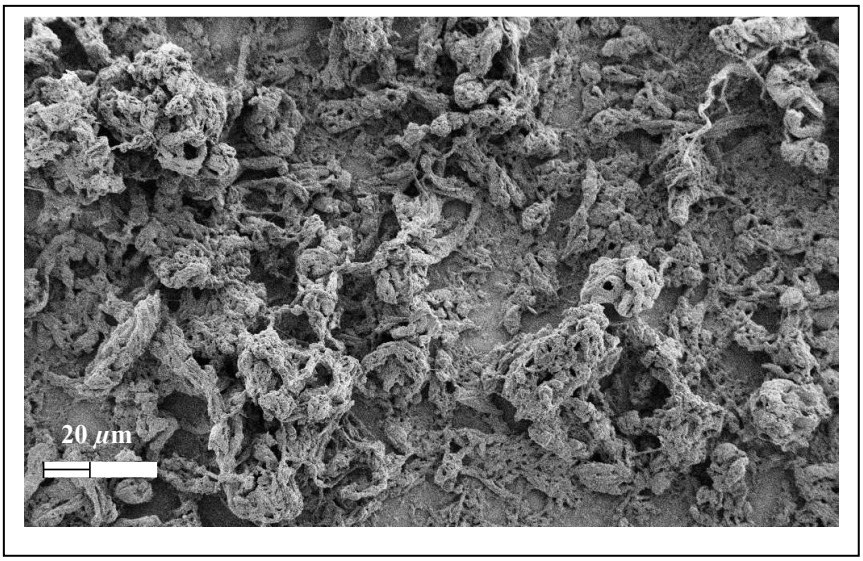

Figure 3.7. SEM micrographs of prepolymer PCL-FLKT-PCL at room temperature with pressure variation **(a)** 3000 psi **(b)** 3500 psi and **(c)** 4500 psi.

In Table 3.2, the pressure and temperature values of the stabilizers that start to become soluble in $scCO_2$ are given so that this information will be important while determining the reaction conditions for fluorinated pentablock PLLA/PCL copolymer synthesis in $scCO_2$ media.

Prepolymer	Pressure (psi)	Temperature (^oC)
PCL-FLKD-PCL	2500	35
PCL-FLKE-PCL	3500	60
PCL-FLKT-PCL	3000	50

Table 3.2. Pressure and temperature values of prepolymers that start to become soluble in $scCO_2$.

Solubility is governed by polymer-polymer interactions and polymer-CO_2 interactions. The solubility of the polymers in $scCO_2$ can be expressed by Gibbs Free Energy (G) or Helmholtz Free Energy (A). Temperature and pressure increases enhance the solubility and this indicates that the entropy effect is dominant factor. The phase behaviors of surfactants were investigated in constant-volume view cell by controlling temperature and P so that Helmholtz free energy was dominant (see Figure 3.8).

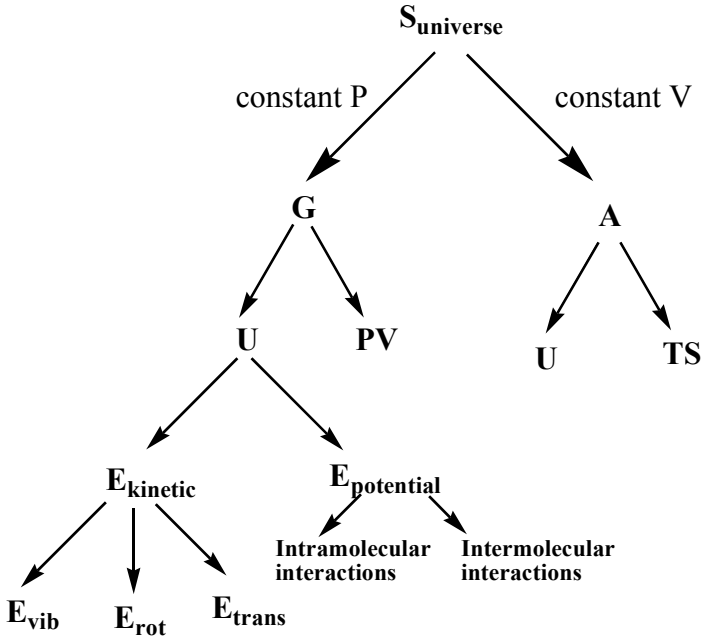

Figure 3.8. Schematic representation of thermodynamic terms

3.2. Synthesis of Fluorinated Block PLLA/PCL Copolymers

Copolymers of PCL and PLLA play a special role in drug delivery systems and the properties of these materials can be adjusted according to the relative copolymer composition [58, 59]. Adjustment of the properties can be also carried out by incorporating branching into the structure to further increase the degradability of the copolymers by decreasing the crystallinity and increasing the terminal groups in the structure [103, 104]. Because of this reason, most of the experiments in $scCO_2$ were concentrated on branched type polymers.

In this part, pentablock copolymers were synthesized using fluorinated stabilizers in $scCO_2$ media and in bulk.

3.2.1. Polymerizations in $ScCO_2$

In biomedical applications, another important criterion besides polymer properties is the product purity, since residues of monomer and solvent may pose significant problems [105]. Supercritical carbon dioxide ($scCO_2$) has attracted great interest as an alternative solvent in the area of polymer synthesis, as a result of such considerations [106].

Relatively little work concerning ROPs in $scCO_2$ has been performed, for these studies are generally concentrated on the homopolymers of ε-caprolactone (ε-CL) [107, 108] and L-lactide (LLA) [95] alone, and work reported on copolymer synthesis in $scCO_2$ is mainly limited to D,L-lactide and glycolide copolymers [109, 110]. Best to our knowledge, there is only one work concerning the copolymerization of ε-CL and LLA in $scCO_2$, being random copolymerization [111]. Especially, utilization of fluorocarbon surfactants as reactive stabilizers for the synthesis of PLLA/PCL copolymers in a non-

solvent, "clean" medium, and correspondingly combining the properties of both the monomers and the stabilizer is still open to investigation.

It is also important for the reactions in $scCO_2$ to choose the soluble materials. Fluoropolymers [5] are one of the few classes readily soluble in CO_2 even at high molecular weight.

The corresponding results for the sequences of polymerization reactions are listed in Table 3.3, respectively.

Run	Mn[a]	Mw[a]	PDI[a]	LLA:ε-CL[b]	Tg (^oC)[c]	Tm(^oC)[c]
1	13200	16400	1.24	1:10	-60.6	55.5
2	14100	16800	1.19	1:20	-61.5	45.5
3	15300	18200	1.19	1:9	-37.5	27.7
4	12100	14000	1.16	1:6	-44.8	53.9
5	18800	22300	1.18	1:4	-38.3	56.5
6	20200	23700	1.17	1:7	-63.3	49.1
7	23400	25200	1.08	3:1	-34.3	43.3
8	13400	17900	1.34	1:3	-38.5	50.9
9	14200	17000	1.20	1:3	-49.3	47.3

[a] Mn, Mw and PDI were recorded by Gel Permeation Chromatography with PS standards.

[b] Ratio of LLA and ε-CL was calculated from ^{1}H-NMR and also confirmed by ^{13}C-NMR.

[c] T_g and T_m were determined by DSC.

Table 3.3. Characterization results of linear and branched pentablock polymers synthesized in $scCO_2$.

3.2.1.1. Structure Characterization

Three types of block copolymers were initially investigated by NMR. Conversions and comparative ratios of the segments were evaluated from the ^{1}H NMR analysis. Conversion of LLA was calculated from the ratio of the integral of characteristic PLLA peak at δ 5.0-5.1 to the integral of LLA monomer peak at δ 5.1-5.2 in the ^{1}H-NMR spectra of the products. PLLA and prepolymer segment ratios were calculated by utilizing the integration of the characteristic proton signals at δ 4.1 for the PCL segments and at δ 5.1-5.2 for the PLLA segments. Figure 3.9.a, 3.10.a and 3.11.a illustrate ^{1}H-NMR spectra of branched and linear block copolymers. The characteristic proton peaks of branched pentablock copolymer (run no: 7) are δ 1.4 ppm (-CH_2-$\underline{CH_2}$-CH_2), δ 1.6 ppm (-CH-$\underline{CH_3}$), δ 1.65 ppm (-CO-CH_2-$\underline{CH_2}$-CH_2- or -O-CH_2-$\underline{CH_2}$-CH_2-), δ 2.3 ppm (-CO-$\underline{CH_2}$-), δ 3.85 ppm (-CF_2-$\underline{CH_2}$-O), δ 3.95 ppm (-CH-$\underline{CH_2}$-O-), δ 4.05 ppm (-O-$\underline{CH_2}$-CH_2-), δ 4.35 ppm (-O-$\underline{CH_2}$-CH-), and δ 5.2 ppm (-O-$\underline{CH}$-(CH_2)(CH_2)-) or (–O-$\underline{CH}$-($COCH_3$)) (Figure 3.9.a). The proton peaks belonging to polycaprolactone and polylactide in the other polymers observed in the expected ranges similar to the peaks of branched block copolymer (Figure 3.10.a and Figure 3.11.a).

In ^{13}C-NMR, only the PCL and PLLA portion of block copolymers can be seen clearly (Figure 3.9.b). The characteristic carbon peaks of fluorolinks are not observed due to their longer relaxation time in NMR [98]. ^{13}C-NMR spectra for linear block copolymers are almost same (Figure 3.10.b and 3.11.b). Characteristic carbon peaks on the PCL block are δ 24 ppm (-CH_2-$\underline{CH_2}$-CH_2-CO-), δ 26 ppm (O-CH_2-$\underline{CH_2}$-CH_2), δ 29 ppm (-CH_2-$\underline{CH_2}$-CH_2-), δ 34 ppm (-$\underline{CH_2}$-CO-), δ 64 ppm (-$\underline{CH_2}$-O-), and δ 174 ppm (-$\underline{CO}$-CH_2-) ppm and ones on PLLA block are δ 16 ppm ($\underline{CH_3}$-CH-), δ 69 ppm (O-$\underline{CH}$-(CH_3)(CO)-), and δ 170 ppm (-$\underline{CO}$-CH-) (Figure 3.9.b, 3.10.b., and 3.11.b).

(a)

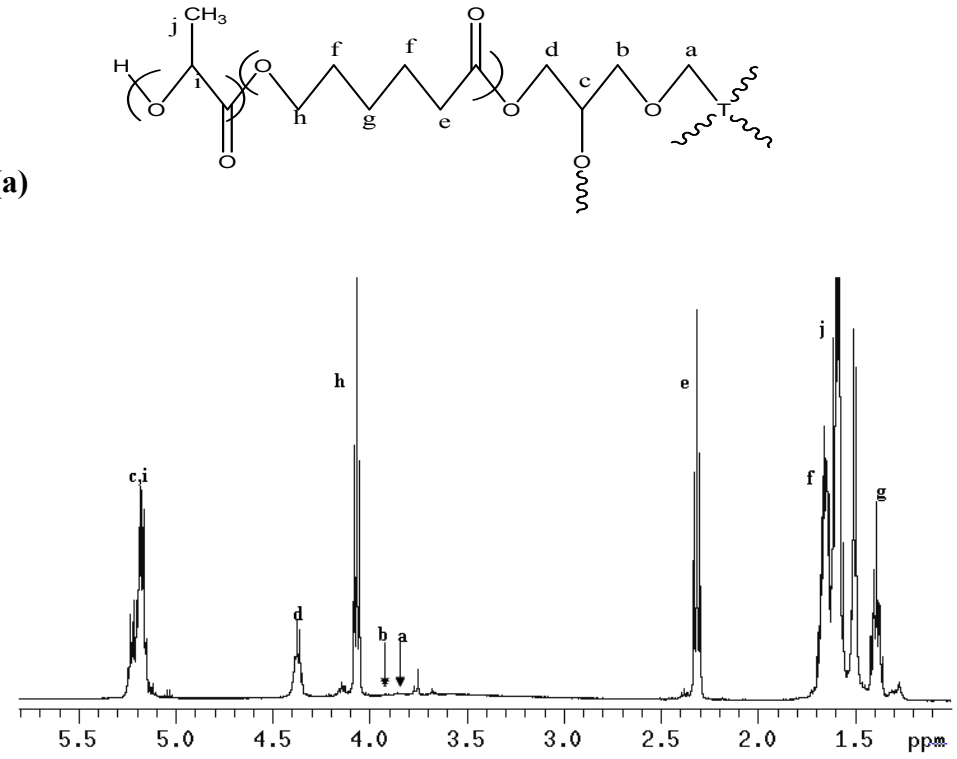

(b)

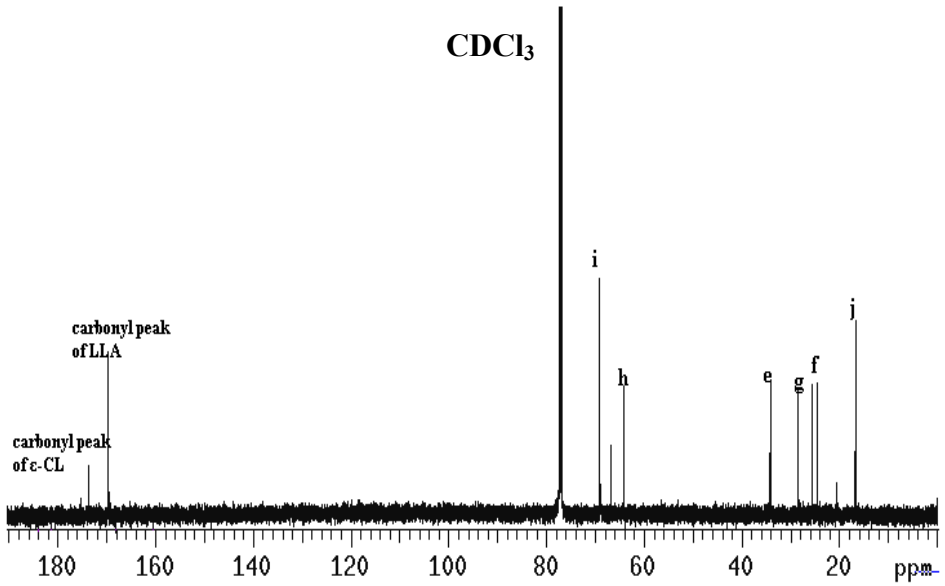

Figure 3.9. **(a)** ^{1}H-NMR and **(b)** ^{13}C-NMR of branched pentablock copolymer (run no: 7) recorded in $CDCl_3$. Only PCL and PLL portion of the polymer is visible in ^{13}C-NMR spectrum.

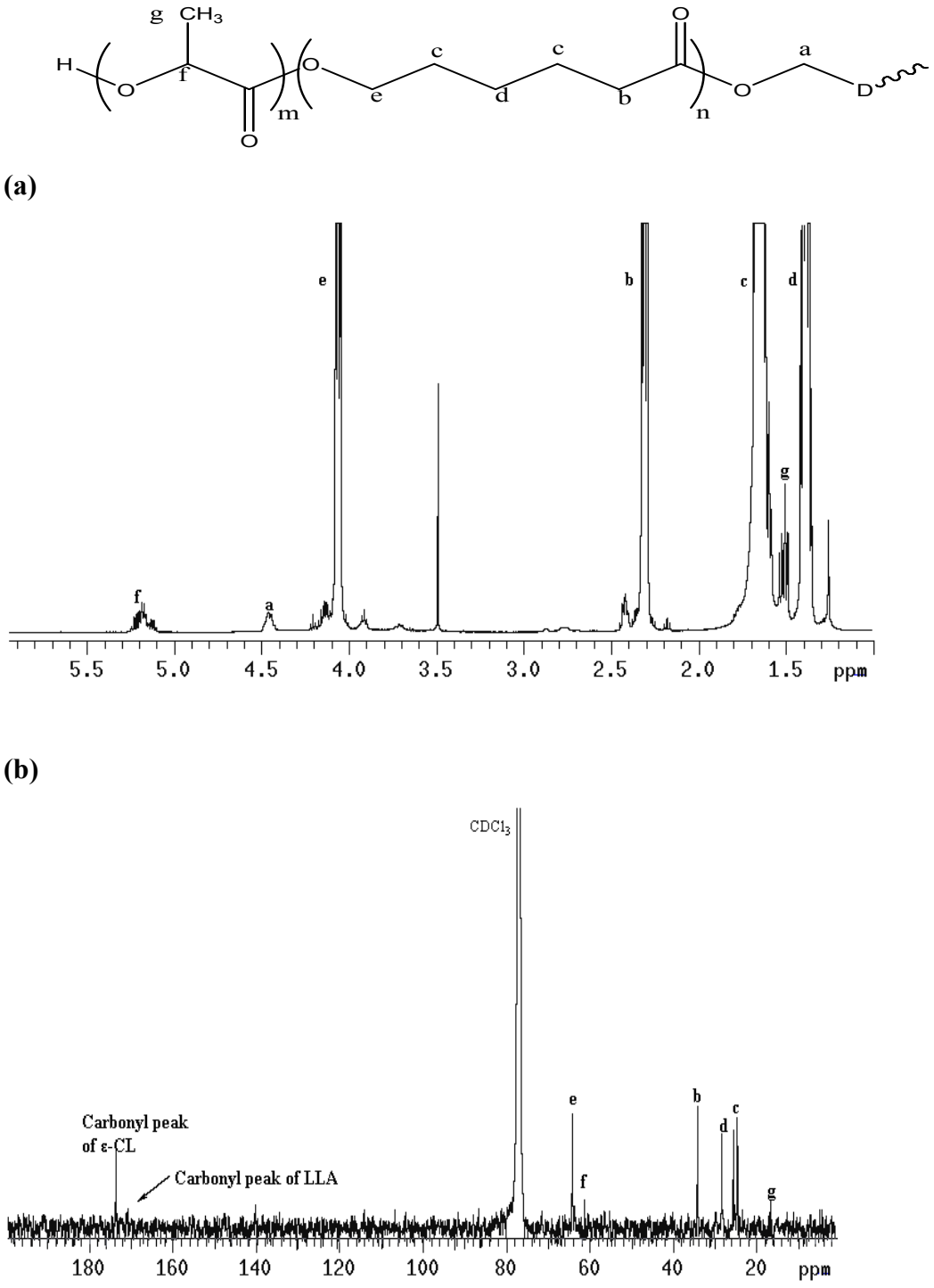

Figure 3.10. (a) ^{1}H-NMR and (b) ^{13}C-NMR of linear block copolymer PLLA-PCL-FLKD-PCL-PLLA (run no: 1) recorded in $CDCl_3$.

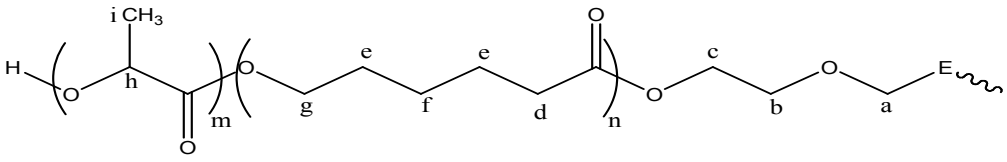

(a)

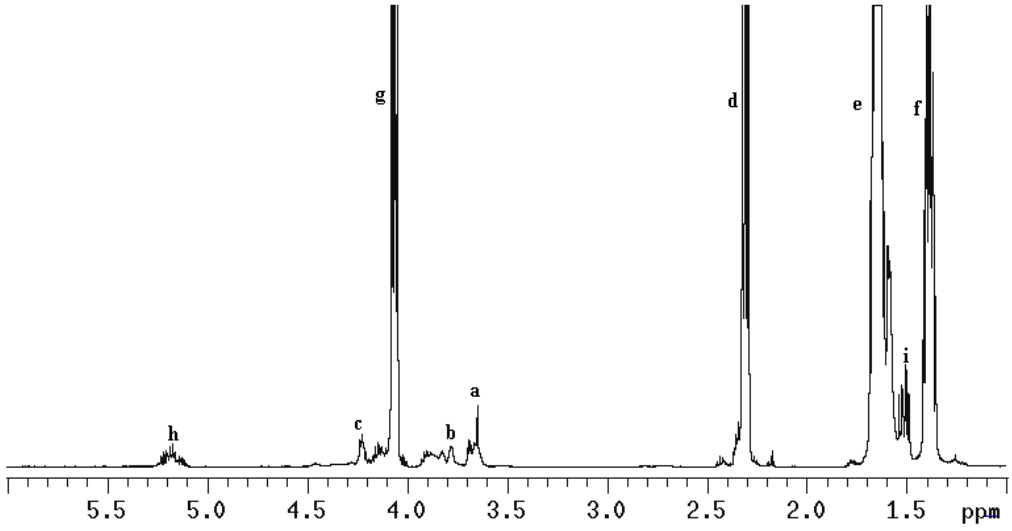

(b)

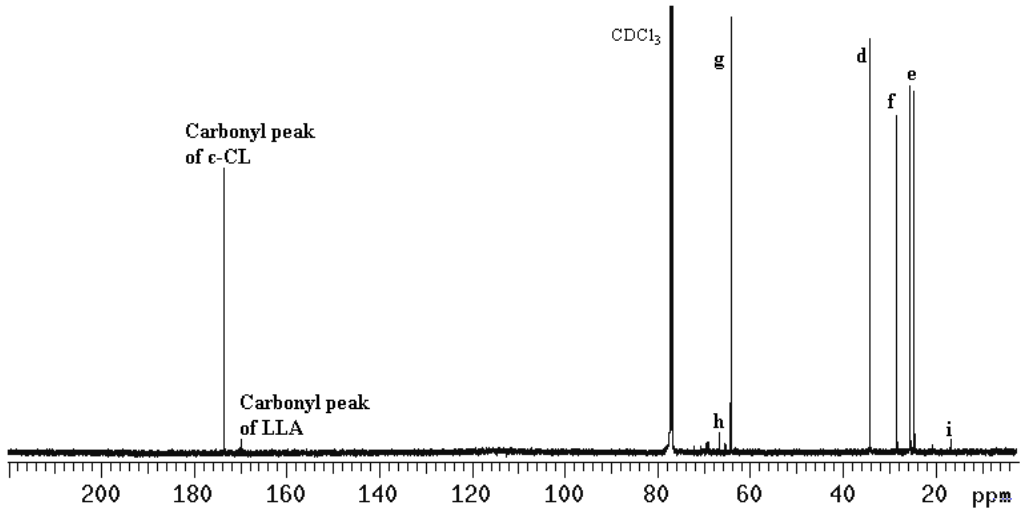

Figure 3.11. (a)^{1}H-NMR and (b) ^{13}C-NMR of linear block copolymer PLLA-PCL-FLKE-PLCL-PLLA (run no: 3) recorded in $CDCl_3$.

3.2.1.2. GPC Results

The M_n values measured by GPC are in the 12,000-24,000 g/mol range. PDI values of 1.08-1.34 were obtained (Table 3.3). Observed M_n values with low PDI values indicated that the polymerizations occured in a control manner. Also, results exhibited that molecular weight can be controlled by the monomer-to-stabilizer ratio.

3.2.1.3. Thermal Analyses

The thermal analysis similarly supports successful copolymerization in $scCO_2$. PLLA is a semicrystalline polymer with a T_g at ~ 57°C. The incorporation of the PLLA segments result in an increase in the initial T_g of the prepolymer. Correspondingly, with decrease in the amount of PLLA, the T_g of the material lowers (Table 3.3). Figure 3.12 shows T_g of block copolymer, and T_m of PCL with a shoulder, and T_m of PLLA is not seen due to lower amount of LLA in polymer compared to the amount of ε-CL. The apperance of shoulder in DSC resulted from the formation of the crystals during the quenching process.

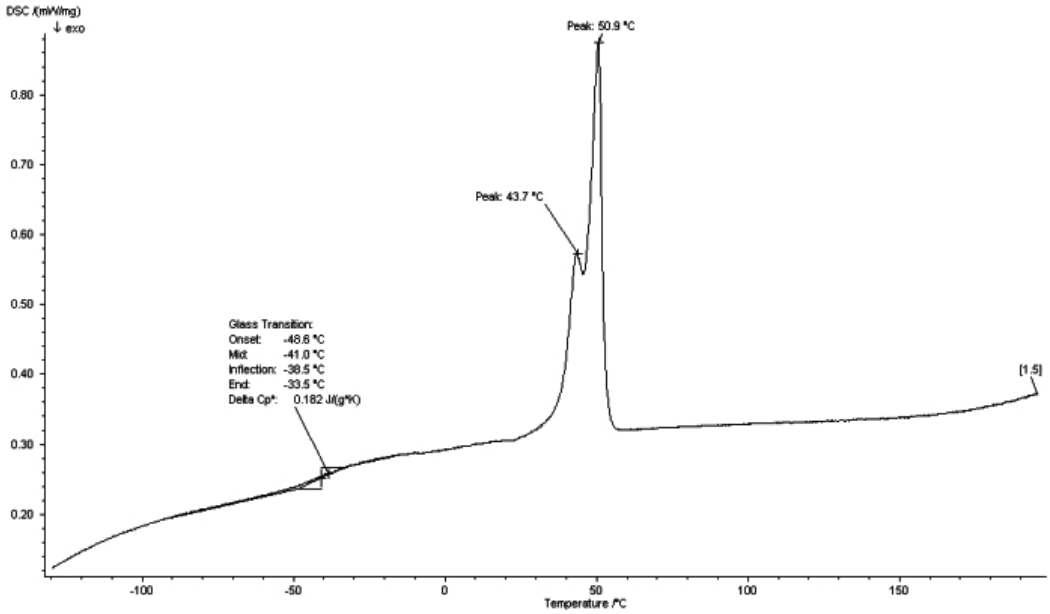

Figure 3.12. DSC of fluorinated block copolymer (PCL/PPLA) (run 8, see Table 3.3).

3.2.1.4. SEM analyses

A SEM image of linear block copolymer including FLK-E obtained after the reaction completition in $scCO_2$ reveals dispersed particles approximately 10 μm in diameter (Figure 3. 13). The formation of particles is a common occurrence in suspension polymerization in which the polymers are insoluble in their monomers [31].

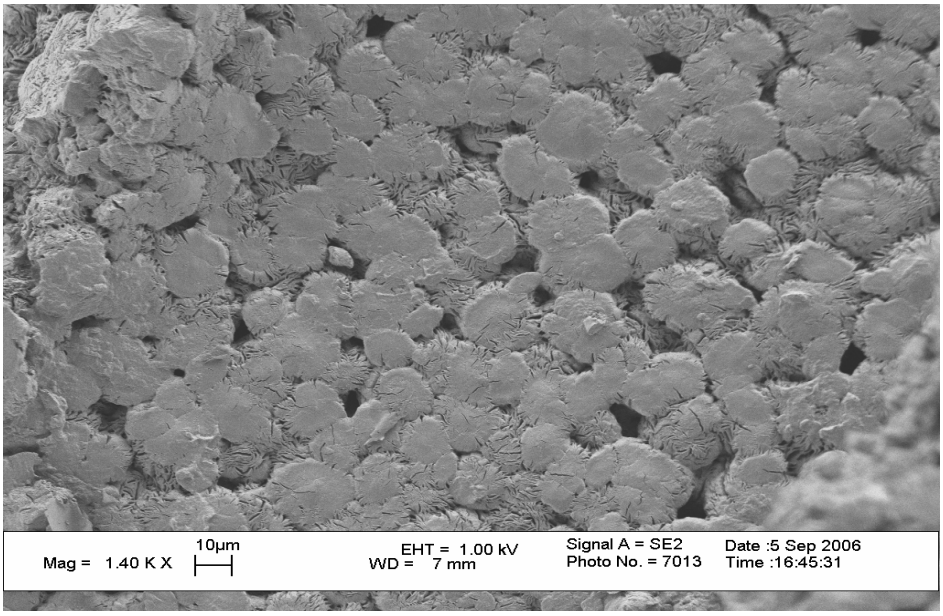

Figure 3.13. SEM image of prepolymer PCL-FLKE-PCL after releasing CO_2.

SEM micrographs of the branched polymers, both taken at two different pressures and temperatures, can be observed in figure 3.14.a and 3.14.b. At 2000 psi and 30^{o}C (Figure 3.14.a), plasticization takes place and the material displays a sticky appearance. Similar to the behavior of the prepolymers, when the pressure is increased to 4500 psi along with a temperature increase to 75^{o}C, the material becomes more flat and porous morphology is observed (Figure 3.14.b). These observations showed that CO_2 at different pressures and temperatures has a significant impact of the material morphologies.

(a)

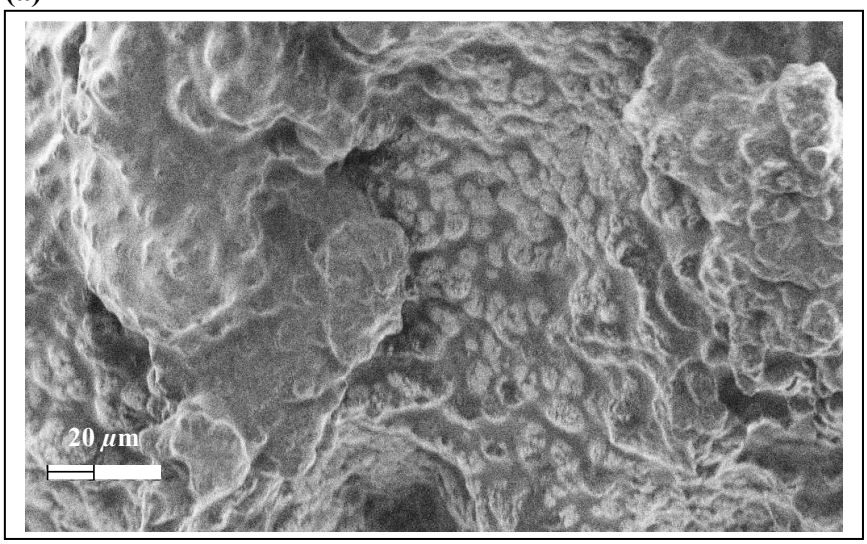

(b)

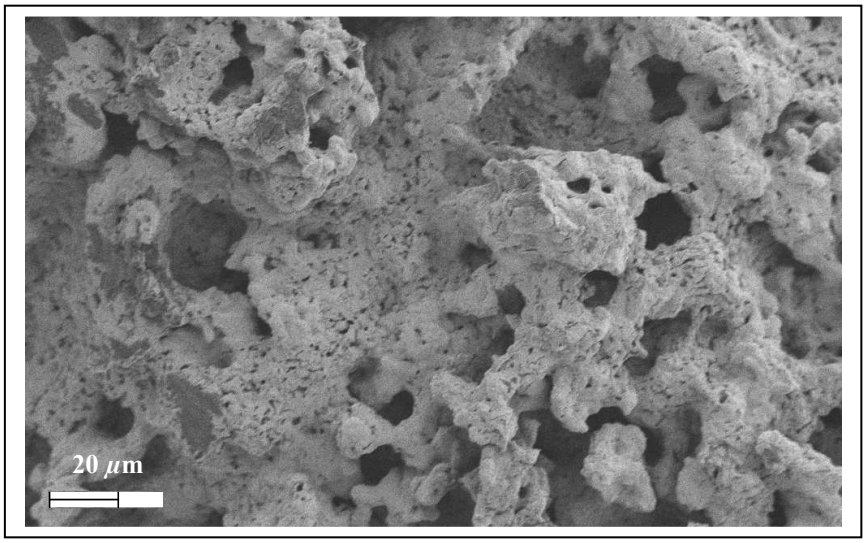

Figure 3.14. Scanning electron microscopy images of branched pentablock copolymer (run no: 7) at **(a)** 2000 psi and 30^{o}C **(b)** 4500 psi and 75^{o}C.

3.2.2. Polymerizations in Bulk

The main purpose for carrying out the polymerizations in bulk is to obtain high molecular weight. Polymer molecular weight is a significant influence on the types of structures produced by electrospinning [112]. Fluorinated prepolymers were reacted with LLA or ε-CL by changing amounts. NMR, GPC and DSC analyses proved that the polymerizations occurred successfully. Table 3.4 gives the results of these analyses. For all experiments, the percent conversions of monomer to polymer are considerably high. In experiment 5, high molecular weight polymer was received when compared to other experiments and this polymer has importance to obtain nanofiber webs in electrospinning process. DSC analyses supported the block copolymer formation. In Table 3.4, T_m (1) and T_m (2) were belonging to PCL and PLLA. PCL and PLLA have melting points of about 60°C and 175°C, respectively [113]. The T_m values of the materials synthesized are near to the theoretical ones. Figure 3.15 represents the melting points of PCL and PLLA blocks (run 6).

Run	Conversion (%)[a]	LLA:ε-CL[a]	Mn[b]	PDI[b]	T_m (1)(°C)[c]	T_m (2)(°C)[c]
1	97	1:2	13000	1.58	55.1	NO
2	94	1:3	12600	1.70	56.0	163.6
3	90	4:1	16000	1.27	44.9	148.3
4	99	3:1	10500	2.08	50.1	161.2
5	99	1:7	40500	1.31	55.9	173.8
6	99	2:1	18600	1.36	55.5	176.4

NO: Not Observed

[a] Conversion was calculated by integrating the monomer peak to polymerized monomer peak from ^{1}H-NMR. Ratio of LLA and ε-CL was also calculated from ^{1}H-NMR

[b] Mn, Mw, and PDI were recorded by Gel Permeation Chromatography with PS standards.

[c] T_m (1) and T_m (2) were determined by DSC.

Table 3.4. Results of characterization of polymers synthesized in bulk

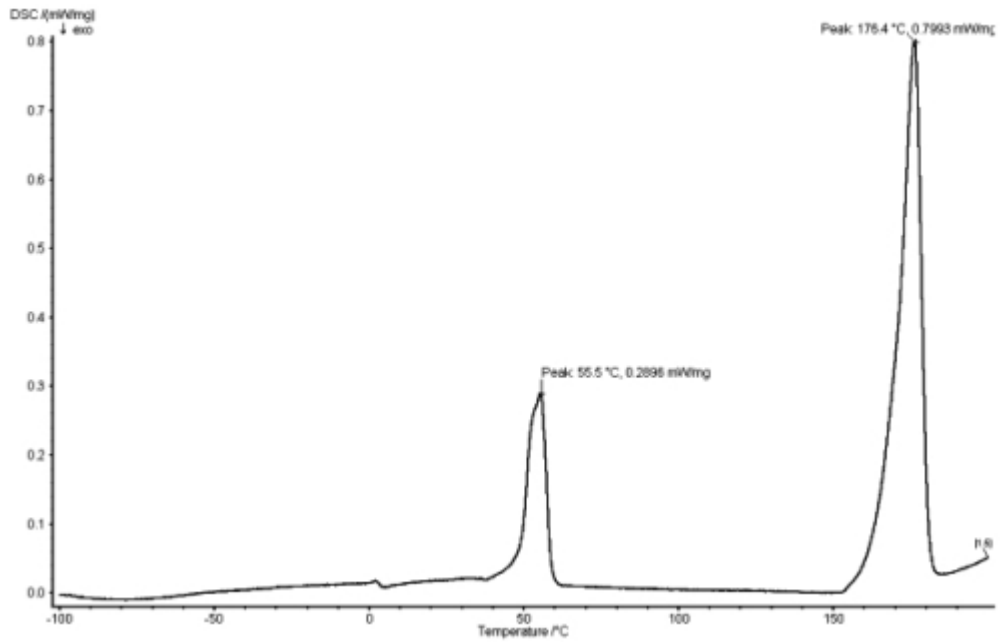

Figure 3.15. DSC of fluorinated block copolymer PCL/PLLA (run 6, see Table 3.4).

3.3. Preparation of Biodegradable Nanofiber Webs via electrospinning

Matrices play a central role in tissue engineering. Biodegradable synthetic polymers exhibit tremendous potential as matrices to manage new tissues. The properties of synthetic polymers can be tailored by using different functional groups (on the backbone or side chain), polymer architectures (linear, branched, comb or star), and combinations of polymer species (polymer blends and copolymer). The choice of PCL and PLLA polyesters is owing to their safety in human applications and the projected approval of FDA. The chemical compositions and the ratio of the monomers used in the polymerization reactions strongly affect the degradation rates of the copolymers.

In the present work, the fluorinated block copolymers were processed into nanofibers by electrospinning. In electrospinning process, there are several factors that affect the fiber diameter and cause the bead formation which is not desirable in some cases: polymer type, molecular weight and its distribution, initial polymer concentration, polymer solution properties (viscosity, surface tension, compatibility with polymer,

etc.), the applied voltage, capillary properties and its distance from the collector system, environmental conditions that the fiber jet moves in and collector system [114]. In order to produce fibers with different diameters with reduced bead formation, the solution composition, applied voltage and collector-tip distance were changed in each trial.

The viscosity of the solution has a profound effect on electrospinning so that the selection of solvent is significant [115]. Some commonly used solvents like DMF, DMSO, CH_3OH, $CHCl_3$ and acetone were tried via altering amounts in the range of 0 to 100 percent in the mixture to find the good solvent mixture. While selecting these solvents, their rates of evaporation were also considered. If the evaporation rate of the solvent is too low, the polymer solution is not evaporated sufficiently and individual fibers may not formed.

Polymers listed in table 3.4 were attempted to prepare non-woven fibrous webs with the polymer:solvent ratios of 1:2, 1:2.5, and 1:3 by applying the voltage in the range of 10-30 kV and adjusting the capillary-collector distance between 5-20 cm. Except the polymer obtained from experiment 5, the other polymers were failed to produce nanofiber webs because molecular weights of these materials were not enough to prepare fibers comparing to experiment 5. Block PLLA/PCL copolymer obtained from the experiment 5 were successfully converted to nanofibers. This success stems from the high molecular weight of the polymer. The molecular weight of the polymer indicates the length of the polymer chains and the polymer length define the amount of entanglement of polymer chains in the solvent. Therefore, high molecular weight polymers result in increasing chain entanglements in the solution and this is required to keep the continuity of the jet during electrospinning. The polymer solution was prepared in 50% DMF and 50% CH_3OH using the polymer synthesized in experiment 5 (polymer:solvent ratio was adjusted as 1:2 (w/w)). A range of fiber diameters was measured from 40 to 360 nm as keeping applied voltage and cappillary-collector distance constant at 15 kV and 10 cm. SEM images of this electrospun material show the fiber formation (Figure 3.16). At high magnifications, branched type fibers were seen clearly (Figure 3.16.b). Branched fibers were formed by the ejection of the smaller jet on the surface of primary jet [116].

The nanofiber scaffolds with seeded cells can be implanted to patient's body to repair the damaged tissues. In the literature, there are many works to improve biocompatibilities of polymeric tissue engineering scaffolds. He et al. [117] coated adhesive protein, collagen, by poly(L-lactic acid)-co-poly(ε-caprolactone) nanofibers and the collagen coated material have higher cell attachment, spreading and viability than the unmodified nanofiber. Xu et al. [118] prepared nanofibrous scaffold from poly(L-lactide-co-ε-caprolactone) by electrospinning and they evaluated the morphology, adhesion and proliferation of human coronary artery smooth muscle cells on this scaffold. In the view of these works, we will continue to improve the aspects of nanofibrous block copolymers for to create "ideal" tissue engineering scaffolds. Scaffolds will also designed to overcome oxygen and nutrient transport limitations by controlling scaffold diameters such as pore size, porosity and pore distribution. The lack of nutrients into the interior of the scaffolds can deform or imitate research results [119].

(a)

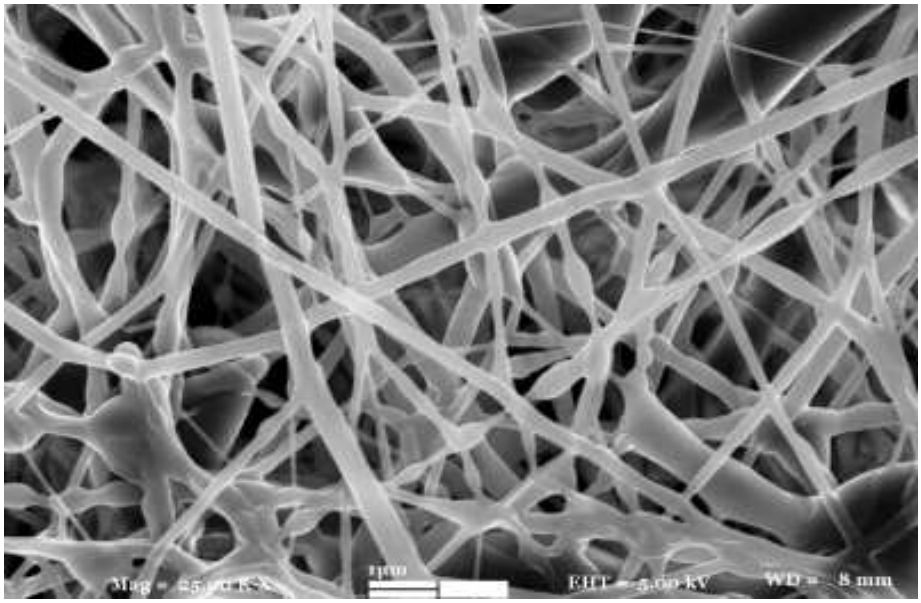

(b)

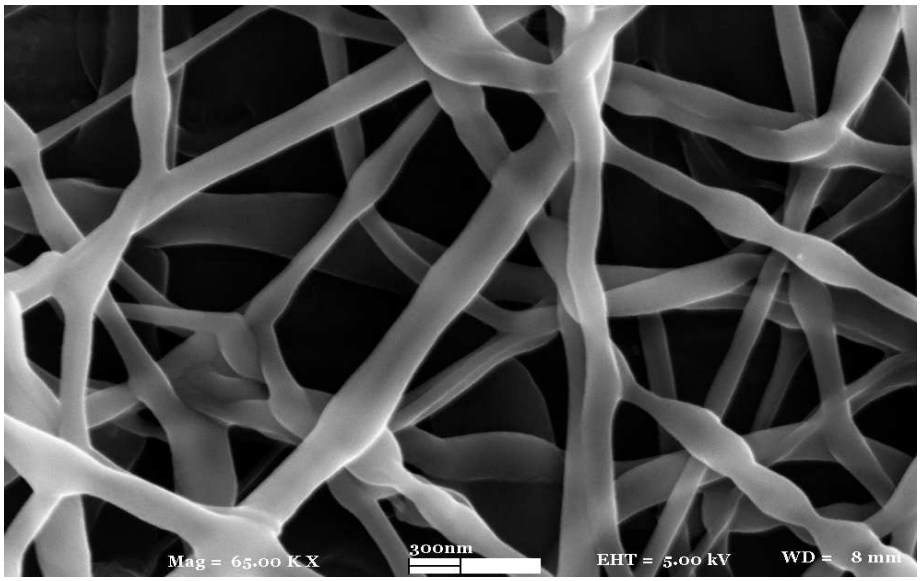

Figure 3.16. (a) and **(b)** Representative SEM images of electrospun polymer belonging to Run 5 (solvent: 50% DMF + 50% CH_3OH, applied voltage: 15 KV and capillary to collector distance: 10 cm) at different magnifications.

CHAPTER 4

SUMMARY AND CONCLUSIONS

$ScCO_2$ can be used as an excellent alternative solvent to traditional organic solvents for the synthesis of biodegradable polymers. This study demonstrated successful biodegradable polymer synthesis in $scCO_2$ media. Another achievement in this work is that perfluoro polyethers were processed into nanofiber webs successfully by the electrospinning process.

Considering the importance of $scCO_2$ in synthetic reactions and the broad applications of electrospun materials, this research was divided into two major parts: the synthesis of biodegradable polymers having the ability to carry oxygen in $scCO_2$ and the fabrication of electrospun polymer fibers.

4.1. Synthesis of Biodegradable Materials in $scCO_2$ media

Three types of triblock fluorinated stabilizers (prepolymers) were initially synthesized by using fluorolinks (FLK-D, FLK-E and FLK-T) as initiators with 100% conversion. With FLK-D and FLK-E, linear polymers were obtained, whereas with FLK-T, branched polymers were received. Since these fluoropolymers have the ability to carry and supply oxygen to tissues and organs, their emulsions are used as blood substitutes as well. Owing to their oxygen-carrying ability in biological systems, these polymers including fluorinated blocks were synthesized in this work.

Before starting the synthesis of block copolymers, the solubility behaviors of fluorinated prepolymers were checked in $scCO_2$ media. Their morphologies at different pressures and temperatures were investigated by SEM analyses.

Block fluorinated (PLLA/PCL), polyester copolymers for biomedical applications were synthesized by ROP mechanism in an environmentally benign solvent, $scCO_2$, with the aid of a reactive fluorinated prepolymer. There were four parameters in $scCO_2$ experiments: catalyst concentration, monomer concentration, pressure and stirring rate. High catalyst ratio was preferred due to the highest conversion in $scCO_2$. Block lengths were controlled by changing monomer concentration. Pressure was kept constant and the stirring rate was adjusted for each reaction.

Copolymers of PLLA/PCL were also synthesized in bulk to obtain high molecular weight that is essential to produce electrospun scaffolds by electrospinning. Different ratios of prepolymer to monomer (LLA and ε-CL) were applied in order to control chain length.

Successful pentablock formation is supported by NMR spectroscopy and the thermal analyses of the materials. The molecular weights of the products were measured with the aid of GPC; the prepolymer and the copolymer possessed average number molecular weights (M_n) in the range of 13,000 and 40,000, respectively. The products obtained in $scCO_2$, have low PDI values in the range of 1.08 and 1.34, compared to the products obtained by ordinary organic solvents. Therefore, the experimental data showed that block copolymers can be prepared in $scCO_2$ with good control on molecular weight. This stems from the dissolving power of CO_2 that can be finely tuned by density or pressure or temperature. In addition, soluble stabilizers in $scCO_2$ effectively stabilized the sequential ROP of LLA in $scCO_2$ leading to the formation of microparticles. High pressures also favored the polymerization because of the decrease in volume during polymerization.

4.2. Preparation of Nanofiber Webs with Oxygen Carrying Systems

In this part, fluorinated block copolymers were processed into nanofibers and fibrous non-woven webs by electrospinning under different conditions. The variables, i.e., the initial polymer concentration, composition of solvent mixture, tip-collector distance and applied voltage were optimized in order to control the fiber formation and to reduce the bead formation. Instead of these variables, polymer molecular weight has also a significant impact on fiber formation. The polymer having high Mn (40500 g/mol) was successfully converted to nanofiber web applying voltage as 15 kV. SEM images were also evidence for the formation of non-woven fibrous structure successfully. Fiber diameters were measured from 40 nm to 360 nm in the sample of block copolymer (PLLA/PCL) prepared with the polymer:solvent ratio of 1:2. This study is still in progress. Future studies will involve in searching the degradation rates in vivo and in vitro.

REFERENCES

[1] G. Manivannan, and S.P. Sawan, in: J. McHardy, S.P. Sawan (Eds.), Supercritical Fluid Cleaning: Fundamentals, Technology and Applications, Vols. 1–21, Noyes Publications, Westwood, NJ, 1998.

[2] R. Span, and W. Wagner, "A new equation of state for carbon dioxide covering the fluid region from the triple-point temperature to 1100 K at pressures up to 800 Mpa", *J. Phys. Chem. Ref. Data*, Vol. 25, 1996, pp. 1509-1596.

[3] N. Bilgin, C. Baysal, and Y. Z. Menceloglu, "Synthesis of fluorinated oligomers for supercritical carbon dioxide applications", *Journal of Polymer Science Part A-Polymer Chemistry*, Vol. 43 (21), 2005, pp. 5312-5322.

[4] J. A. Hyatt, "Liquid and supercritical carbon dioxide as organic solvents", *J. Org. Chem.*, vol. 49, 1984, pp. 5097-5101.

[5] J. M. DeSimone, Z. Guan, and C. S. Elsbernd, "Synthesis of fluoropolymers in supercritical carbon dioxide", *Science*, Vol. 257, 1992, pp. 945-947.

[6] M. R. Clark, and J. M. DeSimone, "Cationic Polymerization of Vinyl and Cyclic Ethers in Supercritical and liquid Carbon Dioxide", Macromolecules, Vol. 28, 1995, pp. 3002-3004.

[7] R. B. Gupta, J. R. Combes, and K. P. Johnston, "Solvent Effect on Hydrogen Bonding in Supercritical Fluids", *J. Phys. Chem.*, Vol. 97, 1993, pp. 707-715.

[8] A. I. Cooper, "Polymer synthesis and processing using supercritical carbon dioxide", *J. Mater. Chem.*, vol. 10, 2000, pp. 207-234.

[9] K. P. Johnston, K. L. Harrison, M. J. Clarke, S. M. Howdle, M. P. Heitz, F. V. Bright, C. Carlier, and T. W. Randolph, "Water-in-carbon dioxide microemulsions: a new environment for hydrophiles including proteins", *Science*, vol. 271, 1996, pp. 624-626.

[10] S. R. P. da - Rocha, K. L. Harrison, K. P. Johnston, "Effect of surfactants on the interfacial tension and emulsion formation between water and carbon dioxide", *Langmuir*, vol. 15, 1999, pp. 6890-6984.

[11] I. Calvo, J. D. Holmes, M. Z. Yates, and K. P. Johnston, "Steric stabilization of inorganic suspensions in carbon dioxide", *J. Supercritical Fluids*, vol. 16, 2000, pp. 247-260.

[12] S. M. Pourmortazavi, F. Sefidkon, and S. G. Hosseini, "Supercritical carbon dioxide extraction of essential oils from Perovskia atriplicifolia Benth", *J. Agric. Food Chem.*, vol. 51, 2003, pp. 5414-5419.

[13] O. Vitzthum, and P. Hubert, "Method for the manufacture of caffeine free black tea", U.S. Patent 4167589, 1979.

[14] U. Van Wasen, I. Swaid, and G. M. Schneider, "Physicochemical principles and applications of supercritical fluid chromatography", *Angew. Chemie*, vol. 19, 1980, pp. 575-658.

[15] V. J. Krukonis, "Processing of polymers with supercritical fluids", *Polymer News*, vol. 11, 1985, pp. 7-16.

[16] K. L. Parks, and E. J. Beckman, "Generation of microcellular polyurethane foams via polymerization in carbon dioxide. 2. Foam formation and characterization", *Polym. Eng. Sci.,* vol. 36, 1996, pp. 2417-2431.

[17] E. Reverchon, "Supercritical fluid extraction and fractionation of essential oils and related products", *J. Supercrit. Fluids*, vol. 10, 1997, pp. 1-37.

[18] C. B. Kautz, U. H. Dahlmann, and G. M. Schneider, "Capacity ratios in supercritical fluid chromatography-Effect the mobile and stationary phases on hexasubstituted benzenes", *Journal of Chromatography A*, vol. 776 (2), 1997, pp. 305-309.

[19] P. Alessi, A. Cortesi, I. Kikic, and I. Colombo, Solvent Removal from Pharmaceutical Products, Proc. 4th Italian Conference on "Supercritical fluids and their applications", Capri, September, pp. 115-120.

[20] San Roman, J., Gallardo, A. and Levenfeld, B. (1994). New Polymers for Biomedical Applications: Synthesis and Characaterization of Acrylic Systems with Parmacological Activity, *Macromolecular Symposia*, 84: 145-158.

[21] J. Kendall, D. A. Canelas, J. L. Young, and J. M. Desimone, "Polymerizations in supercritical carbon dioxide", *Chem. Rev.*, vol. 99, 1999, pp. 543-563.

[22] T. Sarbu, J. Styranec, and E. J. Beckman, "Non-fluorous polymers with very high solubility in supercritical CO_2 down to low pressures", *Nature,* vol. 405, 2000, pp. 165-168.

[23] X. Y. Lang, G. H. Zhang, J. S. Lian, and Q. Jiang, "Size and pressure effects on glass transition temperature of poly (methyl methacrylate) thin films", *Thin Solid Films*, vol. 496, 2006, pp. 1-2.

[24] Z. Guan, J. R. Combes, Y. Z. Menceloglu, and J. M. DeSimone, "Homogeneous free radical polymerizations in supercritical carbon dioxide: 2. Thermal decomposition of 2,2'-Azobis(isobutyronitrile)", *Macromolecules*, vol. 26, 1993, pp. 2663-2669.

[25] E. Kiran, and V. P. Saraf, "Polymerization of styrene in supercritical n-butane", *J. Supercrit. Fluids*, vol. 3, 1990, pp. 198-204.

[26] S. Beuermann, M. Buback, C. Isemer and A. Wahl, "Homogeneous phase free-radical polymerization of styrene in supercritical carbon dioxide", Paper presented at the *NATO ASI* on *Supercritical fluids*, Kemer, Antalya, Turkey, July 1998.

[27] D. A. Canelas, and J. M. DeSimone, "Polymerizations in Liquid and Supercritical Carbon Dioxide", *Adv. Polym. Sci.*, vol. 133, **1997**, pp. 103-140.

[28] T. J. Romack, and J. M. DeSimone, "Synthesis of Tetrafluoroethylene-based, Non-aqueous Fluoropolymers in Supercritical Carbon Dioxide", *Macromolecules*, vol. 28, 1995, pp. 8429- 8431.

[29] J. N. Hay, R. J. Winder, M. R. Giles, and S. M. Howdle, Proceedings of the 6th Meeting on Supercritical Fluids Chemistry and Materials, Nottingham (United Kingdom), Apr. 10/13, 1999, pp. 121-125.

[30] J. M. DeSimone, E. E. Maury, Y. Z. Menceloglu, J. B. McClain, T. R. Romack, and J. R. Combes, "Dispersion Polymerizations in Supercritical Carbon Dioxide", *Science*, vol. 265, 1994, pp. 356-359.

[31] D. Bratton, M. Brown, and S. M. Howdle, "Novel Fluorinated Stabilizers for Ring Opening Polymerizations in Supercritical Carbon Dioxide", *Journal of Polymer Science: Part A: Polymer Chemistry*, Vol. 43, 2005, pp. 6573–6585.

[32] T. Higashimura, M. Sawamoto, and M. Miyamoto, "Progress of Theories of Free Radical Crosslinking Copolymerization", *Macromolecules*, vol. 17, 1984, pp. 265-268.

[33] M. R. Clark, and J. M. DeSimone, "Cationic polymerizations in liquid and supercritical carbon dioxide, *ACS Polymer Preprints*", Vol. 37 (1), 1996, pp. 365-366.

[34] J. Fricke, *AerogelsSpringer proceedings in physics,* Springer, Heidelberg, Vol. 6, 1986, pp. 2-19.

[35] F. M. Kerton, G. A. Lawless, and S. P. Armes, "First example of a conducting polymer synthesised in supercritical fluids", *J. Mater. Chem.*, Vol. 7, 1997, pp. 1965-1966.

[36] E. Kiran, P. G. Debenedetti, and C. J. Peters, "Supercritical Fluids: Fundamentals and Applications". NATO Science Series E: Applied Sciences, Vol. 366, 2000, pp. 12-17.

[37] D. E. Knox, "Solubilities in supercritical fluids", *Pure and Applied Chemistry*, Vol. 77 (3), 2005, pp. 513-530.

[38] J. Mendez-Santiago, and A. S. Teja, "Solubility of solids in supercritical fluids: Consistency of data and a new model for cosolvent systems", *Industrial & Engineering Chemistry Research*, Vol. 39 (12), 2000, pp. 4767-4771.

[39] H. L. Engelhardt, and P. C. Jurs, "Prediction of Supercritical Carbon Dioxide Solubility of Organic Compounds from Molecular Structure", *J. Chem. Inf. Comput. Sci*., Vol. 37, 1997, pp. 478-484.

[40] M. Skerget, Z. Novk-Pintaric, Z. Kenz, and Z. Kravanja, "Estimation of solid solubilities in supercritical carbon dioxide: Peng–Robinson adjustable binary parameters in the near critical region", *Fluid Phase Equilib*., Vol. 203, 2002, pp. 111–132.

[41] F. Rindfleisch, T. P. DiNoia, and M. A. McHugh, "Solubility of Polymers and Copolymers in Supercritical CO_2", *J. Phys. Chem.*, Vol. 100, 1996, pp. 15581-15587.

[42] C. F. Kirby, and M. A. McHugh, "Phase behavior of polymers in supercritical fluid solvents", *Chem. Rev.*, Vol. 99, 1999, pp. 565-602.

[43] S. Kirmizialtin, Y. Z. Menceloglu, and C. Baysal, "New Surfactant Design for CO_2 Applications: Molecular Dynamic Simulations of fluorocarbon-hydrocarbon oligomers", *Journal of Chemical Physics*, Vol. 119 (9), 2003, pp. 4953-4961.

[44] M. A. McHugh, A. Garach-Domech, I. H. Park, D. Li, E. Barbu, P. Graham, and J. Tsibouklis, "Impact of fluorination and side-chain length on poly(methylpropenoxyalkylsiloxane) and poly(alkyl methacrylate) solubility in $scCO_2$", *Macromolecules*, Vol. 35, 2002, pp. 6479-6482.

[45] E. Kissa, "Fluorinated surfactants, synthesis, properties, applications", in: Surfactant Science Series, Vol. 50, Marcel Dekker, New York, 1994.

[46] T. A. Hoefling, R. M. Enick and E. J. Beckman, "Microemulsions in near-critical and supercritical CO_2", *J. Phys. Chem.*, Vol. 95, 1991, pp. 7127-7129.

[47] L. Conte, A. Zaggia, A. Sassi, and R. Seraglia, "Synthesis and characterization of tri-block fluorinated-n-alkanes. Journal of Fluorine Chemistry", Vol. 128, 2007, pp. 493–499.

[48] E. Kissa, "Fluorinated surfactants and repellents", *Surfactant Science Series* 97. Marcel Dekker, New York, 2001.

[49] J. G. Riess, and M. P. Krafft, "Fluorinated materials for in vivo oxygen transport (blood substitutes), diagnosis and drug delivery", *Biomaterials*, Vol. 19, 1998, pp. 1529-1539.

[50] K. C. Lowe, "Fluorinated blood substitutes and oxygen carriers-Review", *Journal of Fluorine Chemistry*, Vol. 109, 2001, pp. 59-63.

[51] M. P. Krafft, "Fluorocarbons and fluorinated amphiphiles in drug delivery and biomedical research", *Advanced Drug Delivery Reviews*, Vol. 47, 2001, pp. 209–228.

[52] C. A. Moody, and J. A. Field, “Perfluorinated surfactants and the environmental implications of their use in fire-fighting foams”, *Environ. Sci. Technol.*, Vol. 34, 2000, pp. 3864–3870.

[53] M. Storck, K. H. Orend, and T. Schmitzrixen, “Absorbable suture in vascular surgery”, *Vasc. Surg.*, Vol. 27, 1985, pp. 413-24.

[54] B. Jeong, Y. H. Bae, D. S. Lee, and S. W. Kim, “Biodegradable block copolymers as injectable drug-delivery systems”, Nature, Vol. 388, 1997, Vol. 860-862.

[55] S. D. Andrew, G. C. Phil, and K. G. Marra, “The influence of polymer blend composition on the degradation of polymer/hydroxyapatite biomaterials”, *J. Mater. Sci.: Mater. Med.*, Vol. 12, 2001, pp. 673–677.

[56] W. Heidemann, S. Jeschkeit, K. Ruffieux, J. H. Fischer, M. Wagner, G. Kruger, E. Wintermantel, and K. L. Gerlach, “Degradation of poly(D,L)lactide implants with or without addition of calciumphosphates in vivo”, *Biomaterials*, Vol. 22, 2001, pp. 2371–2381.

[57] M. K. Cox, in: M. Vert. et al. (Eds.), “Biodegradable Polymers and Plastics”, Royal Society of Chemistry, Cambridge, 1992, p. 95.

[58] A. Schindler, R. Jeffcoat, G. L. Kimmel, C. G. Pitt, M. E. Wall, and R. Zweidinger, in: *Contemporary topics in polymer Science,* Pearce, E.M., Schaefgen, J.R., Eds., Plenum, 1977.

[59] A. Hamitou, T. Ouhadi, R. Jerome, and P. Teyssie, “Soluable bimetallic μ-oxoalkoxides. VII. Characteristics and mechanism of ring opening polymerization of lactones”, *J. Polym. Sci., Polym. Chem. Ed.* Vol. 15, 1977, pp. 865-873.

[60] C. G. Pitt, M. M. Gratzl, A. R. Jeffcoat, R. Zweidinger, and A. Schindler, A., “Sustained drug delivery systems I: the permeability of poly(ε-caprolactone), poly(DL-lactic acid) and their copolymers”, *J. Pharm. Sci*., Vol. 68, 1979, pp. 1534-1538.

[61] C. G. Pitt, F. J. Chasaldo, J. M. Hibionada, D. M. Klimas and A. Schindler, “Aliphatic polyesters I. The degradation of poly(ε-caprolactone) *in vivo*”, *J. Appl. Polym. Sci.,* Vol. 28, 1981, pp. 3779-3787.

[62] C. G. Pitt, A. Schindler and R. A. Zweidinger, in *Drug Delivery Systems*, H. L. Gabelnick, ed., DHEW Publication No. (NIH) 77: 1238, 1977, p. 142.

[63] R. Jerome and P. Teyssie, “Anionic ring-opening polymerization”, Comp. Polym. Sci., New York: Pergamon Press, Vol. 3, 1989.

[64] S. Ponsart, J. Coudane, and M. Vert, “A novel route to poly(ε-caprolactone) based copolymers via anionic derivatization”, *Biomacromolecules,* Vol. 1, 2000, pp. 275-281.

[65] D. Mecerreyes, R. Jerome, and P. H. Dubois, “Novel macromolecular architectures based on aliphatic polyesters: relevance of the ‘coordination-insertion’ ring opening polymerization”. In: Hilborn, J. G., editor. *Advanced Polymer Science*, Berlin: Springer, Vol. 147, 1999, pp. 1-59.

[66] S. G. Kumbar, L. S. Nair, S. Bhattacharyya, and C. T. Laurencin, “Polymeric nanofibers as novel carriers for the delivery of therapeutic molecules”, *Journal of Nanoscience and Nanotechnology*, Vol. 6 (9-10), 2006, pp. 2591-2607.

[67] A. Formhals, “Process and Apparatus for Preparing Artificial Threads”, US Patent 1975504, 1934.

[68] D. H. Reneker, and I. Chun, “Nanometre Diameter Fibres of Polymer, Produced by Electrospinning”, *Nanotechnology*, Vol. 7 (3), 1996, pp. 216-223.

[69] M. M. Demir, I. Yilgor, E. Yilgor, and B. Erman, “Electrospinning of Polyurethane Fibers”, *Polymer*, Vol. 43, 2002, pp. 3303-3309.

[70] D. H. Reneker, A. Yarin, E. Zussman, S. Koombhongse, and W. Kataphinan, “Nanofiber Manufacturing: Toward Better Process Control”, *ACS Symposium Series 918*, Chapter 2, 2006, pp. 7-9.

[71] K. Acatay, E. Simsek, C. Ow-Yang, and Y. Z. Menceloglu, “Tunable, Superhydrophobically Stable Polymeric Surfaces by Electrospinning”, *Angewandte Chemie-International Edition*, Vol. 43 (39), 2004, pp. 5210-5213.

[72] H. L. Schreuder-Gibson, and P. Gibson, “Applications of Electrospun Nanofibers in Current and Future Materials”, *ACS Symposium Series 918,* Chapter 9, 2006, pp. 122-123.

[73] S. N. Reznik, A. L. Yarin, S. A. Theron, and E. Zussman, “Transient and steady shapes of droplets attached to a surface in a strong electric field”, *J. Fluid. Mech.*, Vol. 516: 2004, pp. 349-377.

[74] S. Ramakrishna, K. Fujihara, W. Teol, T. Yong, Z. Ma, and R. Ramaseshan, "Electrospun Nanofibers: solving global issues", *Materials Today*, Vol. 9(3), 2006, pp. 40-50.

[75] T. Dasdia, S. Bazzaco, L. Bottero, R. Buffa, S. Ferrero, G. Campanelli, and E. Dolfine, "Organ culture in 3-dimensional matrix: in vitro model for evaluating biological compliance of synthetic meshes for abdominal wall repair", *J. Biomed. Mater. Res*., Vol. 43, 1998, pp. 204–209.

[76] P. Gibson, H.S. Gibson and D. Rivin, "Transport properties of porous membranes based on electrospun nanofibers", *Colloid. Surf. A*, Vol. 187/188, 2001, pp. 469–481.

[77] Nanotechnology Innovation for Chemical, Biological, Radiological, and Explosive (CBRE): Detection and Protection, The AVS Science and Technology Society (2002), www.wtec.org/nanoreports/cbre/CBRE_Detection_11_1_02_hires.pdf

[78] S. W. Choi, S. M. Jo, W. S. Lee, and Y. R. Kim, "An Electrospun Poly(vinylidene fluoride) Nanofibrous Membrane and Its Battery Applications", *Adv. Mater.*, Vol. 15, 2003, pp. 2027-2032.

[79] C. Drew, X. Y. Wang, K. Senecal, S. Gibson, J. N. He, J. Kumar, and L. A. Samuelson, "Electrospun Photovoltaic Cells", *J. Macromol. Sci., Pure Appl. Chem. A*, Vol. 39 (10), 2002, pp.1085–1094.

[80] D. J. Mooney and A. G. Mikos, "Growing new organs", *Sci. Am.*, Vol. 280, 1999, pp. 60–65.

[81] D. J. Mooney, S. Park, P. M. Kaufmann, K. Sano, K. McNamara, J. P. Vacanti, and R. Langer, "Biodegradable sponges for hepatocyte transplantation", *J. Biomed. Mater. Res.*, Vol. 29, 1995, pp. 959-965.

[82] S. Levenberg, N. F. Huang, E. Lavik, A. B. Rogers, J. Itskovitz-Eldor, and R. Langer, "Differentiation of human embryonic stem cells on threedimensional polymer scaffolds", *Proc. Natl. Acad. Sci. USA*, Vol. 100, 2003, pp. 12741–12746.

[83] A. Atala, D. Mooney, J. P. Vacanti, and R. Langer, "Synthetic Biodegradable Polymer Scaffolds". Printed by Birkhäuser Boston: in Chapter 4: Synthesis and Properties of Biodegradable Polymers Used as Synthetic Matrices for Tissue Engineering, 1997, pp. 51-79.

[84] S. Gong, J. Dong, S. Xue, and J. Wang, A Novel Porous Natural Polymer Scaffold for Tissue Engineering Engineering in Medicine and Biology 27th Annual Conference Shanghai, China, September 1-4, 2005

[85] T. Subbiah, G. S. Bhat, R. W. Tock, S. Paramswaran, and S. S. Ramkumar, "Electrospinning of Nanofibers". *Journal of Applied Polymer Science*, Vol. 96, 2005, pp. 557-569.

[86] E. D. Boland, G. E. Wnek, D. G. Simpson, K. J. Pawlowski, and G. L. Bowlin, "Tailoring Tissue Engineering Scaffolds using Electrostatic Processing Techniques: A study of Poly (glycolic acid) Electrospinning", *J. Macromol. Sci. Pure Appl. Chem.*, Vol. A38 (12), 2001, pp. 1231-1243.

[87] J. C. Schense, J. Bloch, P. Aebischer, and J. A. Hubbell, "Enzymatic incorporation of bioactive peptides into fibrin matrices enhances neurite extension", *Nat. Biotechnol.*, Vol. 18, 2000, pp. 415–419.

[88] B. S. Kim, and D. Mooney, "Development of biocompatible synthetic extracellular matrices for tissue engineering", *TIBTECH*, Vol. 16, 1998, pp. 224–230.

[89] L. G. Cima, J. P. Vacanti, C. Vacanti, D. Ingber, D. Mooney, and R. Langer, "Tissue Engineering by Cell Transplantation using degradable polymer substrates", *J. Biomech. Eng.*, Vol. 113, 1991, pp. 143-151.

[90] D. H. Reneker, A. Yarin, E. Zussman, S. Koombhongse, and W. Kataphinan, "Electrospinning of Bioresorbable Polymers for Tissue Engineering Scaffolds", *ACS Symposium Series 918*, Chapter 14, 2006, pp. 188-203.

[91] H. Yoshimoto, Y. M. Shin, H. Terai, and J. P. Vacanti "Biodegradable nanofiber scaffold by electrospinning and its potential for bone tissue engineering", *Biomaterials*, Vol. 24, 2005, pp. 2077-2082.

[92] J. Brostrom, A. Boss, and I. S. Chronakis, "Biodegradable films of partly branched Poly(L-lactide)-co-poly(epsilon-caprolactone) copolymer: Modulation of phase morphology, plasticization properties and thermal depolymerization", *Biomacromolecules,* Vol. 5, 2004, pp. 1124-1134.

[93] V. W. Dittrich, and R. C. Schulz, "Kinetics and mechanism of the ring-opening. polymerization of L-lactide", Angew. *Makromol. Chem.,* Vol. 15, 1971, pp. 109–126.

[94] J. W. Leenslag, and A. J. Pennings, “Synthesis of High Molecular Weight Poly(L-Lactide) Initiated with Tin 2-Ethylhexanoate”, *Macromol. Chem.*, Vol. 188, 1987, pp. 1809-1814.

[95] D. Bratton, M. Brown, and S. M. Howdle, “Suspension polymerization of L-lactide in supercritical carbon dioxide in the presence of a triblock copolymer stabilizer”, *Macromolecules*, Vol. 36, 2003, pp. 5908-5911.

[96] F. Pilati, M. Toselli, M. Messori, A. Priola, R. Bongiovanni, G. Malucelli, and C. Toselli, “Poly(epsilon-caprolactone)-poly(fluoroalkylene oxide)-poly(epsilon-caprolactone) block copolymers. 1. Synthesis and molecular characterization”, *Macromolecules*, Vol. 32, 1999, pp. 6969-6976.

[97] P. L. Donald, L. M. Gary, and G. S. Kriz, Jr. “Infrared Spectroscopy”. In *Introduction to spectroscopy: A guide for students of organic chemistry*. Phyladelphia: International Thomson Publishing, 1997.

[98] J. B. Lambert, and E. P. Mazzola, “*Nuclear Magnetic Resonance Spectroscopy* by Pearson Education”, Inc. USA, 2004.

[99] T. E. Karis, B. Marchon, D. A. Hopper, and R. L. Siemens, R.L., “Perfluoropolyether characterization by nuclear magnetic resonance spectroscopy and gel permeation chromatography", *J. Fluorine Chem.*, Vol. 118, 2002, pp. 81-94.

[100] W. J. Feast, M. Gimeno, and E. Khosravi, “Approaches to highly polar polymers with low glass transition temperatures. 1. Fluorinated polymers via a combination of ring-opening metathesis polymerisation and hydrogenation”, *Polymer*, Vol. 44, 2003, pp. 6111-6121.

[101] W. J. Feast, M. Gimeno, and E. Khosravi, “Approaches to highly polar polymers with low glass transition temperatures 2. Fluorinated polymers via ring-opening metathesis copolymerisation and hydrogenation”, *J. Mol. Catal.*, Vol. 213, 2004, pp. 9-14.

[102] M. A. Hillmyer, and T. P. Lodge, “Morphological behavior of model poly(ethylene-alt-propylene)-b-polylactide diblock copolymers”*, J. Polym. Sci. Part A: Polym. Chem.*, Vol. 40, 2002, pp. 2364-2376.

[103] V. Langlois, K. Vallee-Rehel, J. J. Peron, A. le Borgne, M. Walls, and P. Guerin, "Synthesis and hydrolytic degradation of graft copolymers containing poly(lactic acid) side chains: in vitro release studies of bioactive molecules", *Polym. Degrad. Stab.*, Vol. 76, 2002, pp. 411-417.

[104] F. Tasaka, H. Miyazaki, Y. Ohya, and K. Ouchi, "Synthesis of comb-type biodegradable polylactide through depsipeptide-lactide copolymer containing serine residues", *Macromolecules*, Vol. 32, 1999, pp. 6386-6389.

[105] N. A. Peppas, and R. Langer, "New Challenges in Biomaterials", *Science*, Vol. 263, 1994, pp. 1715-1720.

[106] A. I. Cooper, W. P. Hems, and A. B. Holmes, "Synthesis of cross-linked polymer microspheres in supercritical carbon dioxide", *Macromol. Rapid. Commun.*, Vol. 19, 1998, pp. 353-357.

[107] F. Stassin, O. Halleux, and R. Jerome, "Ring-opening polymerization of epsilon-caprolactone in supercritical carbon dioxide", *Macromolecules,* Vol. 34, 2001, pp. 775-781.

[108] F. C. Loeker, C. J. Duxbury, R. Kumar, W. Gao, R. A. Gross, and S. M. Howdle, "Enzyme-catalyzed ring-opening polymerization of epsilon-caprolactone in supercritical carbon dioxide", *Macromolecules,* Vol. 37, 2004, pp. 2450-2453.

[109] D. D. Hile, and M. V. Pishko, "Ring-opening precipitation polymerization of poly(D,L-lactide-co-glycolide) in supercritical carbon dioxide", *Macromol. Rapid. Commun.,* Vol. 20, 1999, pp. 511-514.

[110] D. D. Hile, and M. V. Pishko, "Emulsion copolymerization of D,L-lactide and glycolide in supercritical carbon dioxide", *J. Polym. Sci, Part A: Polym. Chem.,* Vol, 39, 2001, pp. 562-570.

[111] F. Stassin, and R. Jerome, "Polymerization of (L,L)-lactide and copolymerization with B-caprolactone initiated by dibutyltin dimethoxide in supercritical carbon dioxide", *J. Polym. Sci. Part A: Polym. Chem*., Vol. 43, 2005, pp. 2777-2789.

[112] W. Lui, X. Li, S. Zhou, and J. Weng, "Investigation on process parameters of electrospinning system through orthogonal experimental design", *Journal of Polymer Science*, Vol. 103, 2007, pp. 3105-3112.

[113] C. Teng, K. Yang, P. Ji, and M. Yu, "Synthesis and Characterization of Poly(L-lactic acid)-Poly(ε-caprolactone) Multiblock Copolymers by Melt Polycondensation", *Journal of Polymer Science: Part A: Polymer Chemistry*, Vol. 42, 2004, pp. 5045-5053.

[114] N. Bolgen, Y. Z. Menceloglu, K. Acatay, I. Vargel, and E. Piskin, "*In vivo* performance of antibiotic embedded electrospun PCL membranes for prevention of abdominal adhesions", *J. Biomater. Sci. Polymer Edn.,* Vol. 16, 2005, pp. 1537-1555.

[115] H. Q. Liu and Y. L. Hsieh, "Ultrafine fibrous cellulose membranes from electrospinning of cellulose acetate", *J. Polym. Sci. B: Polym. Phys*., Vol. 40, 2002, pp. 2119-29.

[116] S. Koombhongse, W. X. Liu, and Reneker, "Flat polymer ribbons and other shapes by electrospinning", *Journal of Polymer Science Part B-Polymer Physics*, Vol. 39 (21), 2001, pp. 2598-2606

[117] W. He, Z. W. Ma, T. Yong, W. E. Teo, and S. Ramakrishna, "Fabrication of collagen-coated biodegradable copolymer nanofiber and their potential for endothelial cell growth", *Biomaterials*, Vol. 26, 2005, pp. 7606-7615.

[118] C. Y. Xu, R. Inai, M. Kotaki, and S. Ramakrishna, "Aligned biodegradable nanofibrous structure: a potential scaffold for blood vessel engineering", *Biomaterials*, Vol. 25, 2004, pp. 877-886.

[119] U. Boudriot, R. Dersch, A. Greiner, and J. H. Wendorff, "Electrospinning Approaches Toward Scaffold-A Brief Overview", *Artifical Organs*, Vol. 30 (10), 2006, pp. 785-792.

APPENDIX

(a)

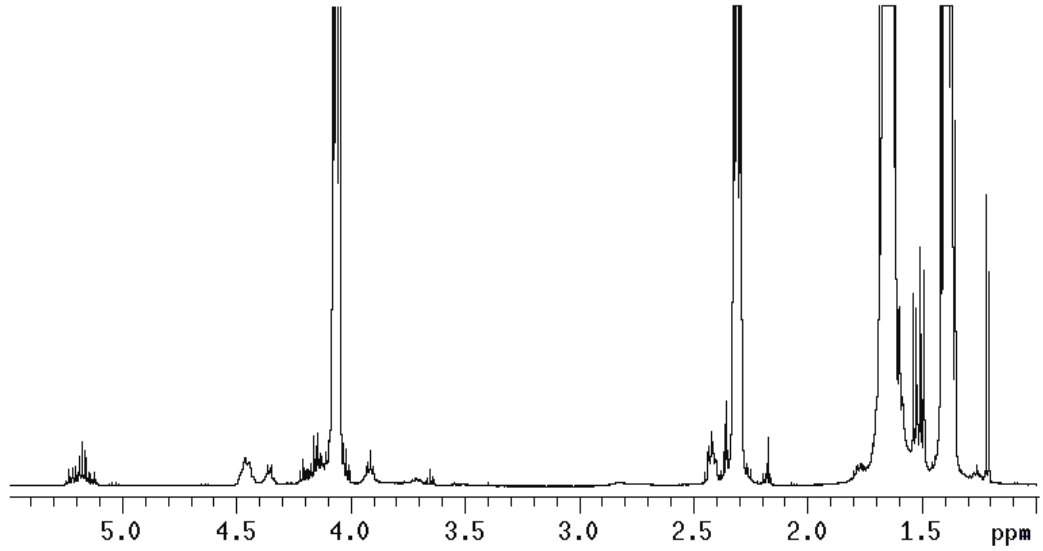

(b)

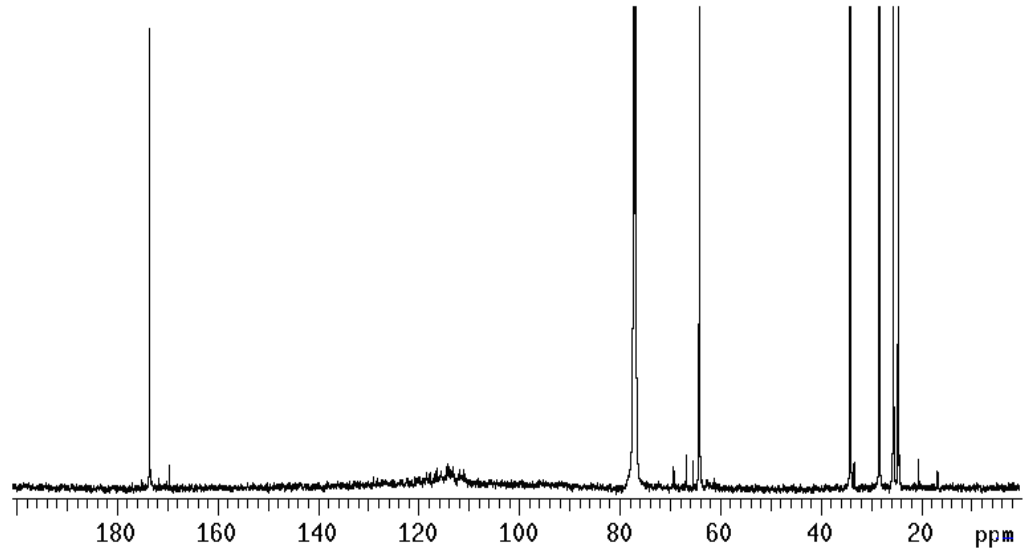

Figure A. 1. (a) ^{1}H-NMR and **(b)** ^{13}C-NMR of branched pentablock copolymer (run no: 2, look Table 2.3) recorded in $CDCl_3$.

(a)

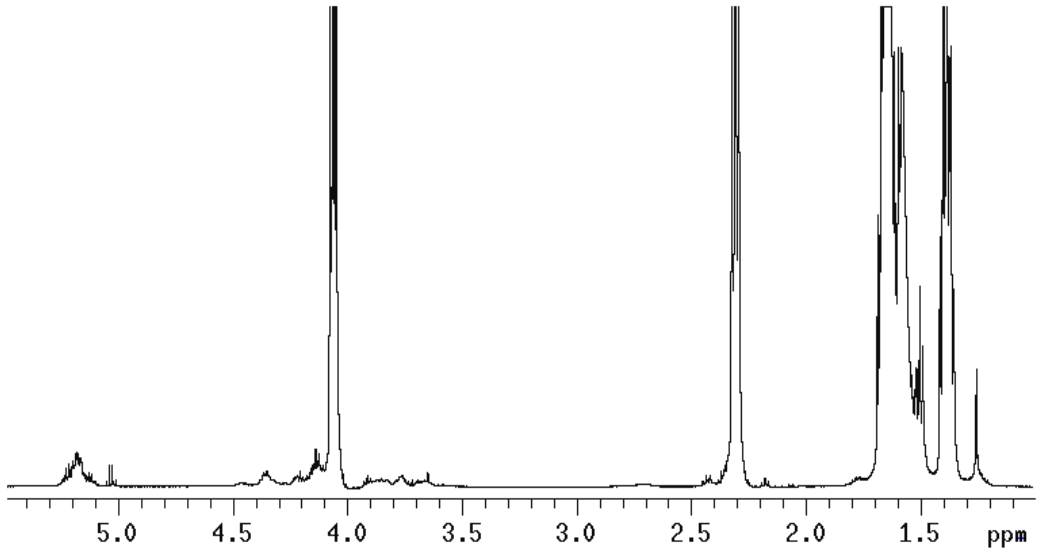

(b)

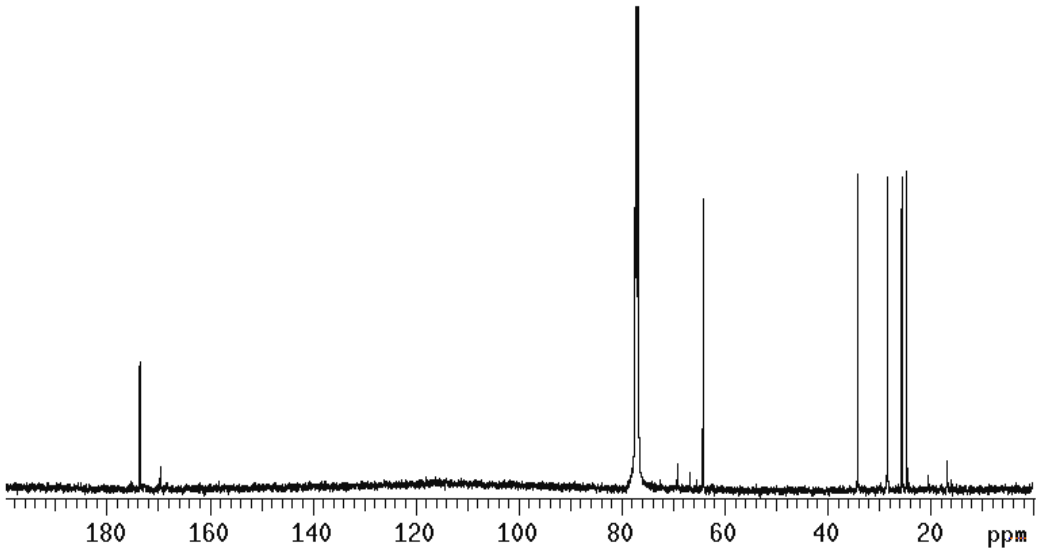

Figure A. 2. (a) ^{1}H-NMR and **(b)** ^{13}C-NMR of branched pentablock copolymer (run no: 4, look Table 2.3) recorded in $CDCl_3$.

(a)

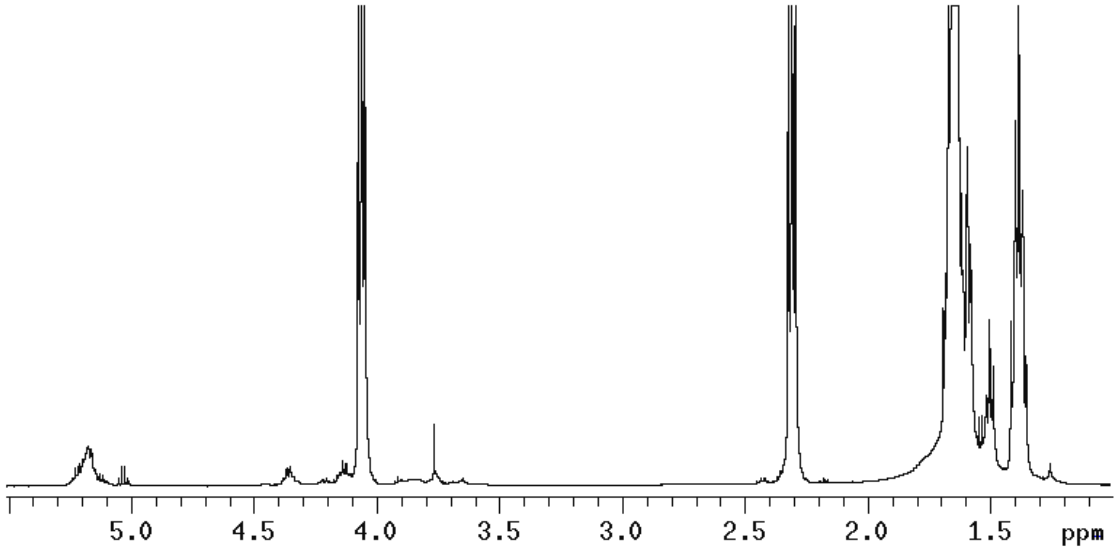

(b)

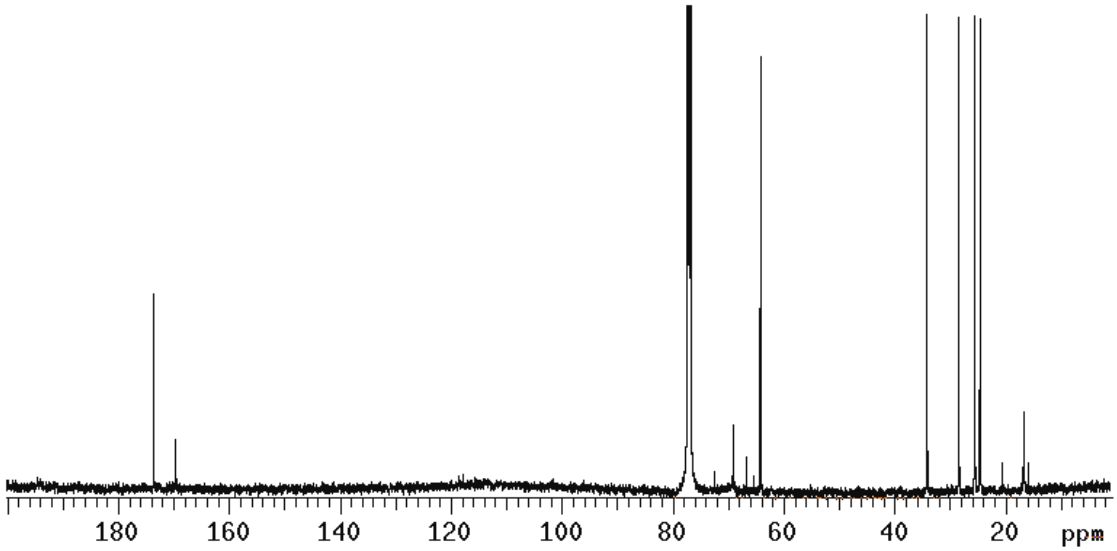

Figure A. 3. (a) ^{1}H-NMR and **(b)** ^{13}C-NMR of branched pentablock copolymer (run no: 5, look Table 2.3) recorded in $CDCl_3$.

(a)

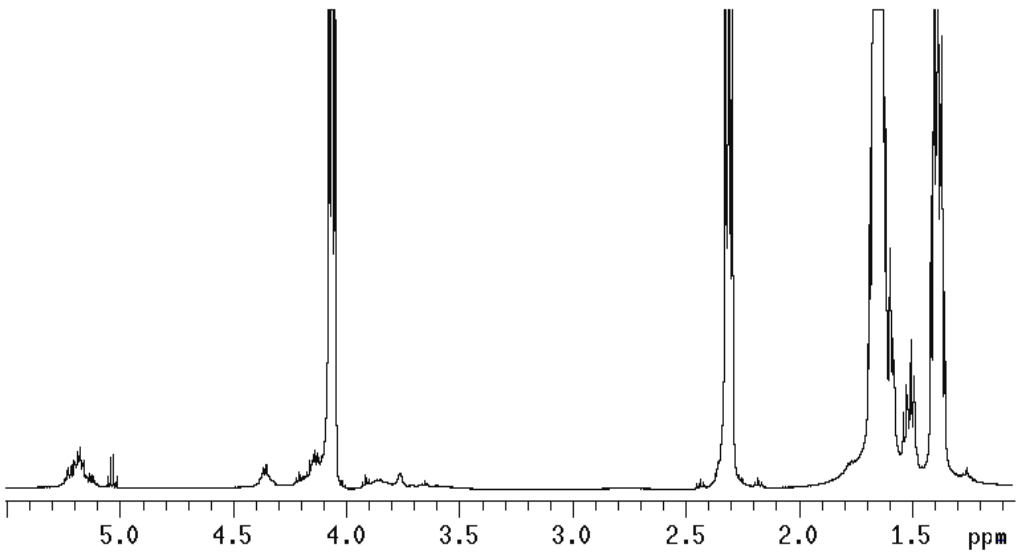

(b)

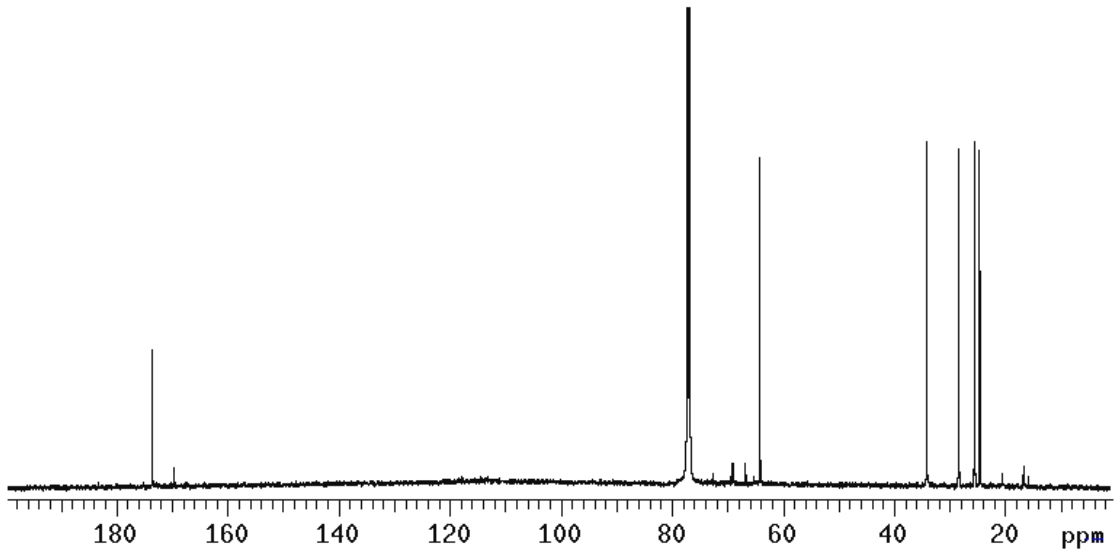

Figure A. 4. (a) ^{1}H-NMR and **(b)** ^{13}C-NMR of branched pentablock copolymer (run no: 6, look Table 2.3) recorded in $CDCl_3$.

(a)

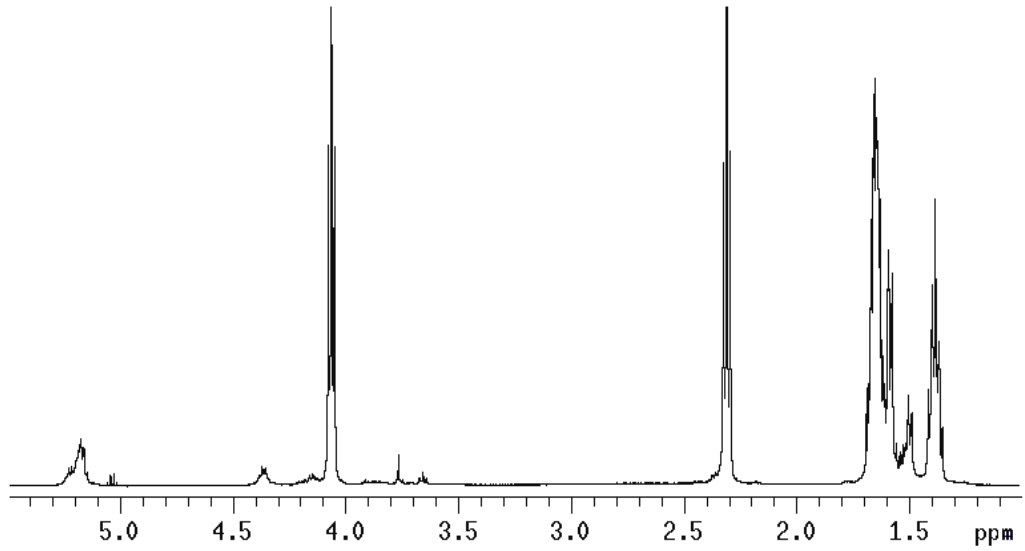

(b)

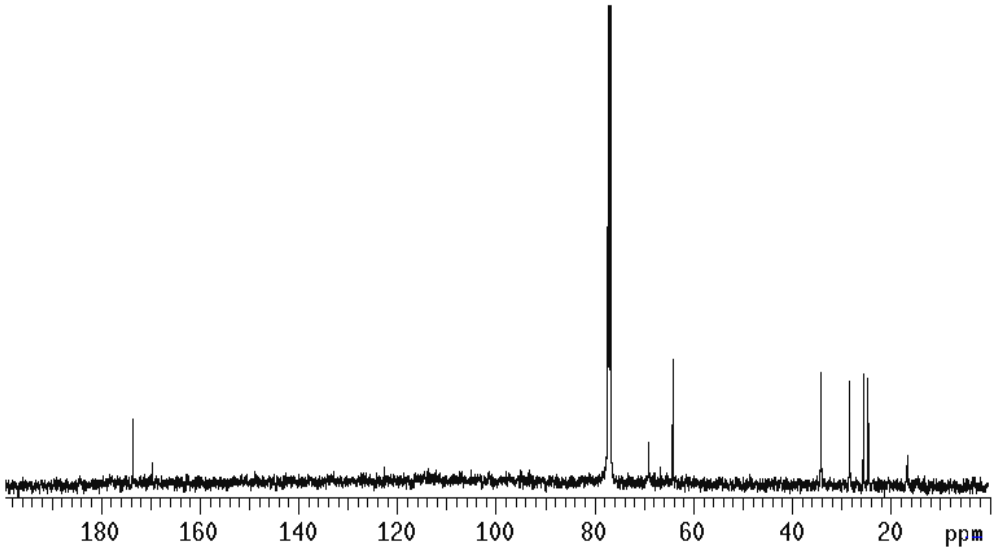

Figure A. 5. (a) ^{1}H-NMR and **(b)** ^{13}C-NMR of branched pentablock copolymer (run no: 8, look Table 2.3) recorded in $CDCl_3$.

(a)

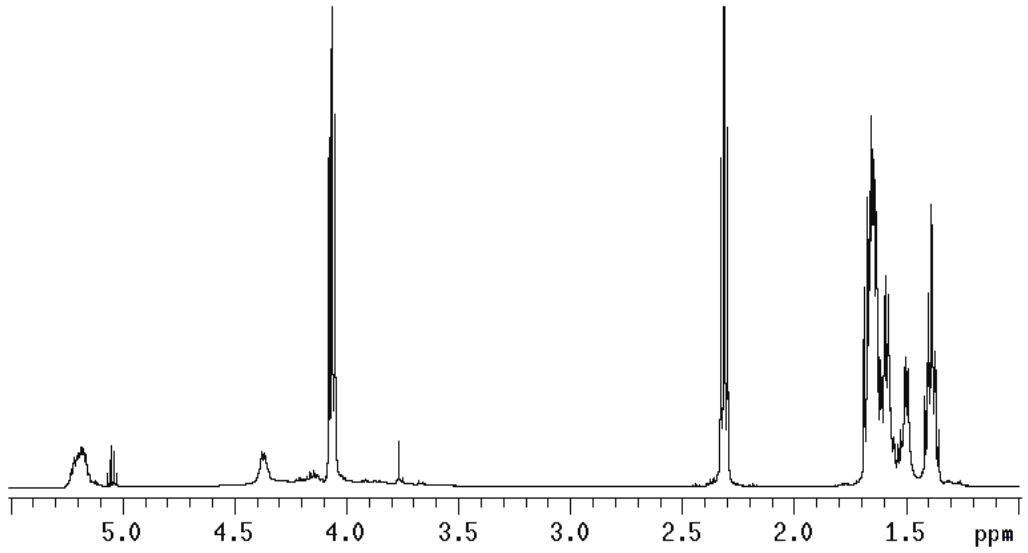

(b)

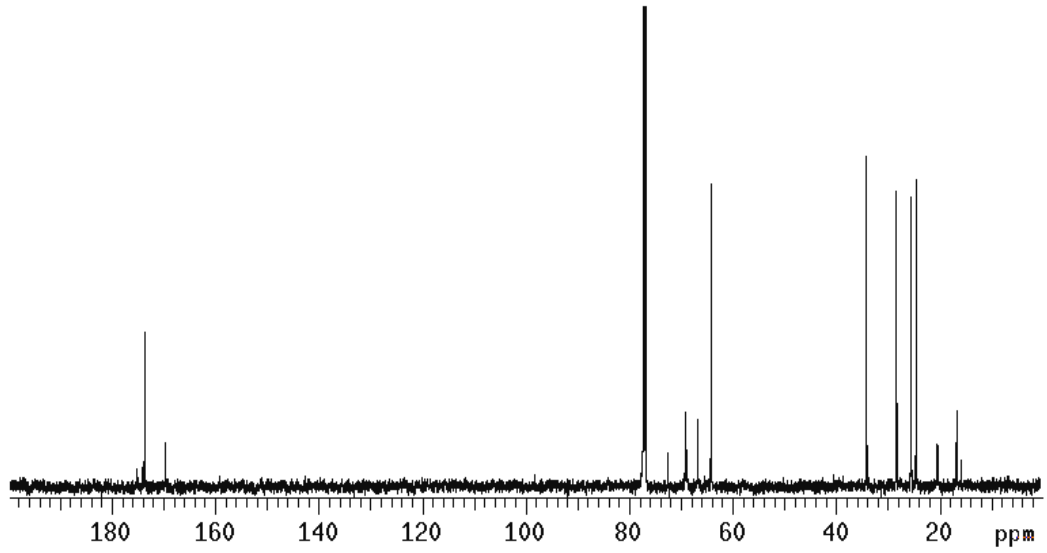

Figure A. 6. (a) ^{1}H-NMR and **(b)** ^{13}C-NMR of branched pentablock copolymer (run no: 9, look Table 2.3) recorded in $CDCl_3$.

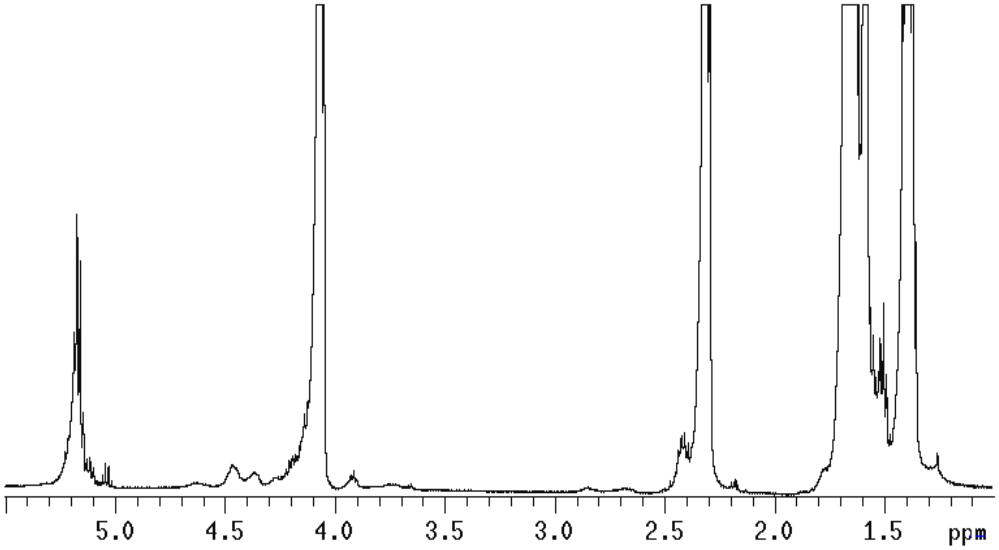

Figure A. 7. ^{1}H-NMR of fluorinated block copolymer synthesized in bulk (Run 1, look Table 2.4) recorded in $CDCl_3$.

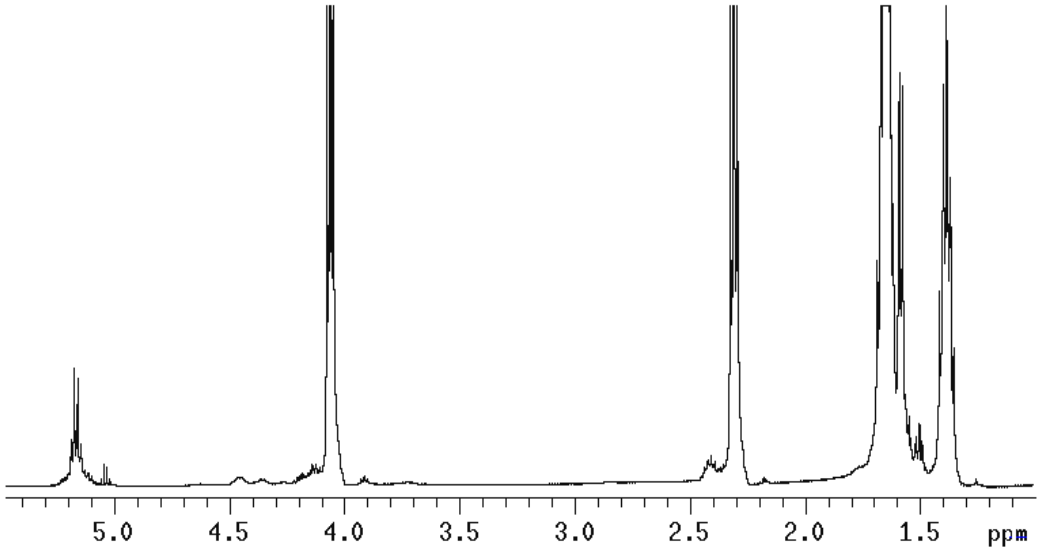

Figure A. 8. ^{1}H-NMR of fluorinated block copolymer synthesized in bulk (Run 2, look Table 2.4) recorded in $CDCl_3$.

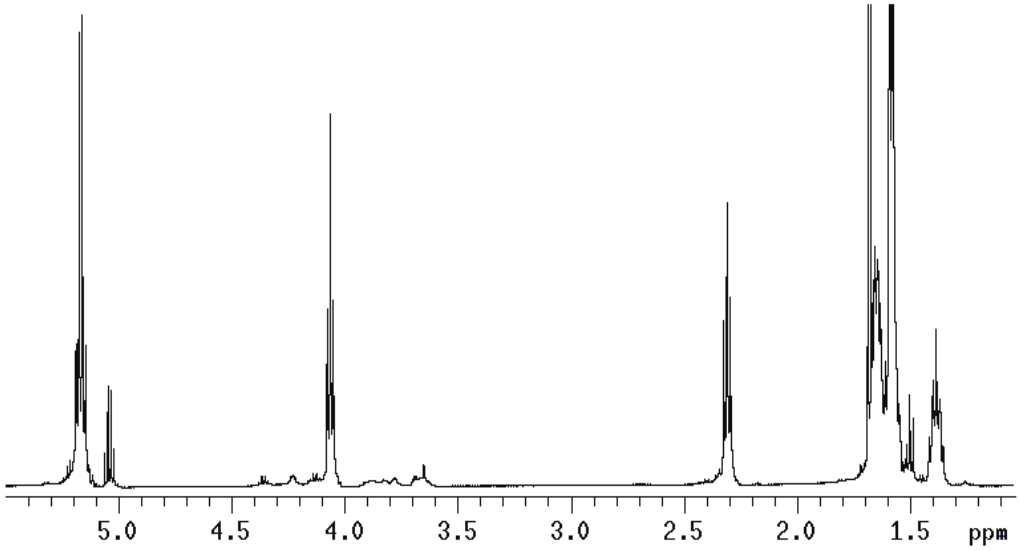

Figure A. 9. ^{1}H-NMR of fluorinated block copolymer synthesized in bulk (Run 3, look Table 2.4) recorded in $CDCl_3$.

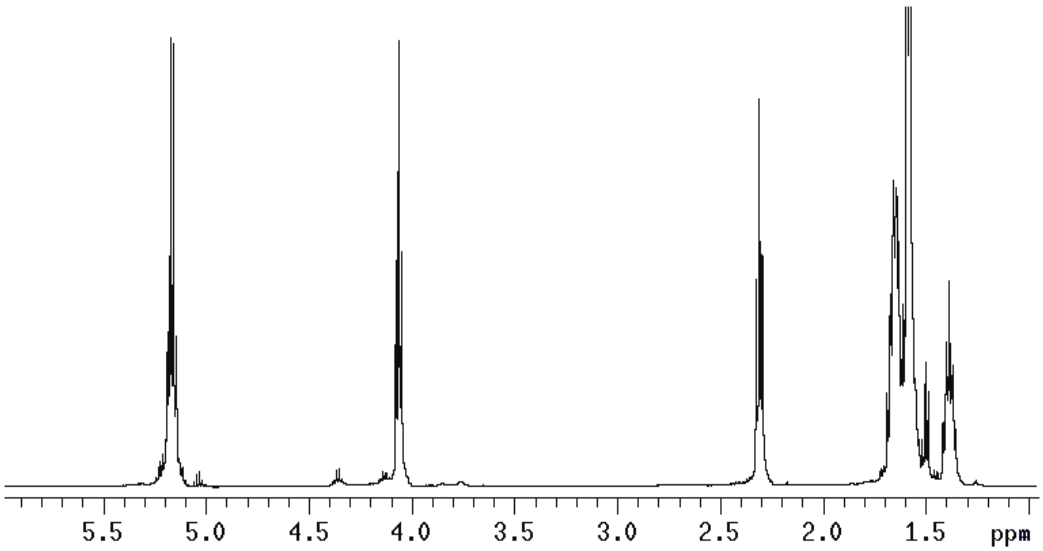

Figure A. 10. ^{1}H-NMR of fluorinated block copolymer synthesized in bulk (Run 4, look Table 2.4) recorded in $CDCl_3$.

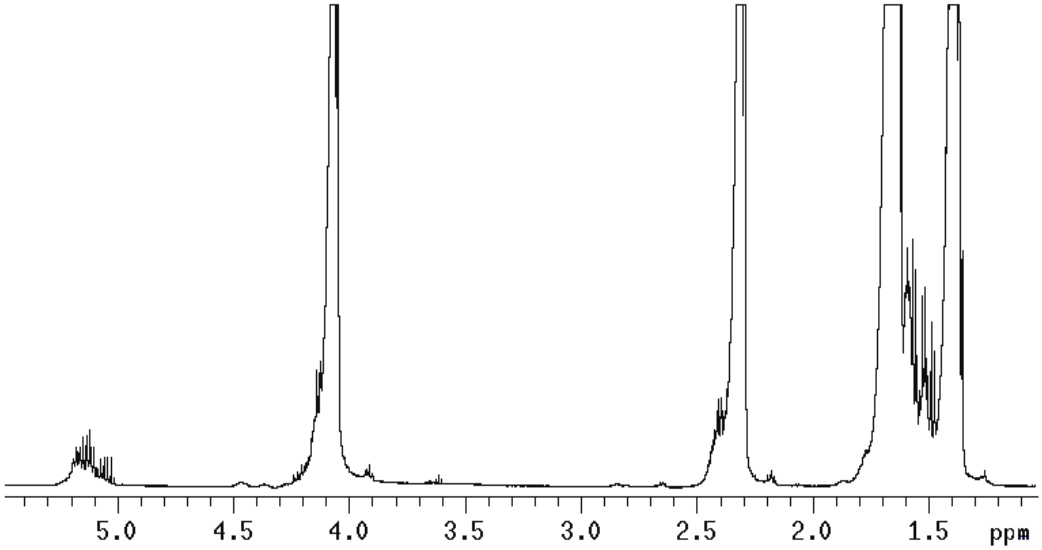

Figure A. 11. ^{1}H-NMR of fluorinated block copolymer synthesized in bulk (Run 5, look Table 2.4) recorded in $CDCl_3$.

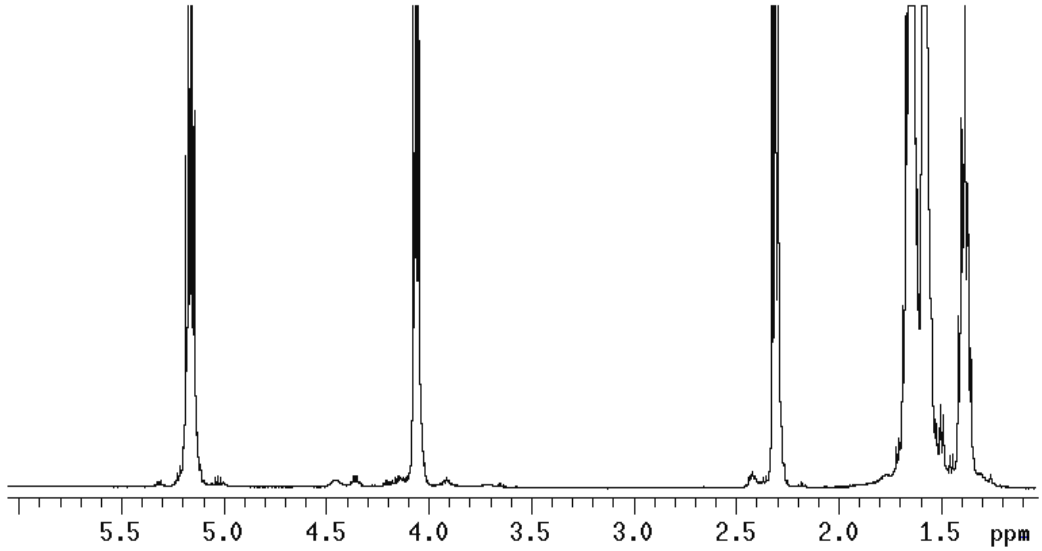

Figure A. 12. ^{1}H-NMR of fluorinated block copolymer synthesized in bulk (Run 6, look Table 2.4) recorded in $CDCl_3$.